Inscription of in-fibre photonic devices by an infrared femtosecond laser

Amós Martinez

Doctor of Philosophy

ASTON UNIVERSITY

September 2005

Aston University

Inscription of in-fibre photonic devices by an infrared femtosecond laser

Amós Martinez

Doctor of Philosophy

September 2005

In recent years, the inscription of embedded photonic devices in transparent materials by means of tightly focused infrared femtosecond laser pulses has been the subject of intense research. There are multiple advantages associated to femtosecond inscription, particularly due to the highly deterministic and nonlinear nature of the absorption process. Nonlinear photo-absorption implies that structural modifications in the material can be confined to the region where the laser is focused; therefore by translating the sample with respect to the focal point, buried, three dimensional structures can be inscribed. The highly deterministic nature of the process permits previously unattainable levels of control in the dimensions and properties of the inscribed structures. The flexibility of the method is further illustrated by the multitude of devices that have been implemented, including waveguides, 3D couplers, lasers, photonic crystals, data storage and gratings. Femtosecond laser inscription has been primarily applied to a wide variety of glasses, but studies have also demonstrated the validity of the method applied to other transparent materials such as crystals or polymers.

In this work, a point by point method for the inscription of fibre Bragg gratings using a tightly focused infrared femtosecond laser is implemented for the first time. Fibre Bragg gratings are wavelength-selective, retro-reflectors which have become a key component in optical communications as well as offering great potential as a sensing tool. Standard methods of fabrication are based on UV inscription in fibre with a photosensitive core. Despite the high quality of the gratings, a number of disadvantages are associated with UV inscription, in particular, the requirements of a photosensitive fibre, the low thermal stability and the need to remove the protective coating prior to inscription. By combining the great flexibility offered by the point by point method with the advantages inherent to inscription by an infrared femtosecond laser, the previous disadvantages are overcome.

The method here introduced, allows a fast inscription process at a rate of ~1mm/s, gratings of lengths between 1cm and 2cm exhibiting reflections in excess of 99%. Physical dimensions of these gratings differ significantly from those inscribed by other methods, in this case the grating is confined to a fraction of the cross section of the core, leading to strong and controllable birefringence and polarisation dependent loss.

Finally, an investigation of the potential for their exploitation towards novel applications is carried out, devices such as directional bend sensors inscribed in single-mode fibre, superimposed but non-overlapping gratings, and single-mode, single-polarisation fibre lasers, were designed, fabricated and characterised based on point by point femtosecond inscription.

Keywords: femtosecond lasers, fibre Bragg grating, micromachining, fibre sensors, fibre lasers.

No consigo entender por qué todo tiene que estar bien hecho, no me atrevo a salir de la cama y afrontar todos los días la tiranía de la perfección.

Héroes, Ray Loriga

Acknowledgements

First of all, I would like to express my gratitude to my supervisor Dr Igor Khrushchev, throughout this three-year long rollercoaster, his guidance and help has been fundamental for the success of this project. More importantly, I would like to thank him for his objective advice in many aspects away from the strictly academic. Since I am a fairly introvert, individual person (for a Spaniard), I never seek or expected this advice, but I do highly appreciate it, for it was always very helpful. I would like to extend this gratitude to Prof Ian Bennion, who has been understanding and supportive and always offered me his advice in the cross-roads that I have encountered in the way.

I would also like to thank Mr Michael Dubov, we have worked together for most of my PhD and he has helped me find my way around the lab. We went through many patches of frustration and excitement inside a small room with a tropical microclimate for over 300 days a year. So thank you for bearing with me and my ways.

I feel particularly obliged to Dr Yicheng Lai and Dr Tom Allsop. The fact that they were interested in our work and joined our efforts has been the key to the flourishing of this project. Their endless supply of ideas, as well as theoretical and experimental expertise has been a great example to me. Of course up with those two, I would like to include Ms Jovana Petrovic, I know I get in her nerves more often than not but she has always been supportive and has offered her help and her thoughts and she is still my preferred source of information and search engine.

Thanks to Helen Dobb, Dr Youfang Hu, John Mitchell and Andy Main, I must apologise for not been able to make up the time, to realise all the ideas that you brought to me. Finally I must say a big thank you to Rachel Won, not only for the UV gratings used in this work, but also for all the support while writing this thesis.

I would like to thank and congratulate everybody from the Photonics Research Group, since they make it a great and comfortable place to work. In particular I like to thank Bert Biggs, his help and understanding is greatly appreciated, without him the labs could not run so smoothly.

To my aunt Conchi

Table of Contents

List of figures

Chapter 1: Introduction

The advent of high power femtosecond lasers has recently given way to new areas of research particularly in micromachining and bulk material modification. The high intensities that can be achieved in femtosecond pulses despite modest average powers lead to a fundamentally different interaction between laser and matter than that observed for longer pulses and CW light [1,2]. Early in the 1990s it was observed that by machining with ultrashort pulses the heat-flow to the surrounding material was essentially eliminated [3]. This property led to high precision micromachining in a wide variety of materials and immediate presence of ultrafast lasers for micromachining in industry.

Soon after, it was demonstrated that glass modification in the bulk of the material [4], rather than ablation, was possible by tightly focusing the femtosecond pulses inside the material. This led to novel areas of research with potential applications in optical communications and photonics in general. By glass modification, we refer to the refractive index modification of the volume in which the pulse was focused. Similar modifications have been also induced in materials such as, polymers [5], or crystals [6]. The potential advantages of this technique are the flexibility to modify the properties of a wide variety of materials and the possibility to produce buried and three-dimensional structures.

Femtosecond inscription provides great flexibility to inscribe three-dimensional structures. This is because the modifications rely on highly nonlinear absorption processes. By focusing the beam, the material modification can be confined to a small volume where the intensity reaches its threshold for the substrate material. In this work, we will define the intensity threshold for a material as the minimum laser intensity required to create a permanent detectable modification in such material. Numerous techniques have been proposed and used in literature to measure this material dependent intensity threshold, including examination by optical microscopy [1, 7], monitoring of changes in transmission of the laser source [7, 8], measuring of plasma emission [8, 9] and monitoring of the dark field scattering [7, 10]. Interferometric techniques of optical microscopy such as differential interference contrast (DIC) [20] and Nomarski microscopy [1] offer submicron resolution, however in-situ diagnosis is not available using microscopy techniques. Plasma emission may be monitored using a photomultiplier tube [8] or a standard CCD camera [9], with such reports indicating the presence of plasma leads to a permanent structural modification. Other techniques monitor the transmission variations of the femtosecond laser beam [8] or a probe beam such as a He-Ne laser [8, 10] measure the intensity threshold. The measured threshold from different sources varies significantly due to the large number of variables such as; pulse duration, wavelength and repetition rate of the laser, material composition and purity of the substrate and focusing conditions.

In chapter 2 the highly nonlinear absorption of the laser beam during femtosecond inscription will be discussed. The strong dependence of the absorption process on laser intensity means that after tight focusing threshold intensity may be reached solely in the focal region, limiting the effects in the surrounding area. Femtosecond lasers have, therefore, been applied to create various buried structures including; waveguides [4], couplers [11], amplifiers [12], photonic crystals [13], data storage components [14] and gratings [15]. The immense potential of this method has led to much interest within the research community and rapid growth in the number of publications and researchers involved. The commercial presence of the femtosecond inscription of photonic devices will be determined by a number of factors. The development of more cost-effective and user-friendly femtosecond lasers is evidently a major requirement. But it is also necessary to demonstrate that the performance of devices fabricated by these methods can compete and exceed the performance of those fabricated by existing methods.

In this work, we will concentrate on the inscription of fibre Bragg gratings by a tightly focused infrared femtosecond laser. Bragg gratings are wavelength selective retro-reflectors based on the inscription of a periodic structure in the core of the fibre. Conventionally these devices are inscribed by UV laser sources [16]. These methods have been developed for over a decade and now are capable of producing highly complex structures to suit the requirements of numerous applications in communications [17] and sensing [18]. The initial motivation to carry out this work was the fact that femtosecond inscription should not experience many of the limiting factors observed in UV inscribed gratings. These restrictions include the need of a photosensitive fibre [19], the low thermal stability of structures inscribed by UV laser sources [20] and the limited flexibility to inscribe complex structures using the standard methods of inscription [16]. The absorption process and material modification during femtosecond inscription are fundamentally different. Thus the limitations found during UV inscription can be overcome.

After implementing a point by point method for the inscription of fibre Bragg gratings by an infrared femtosecond laser, we concentrated on investigating the unique characteristics of the inscribed structures and developing novel applications for these devices. The following section summarises the major achievements of this work.

1.1 Contributions of this work

In this work, a novel method for the fabrication of fibre Bragg gratings using a tightly focused infrared femtosecond laser beam is presented. This method is based on a point by point technique in which each grating pitch is inscribed independently by a single laser pulse. There are limited reports of point by point inscription with UV sources [21], and to this date, this

technique has not been able to compete with holographic or diffractive techniques [19], and has been rarely used for standard applications.. However taking advantage of the properties of femtosecond pulses it was possible to develop a rapid flexible inscription technique which produced high quality gratings with numerous attractive properties.

- *Inscription point-by-point of highly reflective Bragg gratings and first order gratings.* The gratings reported in literature using point by point and a UV laser source presented a reflectivity that did not exceed 70% [21]. In contrast, inscription by the method developed in this work allows the inscription of gratings with reflectivity in excess of 99.9%. Furthermore inscription of first order fibre Bragg gratings for a resonant wavelength of 1550nm is demonstrated for the first time for a point-by-point method. Unlike other reported point-by-point methods, the alignment and inscription processes are fast, with a writing speed of approximately 1mm/s. The writing speed, v_i is set by the repetition rate of the laser, f_{rr}, in our system 1kHz and the length of the grating pitch, Λ, that is to be inscribed, equation 1.1;

$$V_i = f_{rr} x \Lambda \qquad (1.1)$$

These writing speeds are not only much higher that those reported in other point-by-point methods [21, 22] but it is also competitive against other methods such as phase-mask or holographic inscription in this respect.

- *Inscription in non-photosensitive fibre.* Inscription by standard methods requires the use of photosensitive doped fibre or fibre which has undergone photosensitisation procedures (such as hydrogenation). This is not the case for femtosecond inscription. High quality gratings were inscribed in standard single-mode fibre and other non-photosensitive fibres.

- *Inscription of gratings with high thermal stability.* Gratings inscribed by the method proposed in this work exhibit improved thermal stability compared to gratings based on UV-inscription. Stability as high as 1000°C is demonstrated. This represents a higher thermal stability than has ever been reported by UV inscribed gratings. Standard UV inscribed gratings rapidly deteriorate at temperatures which range between 200°C and 500°C for type I and type IIA gratings.

- *Inscription through the protective coating of the fibre.* Standard methods of inscription require the removal of the acrylic coating that protects the fibre. This process is not only time consuming, but it is also detrimental to the mechanical strength of the fibre. A number of methods have been proposed to inscribe through the coating of the fibre, however they are based on special fibres with high dopant concentrations and near UV light [23] or special coatings transparent to UV light [24-26]. In this work, we present for the first time the inscription of fibre Bragg gratings through the coating of a standard fibre.

- *Inscription of axially confined gratings.* Confinement of induced modification of material within a fraction of the fibre cross-section with an area much smaller than the core area is demonstrated by this technique. Multiple potential applications based on this property are outlined in this work.

- *Inscription of gratings with strong polarisation dependence.* The birefringence induced by the inscription process was measured to be significantly higher than that reported in standard UV methods [19]. Furthermore, this polarisation dependence can be increased by changing the conditions of inscription. Highly birefringent gratings may be considered for a number of applications, a suitable technique to create the polarisation sensitivity and possible applications are studied in this work.

- *Inscription of fibre Bragg gratings with directional bending sensitivity.* Gratings inscribed offset from the centre of the core induce an asymmetry in the fibre. This leads to directional sensitivity of the device. A novel directional bending sensor is demonstrated based on such devices.

- *Fabrication of fibre lasers.* A fibre laser inscribed by an infrared femtosecond laser is fabricated for the first time. Inscription of highly reflective gratings is demonstrated in non-photosensitive Er:Yb codoped fibre, and the strong polarisation sensitivity of the gratings is used to ensure single-mode, single polarisation operation. Furthermore, Stable operation of the laser is demonstrated at temperatures as high as 600°C.

- *Long period grating fabrication.* Using the same set-up as used for the inscription of fibre Bragg gratings, long period gratings were inscribed, the polarisation and thermal properties were compared to those of the fibre Bragg gratings.

- *Asymmetrisation of standard fibres.* Taking advantage of the flexibility of femtosecond inscription, asymmetry was photo-induced in the cladding of standard fibres in which a long period grating had been inscribed and the sensitivity to bending was studied. This procedure leads to directional sensitivity, methods to further improve the design are analysed.

1.2 Structure of the thesis

This work, details the development of a method for the inscription of fibre Bragg gratings and other in-fibre devices by a tightly focused infrared femtosecond laser. For this reason, chapter 2 introduces the technology of femtosecond inscription. The development of solid state femtosecond lasers, which led to the advent of femtosecond micromachining, is outlined. This will lead to a discussion on the recent developments of more compact and user-friendly solid state femtosecond laser and femtosecond fibre lasers and the impact that it may have towards realising the commercialisation of this technology. In addition, chapter 2 overviews the

interaction between the tightly focused ultrashort pulse and the material, and how it leads to refractive index modification in buried localised areas. Finally the major advances towards the fabrication of photonic devices are summarised.

Chapter 3 gives an synopsis of the basic methods use for the fabrication of fibre Bragg gratings using the conventional UV-based techniques. The characteristics of these gratings will be summarised, focusing particularly on those which differ from the characteristics of femtosecond inscribed gratings. This chapter will be concluded with a look at the main applications that make use of fibre gratings.

The technique used in this work for the inscription of fibre Bragg gratings is detailed in chapter 4. The dimensions and refractive index modification of the structures are analysed using microscope imaging and quantitative phase microscopy (QPM). The spectral properties are fully characterised, and the effect of varying various inscription parameters investigated. The characteristics of these gratings are compared with gratings inscribed by UV technologies. Finally, the inscription of long period gratings in standard fibres is also demonstrated.

The distinctive characteristics of these devices are introduced and potential applications are discussed in chapter 5. The thermal properties are investigated as well as the characteristics and advantages of inscription through the coating. Two different configurations for bending sensing based on the unique flexibility of femtosecond inscription are proposed, both methods offering directional discrimination in standard fibre. The possibility of inscribing superimposed but non-overlapping gratings is also studied. In chapter 6, fibre lasers are inscribed for the first time by a femtosecond laser. Particularly interesting is the possibility of inscribing directly in Er:Yb co-doped fibre a non-photosensitive fibre and the fabrication of single-mode, single polarisation lasers with stable laser operation at temperatures as high as 600°C for several hours.

Chapter 7 gives conclusions on the bulk of this work and chapter 8 indicates the directions that we will take in the future towards the development of this technique in order to demonstrate its advantages and applicability in a commercial environment.

CHAPTER 2: Inscription of photonic devices by femtosecond lasers

2.1 Introduction

Optical breakdown induced in transparent materials by femtosecond laser pulses has been the subject to a great deal of attention since the development of ultrafast solid state lasers and posterior methods of amplification. This interest is justified by the great flexibility and precision to inscribe tightly confined structures either in the surface or bulk of the material. The interaction between femtosecond laser pulses and transparent materials, particularly glasses can be broadly categorised in three regimes; surface ablation, embedded voids in the bulk of the material and structural modifications in the bulk of the material. Which regime is present in each case depends on parameters such as pulse energy, pulse duration, intensity at focal point and nature and bandgap of the material. Inscription of structural modifications in the bulk of a material offers great flexibility for the fabrication of photonic devices in transparent materials.

The commercialisation of this technology depends primarily on three major aspects which are currently under intense investigation; the development of femtosecond lasers towards more cost effective and user-friendly systems, better understanding of the processes that take place during femtosecond inscription within the material and finally improving the inscription process towards the fabrication of devices that can compete with those fabricated by existing technologies. This chapter offers an introduction to the various aspects of inscription by femtosecond lasers. The developments in femtosecond laser technology are reviewed; followed by a study on the processes that take place during laser-matter interaction, finally the major milestones in device fabrication are described.

2.2 Development of ultrafast Solid State Lasers

The development in the 70's of modelocked dye lasers, demonstrated the feasibility of femtosecond laser pulsing. However, and despite the inherently broad bandwidths of organic dyes, tuning restrictions and the presence of dyes and solvents limited severely their commercial presence. Furthermore, the peak powers reached by such dye lasers were modest [27]. Dye lasers are large devices with high maintenance requirements and unable to deliver output powers exceeding 10mW. The high electrical consumption and the hazards involved in their operation made them unreliable for most applications.

The first broad-bandwidth solid state lasers [28] and subsequent demonstration of self-modelocking in Ti:Sapphire lasers opened the door for ultrashort pulse generation, with ultrahigh peak powers and good tunability. Ti:Sapphire crystal amplifies wavelengths from 700nm to 1100nm and can support pulses shorter than 4 femtoseconds. For Ti:Sapphire lasers to produce a periodic sequence of pulses, it is necessary to phase lock the millions of longitudinal modes present in the operation of the lasers, it was therefore important the observation of self-modelocking of Ti:Sapphire lasers which permitted femtosecond operation with a single optical cavity [29], reducing the cost and dimensions as well as improving the operability. The optical Kerr-effect induced in the gain media due to the high intensities enhanced the modelocking process by discriminating in favour of the pulsed regime. The Kerr-effect produces a combine effect of self-focusing and a self-phase modulation.

The intensity threshold for laser modification by an infrared femtosecond laser on transparent dielectrics such as silicates and borosilicates ranges, according to literature, between 10^{13}W/cm^2 and 10^{14}W/cm^2 [7, 9, 10, 30, 31]. Direct amplification of femtosecond pulses is limited due to the high peak powers characteristic of ultrashort pulses. At high pulse energies, the peak intensities of a femtosecond pulse can damage conventional laser optics; limiting the maximum laser intensities after strong focusing to about 10^{15} W/cm^2. In 1985, Chirp Pulse Amplification (CPA) was proposed [32], this technique stretches the pulse temporally, and thus the intensity of the pulse is reduced and can then be amplified without damaging the system, and then compressed back to femtosecond regime to achieve intensities over 10^{21} W/cm^2. These high power solid state lasers exceeded significantly the necessary energy levels for material modification and therefore the requirements for strong focusing were reduced and this method of inscription became more flexible, as a result work on micromachining and ablation with such systems started [7].

The main advantages of such laser systems in micromachining are a well-defined threshold, a reduced fluence required to start ablation, and a reduced thermally affected area allowing the inscription of high quality sub-diffraction limited structures [1-3]. The downside for the amplified

Ti:sapphire system is the high cost, large dimensions and high energy consumption of the system.

The demonstration of photo-induced bulk change rather than ablation in transparent materials by tightly focused femtosecond laser initiated a new important area of research with enormous potential due to a very broad range of applications in the fabrication of photonic devices, the list of devices that have been fabricated by femtosecond lasers includes waveguides [4, 30, 33], couplers [11, 34], amplifiers and lasers [12, 35], data storage [5, 14] photonic crystals [13] and in-fibre gratings [15, 36-38]

The nature of the laser-matter interaction at these intensity levels implies that it can be applied to a range of materials such as various glasses [4, 11-15], crystals [6, 39-40], and polymers [5, 41-43] with similar effects. For this technology to develop from research laboratories towards widespread industrial applications, it will be crucial not only to develop methods of inscription of photonic devices by femtosecond lasers, but also to further develop femtosecond laser towards higher compactness, lower maintenance devices.

To this date, most of the research in femtosecond inscription has been carried out on one of the following three systems; amplified Ti:Sapphire lasers with kHz repetition rate and high pulse energy of approximately 1mJ [1], regeneratively amplified Ti:sapphire laser with 100kHz to 250kHz and up to 1W average power [4, 44] and Ti:Sapphire stretched cavity oscillator with MHz repetition rate and lower peak powers of the order of 10nJ [10]. The merits of both options for the inscription of various photonic devices will be discussed below; however both are complex and expensive systems with very limited commercial potential. Important advances have been reported recently in the development of femtosecond lasers more suitable for industrial applications. The use of two particularly interesting femtosecond laser systems has been recently reported. One is a diode-pumped cavity dumped Yb:glass femtosecond laser oscillator with s repetition rate of the order of 200kHz, pulse energy of ~300nJ and a pulse duration of 250fs [35]. The second system is a compact femtosecond Yb-fibre laser with variable repetition rate, and energies higher than 2.5μJ at 100kHz repetition rate, and higher than 150nJ at 5MHz repetition rate [33]. The pulse duration in this laser is approximately 375fs. As well as offering a more compact and economical solution to femtosecond applications, the feasibility of using these lasers for waveguide inscription has been demonstrated, and while shorter pulse durations may be desirable future systems used commercially for femtosecond inscription are expected to be based on similar configurations.

2.3 Laser-matter interaction in femtosecond phenomena: Photo-absorption

The study of laser-matter interaction of femtosecond pulses is a topic that deserves much attention in its own right. Soon after the chirped pulse amplification technique was developed, it was observed that bulk damage during femtosecond irradiation deviated significantly from those predicted by models based on longer pulses from tens of picoseconds to nanoseconds [1].

The most accepted interpretation of photoinduced material breakdown or damage for pulse durations of the order of tens of picoseconds indicates that electrons at the conduction band, which oscillate in response to the laser field, increase their energy by absorbing electrons in inelastic collisions with the lattice. These free electrons will later scatter with the lattice transferring the laser energy into the lattice, with the resulting emission of phonons. When a free electron achieves kinetic energy equal to the energy bandgap of the material, subsequent impact ionisation promotes another valence electron into the conduction band, creating an avalanche effect. Damage takes place when the pulse energy is sufficient to heat the dielectric material through electron avalanche until it melts or fractures [1, 7].

While the mechanisms that lead to structural changes in dielectrics and other transparent materials during and after femtosecond laser irradiation are not yet fully understood; photon absorption is reasonably well known [7], and consists on highly nonlinear photo-absorption processes, such as multiphoton absorption and avalanche ionisation. Current research is mainly aimed at understanding the way in which the energy from the pulse transfers into the lattice of different materials and for different laser parameters. In this section, the absorption mechanisms of tightly focused femtosecond pulses by transparent materials will be reviewed. The manner in which the energy transfers into the lattice and how that may lead to different types of optical changes depending on the level of intensity and the nature of the material are also outlined. Finally the influence of inscription parameters, such as repetition rate, wavelength and focusing conditions will be considered.

2.3.1 Nonlinear Photo-ionisation

In a transparent material, there is not linear absorption of the incident laser light. Significant transfer of energy to the material is only possible by nonlinear photon absorption. Thus, only at regions where the intensity reaches its threshold, absorption will be enough to modify or ablate the material. It is this property that enables the inscription of buried structures in transparent

materials; this is possible when the pulse is tightly focused in the bulk of the material and its energy is such that the threshold intensity is only reached at or in the vicinity of the focal point.

During the processes of ablation and structural changes, two nonlinear mechanisms for the excitation of bound electrons to the conduction band are present; those are photo-ionisation and avalanche ionisation. A single photon of infrared light does not have enough energy to promote an electron from the valence band to the conduction band of a transparent material; therefore if the atoms are to be photo-ionised alternative processes must take place. These processes are multiphoton ionisation and tunnelling ionisation [1, 7].

Multiphoton ionisation refers to the simultaneous absorption of various photons of the laser beam by a bound electron that absorbs enough energy to be promoted to the conduction band. The multiphoton ionisation rate is strongly dependent on the laser intensity, following equation 2.1;

$$P(I) = \sigma_K I^K \tag{2.1}$$

Where σ_k is the multiphoton absorption rate for k-photon absorption and k is the minimum number of photons that satisfy $k\hbar\omega \geq E_g$. In the case of fused silica and assuming an infrared laser source with 800nm radiation, it is a six photon process. This means that in order to photo-ionise the electron in the atom, it must interact simultaneously with six photons, the photon density must consequently be extremely high [45]. Figure 2.1a illustrates the process of multiphoton absorption.

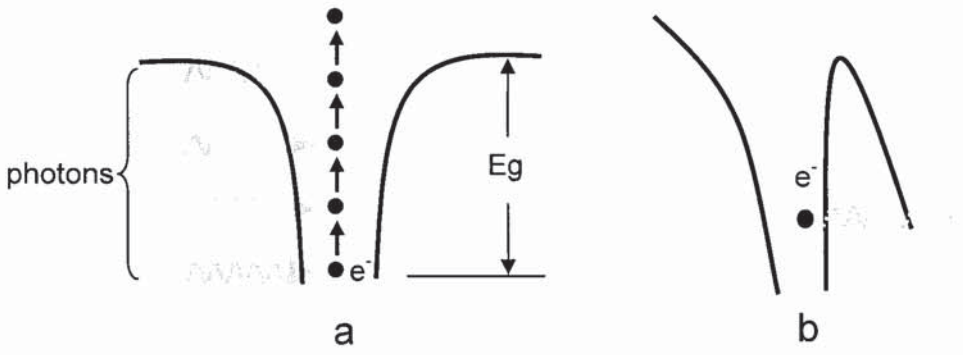

Figure 2.1: (a) Diagram of multiphoton ionisation. The bounded electron requires the energy of various photons simultaneously to be liberated from the ion, (b) Diagram of tunnelling ionisation. The bounded electron can tunnel through the potential barrier to a free state as the laser electric field reduces the potential well of the lattice (adapted from [7]).

Multiphoton absorption is responsible for the deterministic nature of the threshold in femtosecond laser breakdown, opposed to the statistical nature of interactions with longer pulses. It is fundamental in the creation of the seed electrons required for avalanche ionisation process during femtosecond inscription [2, 7-8].

An alternative non-linear process for photo-ionisation is tunnelling. Tunnelling ionisation takes place when the electric field of the laser suppresses the Coulomb well that binds a valence electron to its atom. If the laser intensity is large enough the electron could tunnel through the barrier and become free. This process is illustrated in figure 2.1.b.

The balance between multiphoton and tunnelling ionisation in the overall femtosecond ionisation process is dependent on parameters such as the bandgap of the material, photon energy, and the electric field and intensity of the laser. Various reports indicate that the dominant process can be estimated from the adiabatic or Keldish parameter [7], γ, from equation 2.2. This criterion indicates that when the Keldish parameter is larger than 1.5 ($\gamma>1.5$), photo-ionisation is mainly a multiphoton process, if γ is smaller than 1.5 tunnelling is the dominant process. Both processes have a similar impact in the intermediate region ($\gamma=1.5$).

$$\gamma = \frac{\omega}{e}\left[\frac{mcn\varepsilon_o E_g}{I}\right]^{1/2} \qquad (2.2)$$

Where ω is the laser frequency, I is the laser intensity at the focal point, m and e are the reduced mass and charge of the electron and c is the velocity of light, n is the refractive index and E_g is the band gap of the material. There is an on-going debate on the validity of this criterion with some reports indicating deviations from it [7].

Photo-ionisation rates depend strongly on the laser intensity, particularly multiphoton ionisation which in the case of silica has a sixth power dependence on the intensity. The strong nonlinear dependence of multiphoton rates on intensity causes the threshold to be sharply defined for this type of interaction, contrasting with longer pulses in which much of the absorption depends on the density of defects which act as source of seeded electrons for the avalanche ionisation. This characteristic of femtosecond laser inscription is advantageous for micromachining, since such highly determine threshold has been used for the inscription of sub-diffraction limited structures [1].

2.3.2 Avalanche Ionisation

This process consists on the progressive absorption of photons from the laser beam by an electron which is already in the conduction band. This electron, commonly known as seed electron, can linearly absorb laser energy through resonant absorption; this is by colliding with bound electrons and the lattice through de-phasing and therefore conserving the energy and momentum. This process is known as inverse Bremsstrahlung or Joule's heating and allows the electron to absorb energy from the photons [41]. After the electron has absorbed a number of photons, n, such that its energy is greater than the band gap, E_g, as given by equation 2.3, it can ionise a bound electron by direct collision, leaving two electrons at the bottom of the conduction band that can continue the avalanche effect.

$$n\hbar\omega \geq E_g \tag{2.3}$$

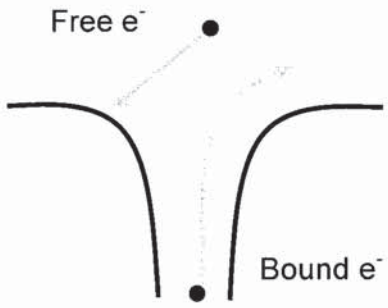

Figure 2.2: Avalanche ionisation, free electrons absorb the energy of incoming photons by Joule's heating, when they have gained enough energy they can ionise bounded electrons, with the consequent cascade effect [7].

The electron density in the conduction band grows due to avalanche at a rate η, given by equation 2.4;

$$\frac{dn}{dt} = \eta n \tag{2.4}$$

The avalanche ionisation rate, η, is linearly dependent on the intensity [12], η=αI, where α is the avalanche ionisation coefficient. It is worth noting that while avalanche is a nonlinear process,

since it is a linear function of the intensity, it is not as highly nonlinear as multiphoton ionisation, which for silica irradiated with an 800nm source is a function of the sixth power of the intensity.

The absorption of incident light by Joule's heating does not take place only during femtosecond laser irradiation; on the contrary, it is the dominant cause of absorption during laser-matter interaction of longer pulses. The main difference between the longer pulses and femtosecond pulses concerns the source of the seeded electrons that start the avalanche process. While for longer pulses avalanche requires the initial presence of seeded electrons from either thermal excitation or defects in the material, during femtosecond irradiation, nonlinear photo-ionisation provides sufficient free electrons to start avalanche.

The origin of the seeded electrons indicates an advantage of the femtosecond material processing, since in this case, seed electrons are provided by the multiphoton process and the role of the impurities of the material can be neglected. Hence, the threshold for femtosecond inscription is an intrinsic property of the material for the given writing conditions and can be calculated accurately. For longer pulses, only a statistical approximation of the threshold is possible.

2.4 Laser-matter interaction in femtosecond phenomena: Material modification

Permanent structural changes are printed on the surface or in bulk of the material after interacting with femtosecond laser radiation at energies above certain material-dependent intensity threshold, which is of the order of 10^{13}W/cm^2 for most transparent dielectrics. Various mechanisms are known to lead to that modification and the morphology of that structural change is dependent on the nature of that mechanism. Which of these mechanisms causes the modification depends on a number of parameters, including pulse energy, focusing conditions, repetition rate of the laser and number of incident pulses as well as on the properties of the material.

For instance, if the absorption of the pulse leads to an increase of temperature sufficient to melt a small area in the focal region, the material may re-solidify non-uniformly leading to density and refractive index variations. This type of changes, sometimes accompanied by the presence of colour centres [9, 11, 46], is applied to the fabrication of waveguides. At higher laser intensities, absorption of the pulse energy leads to micro-explosions and a resultant shock wave expanding towards the surrounding region [47]. This explosive expansion leaves a less dense central region or a void, surrounded by a denser corona; such modifications have been proposed for the inscription of devices such as data storage or photonic crystals. Other than localised melting and densification, and micro-explosions, there is a third case, which is particularly interesting for the inscription of waveguides and consists of the material modification by a femtosecond laser with a high repetition rate (>1MHz). In this case, and at energy levels in the range of localised melting, material changes in the focus and surrounding region are created by cumulative heating effects [48]. In this case, the temperature in the focal region gradually increases due to the progressive absorption of various pulses before thermal dissipation is completed, the temperature can be increased until permanent changes are reached, working below the pulse energy threshold from a single pulse. A final and seldom investigated regime of material modification leads to an increased birefringence of the host material. These changes take place at intensities between those of micro-explosion and index change. This birefringence is due to a self-organised, periodic refractive index modulation produced by a pattern of interference between the incident laser irradiation and on electron acoustic wave generated within the material [44].

2.4.1 Plasma formation, index modification and ablation in glass materials

As it was detailed in the previous section, the process begins with the absorption of the pulse energy in the focal region by multiphoton seeded avalanche photo-absorption. This leads to the creation of an electron plasma that may lead to index modification or damage in the material. The density of this plasma is going to determine ultimately the nature of the modification. Therefore, It is important to understand the evolution of the electron plasma, which can be described by the rate equation 2.5 [45]:

$$\frac{\partial n}{\partial t} = \sigma_k I^k + \alpha n I - \frac{n}{\tau} \tag{2.5}$$

The first term in the right hand side of equation 2.5 corresponds to multiphoton ionisation, where k indicates the number of photons that must be absorbed simultaneously to promote and electron to the conduction band, σ_k is the multiphoton absorption coefficient and I is the intensity of the pulse. The second term corresponds to avalanche ionisation, where α is the avalanche coefficient, and n is the number of free electrons. The last term indicates the linear losses in electron population with τ, indicating the rate in which it takes place.

The intensity and wavelength of the laser pulse and the energy bandgap of the material will dictate the properties of the plasma and the final characteristics of the modified area [31]. In particular, the plasma can reach a density level after which it becomes strongly absorbent to the incident laser wavelength. Reaching this plasma density level, known as critical plasma density leads to the efficient absorption of the tail of the pulse, leading to micro-explosions. Thus, the density of the plasma is directly related to the refractive index modification and the ablation processes. Refractive index modification takes place when the plasma created is of low-density; therefore well below the critical plasma density for the given incoming beam [9, 48]. The critical plasma density for silica as a function of the incoming light is given by equation 2.6;

$$n_c = \frac{0.112x10^{34}}{\lambda^2(nm)} \left(1/m^3 \right) \tag{2.6}$$

where n_c is the critical electron density (approximately $10^{27}cm^{-3}$ for fused silica and an incoming beam emitting at 800nm) and λ is the wavelength of the incoming laser beam. When the intensity is below the threshold for ablation, the pulse energy is only partially absorbed by the lattice. As the intensity of the pulse increases, the plasma reaches its critical level it becomes very absorbing and most of the pulse is therefore transferred to the material, at even higher

intensities the plasma becomes reflective which may lead to the creation of damage features with conical shape [48].

We can therefore consider three regimes of laser-matter interaction regarding the nature of the plasma. At lower intensities absorption, is predominantly an avalanche process, the front part of the pulse provides a number of seed electrons through multiphoton ionisation, and avalanche starts from this seeded electrons. This regime typically takes place up to intensities in the order of $10^{13}W/cm^2$ for a silica sample at incident wavelengths of approximately 1μm, the plasma has low density and low absorption, much of the pulse does not contribute to the structural modification. This interaction leads to positive refractive index changes in the focal region due to the compaction after re-solidification of the material, and is the basis for the fabrication of devices such as waveguides [48].

At higher intensities, the threshold for most glasses is commonly reported to lie between $10^{13}W/cm^2$ and $10^{14}W/cm^2$ for silica, the dominant mechanism is multiphoton ionisation, this leads to full ionisation in tens of femtoseconds and after surpassing the critical density for the corresponding incident wavelength, to strong absorption and ablation [31]. The absorption of most of the pulse in such a small volume produces micro-explosions and thus micro-cracks or voids in the material [3]; this effect is undesirable for the inscription of waveguides, but if the dimensions and properties of the structure are well controlled, it is useful for micromachining and data storage [14], due to the high optical contrast needed for such applications. At even higher energies plasma becomes highly reflective. This leads to a shielding effect and to a large area damage structure which propagates towards the direction of the incoming beam. This regime is undesirable for the fabrication of photonic devices, and generally not applicable to micromachining [14, 48].

The dynamics of the energy transfer from the electron plasma into the lattice is not well-known but particularly for glasses has been the subject of intense research [7, 48]. These studies indicate the following approximate temporal evolution. First, the energy of the pulse is transferred to the electrons in the duration of the pulse. The energy of the electron plasma is transferred the surrounding lattice in a few tens of picoseconds, creating an ion plasma and breaking the bonds of the lattice this process takes approximately 100ps, during the electron-ion interaction, phonon emission ensures the conservation of momentum. The phonon emission creates a pressure wave that propagates away from the focal region influencing the final morphology of the index change [48]. The pressure wave is a result of a thermo-elastic stress induced by the rapid temperature elevation of the region that absorbs the pulse, as it propagates it may lead to the creation of concentric rings with positive or negative refractive index changes. The pressure wave is totally damped in tens of nanoseconds. Finally, thermal dissipation is completed in approximately 1μs. The newly formed bonds are subject to strains which increase the density and therefore higher refractive indexes are present in those areas.

Apart from densification after localised melting, there are other minor contributors responsible for the refractive index changes in glasses, such as the presence of colour centres [9, 47] and strains due to the propagation of the pressure waves [9]. Studies indicate that these colour centres and strains can be erased by annealing, however the refractive index is only reduced by a small percentage indicating that femtosecond inscription does create colour centres but they account only marginally to the refractive index modification [9, 11, 46].

2.4.2 Comparison between high and low repetition rate

During the interaction of subpicosecond pulses and matter, energy is absorbed by the electrons much faster than it is transferred to the lattice, since the lattice does not heat appreciably during the pulse there is no modification of the electron-lattice scattering rates, and there is no need to account for the thermal and mechanical stresses as it would be for longer pulses (picosecond and nanosecond regime). However, thermal effects may be caused by the interaction between a region in the material that has just absorbed the energy from a pulse and ensuing pulses in the pulse train.

Incubation effects are particularly relevant for laser system with a high pulse repetition rate. In this case, the time interval between pulses is not sufficient to allow the dissipation of the heat created by the absorption of the individual pulses, thus the focal region acts a heat point source with a temperature that increases with the number of pulses [48]. It has been observed that the refractive index modification continues to take place after the pulse has passed; this change is caused by thermal diffusion from the heated region and is expected to continue for an approximate time of 100ns for glasses such as silica [9].

In the context of femtosecond inscription, it is possible to categorise the laser systems according to the pulse repetition rate. The first type of systems consists of Ti: Sapphire lasers amplified using chirp pulse amplification, that emit very high peak powers at low repetition rates, generally from 1KHz to 5KHz. In this case, the material has sufficient time to cool down between pulses (between 0.2ms and 1ms), thus, cumulative heating effects do not take place and the effect of each pulse must be considered individually. The second type of lasers consists of a long laser cavity particularly suitable for the inscription of waveguides, this type of lasers produce lower pulse energies but the repetition rate is significantly higher at up to 25MHz, the time between pulses in this case is tens of nanoseconds, and before thermal diffusion has been completed the next pulse in the train is been absorbed. This leads to an alteration of the absorption of pulses in the low plasma regime with cumulative heating effects, which leads to the isotropic distribution of the refractive index change from the focal point.

At low repetition rates, below 1MHz the material has time to cool down between pulses, the focusing conditions and the material properties for successive pulses would be different due to the effect of previous pulses and therefore the area is modified both in dimensions and magnitude of the refractive index modifications. The threshold for index modification does not change by increasing the number of pulses.

At higher repetition rates over 5MHz the lattice does not have time to fully stabilise before the next pulse is absorbed, and thus, the cumulative heating effect is significant. Point-like structures inscribed by multiple pulses in this regime are spherical due to the required tight focusing (necessary since these systems only operate at low peak powers), and because it is essentially a thermal effect (thermal diffusion is isotropic). Structures produced in this regime are spherical rather than elliptical. In effect, the material sees a point-source of heat at the focal point of the laser. With high repetition rate lasers the threshold can be reduced by increasing the number of pulses that are absorbed by a given area. Another interesting characteristic in this regime is that the dimensions of the structure are proportional to the number of pulses applied and the magnitude of the refractive index change is proportional to the pulse energy. These properties allow a high level of control in designing the desired photonic device in a simple manner.

Regeneratively amplified laser systems offer a intermediate repetition rate in the range between 100kHz and 300kHz [4, 49], such systems have an improved performance with respect to the systems that operate at repetition rates up to 5kHz, but cumulative heating such as observed for high repetition rate systems (>1MHz) does not take place, and therefore the features inscribed are elliptical.

Summarising, the affected area in the fast repetition rate cases effectively increases as the number of pulses increases while in low repetition rate system the transmission through affected areas will see different conditions after the initial pulse but all the created heat would have been dissipated before the next pulse arrives. It is worth noting that for other materials such as polymers, the cumulative heating effects have been observed even at repetition rates as low as 1kHz indicating a thermal diffusion rate significantly slower than for glasses.

2.5 Applications of material processing by a femtosecond laser

Femtosecond lasers have been used for a variety of micromachining tasks [27], it has been demonstrated that they can cleanly ablate a wide variety of materials without affecting the surrounding area with molten material as is generally observed for other laser-based techniques. More importantly it has been demonstrated that for large band-gap materials in which linear absorption is not present, it is possible to locate the damaged or modified region in the bulk of the material without affecting the surroundings [14]. It is therefore possible to produce three-dimensional structures within the bulk of the material by producing micro-voids or change the refractive index of a volume inside the material.

The characteristics of the modified area depend on the parameters of inscription, as reported in the previous section, and may be selected in accordance with the specific needs of the application. Another key advantage that can be attributed to femtosecond inscription is that it is applicable to a variety of materials including glasses, polymers and crystals adding to the flexibility and integrating capabilities of the method.

Various photonic devices have been fabricated and others proposed based on tightly focused femtosecond laser inscription. This section reviews the most relevant advances and comments on the main obstacles that must be overcome by this technology to become a commercial reality. Depending on the level of laser intensity, it is possible to create different types of structures inside dielectric materials. Low intensities produce smooth positive refractive index changes, while higher intensities would lead to micro-voids and cracks. Recent studies also investigate the creation of birefringent regions after irradiation by intermediate intensity levels [44]. By controlling appropriately the pulse energy of the femtosecond laser and the focusing conditions, devices such as waveguides, data storage or photonics crystals can be created.

2.5.1 Surface micromachining: Femtosecond laser ablation

Micromachining has been identified from early days as one of the key applications of high power femtosecond laser. Its unique properties have ensured commercial success in a wide range of applications from the micromachining of metals with sub-micron precision to surgical applications [27].

Ablation by tightly focusing the laser beam is already available with alternative high power lasers, such as CO_2 and Nd:YAG lasers. The mechanisms that lead to the material removal are

fundamentally different. In the case of microsecond and nanosecond pulse lasers the removal of the material is accompanied by thermal diffusion of the pulse energy into the surrounding material, that leads to the presence of debris and surface contamination in the surrounding area. During ablation by a femtosecond laser the energy is deposited in the focus too rapidly for the heat to diffuse into the surrounding non-irradiated areas, ensuring smooth, precise features. Another significant advantage of micromachining by ultrashort pulses is the deterministic nature of the ablation threshold. It is therefore feasible to create features smaller that the focal point by carefully adjusting the pulse energy to reach the threshold only at its central part.

The two above mentioned properties have granted this technology commercial success in diverse areas of micromachining including neurosurgery or the restoration of lithographic photo-masks, despite the current complexity, cost and bulkiness of available amplified femtosecond lasers. On-going development of more user-friendly femtosecond systems will undoubtedly benefit the establishment of the femtosecond micromachining technology.

2.5.2 Applications for buried positive refractive index changes

The inscription of waveguide has been subject of intense research since the feasibility of the method was first demonstrated in 1996 [4]. Properties such as; simplicity, versatility, three dimensional capabilities, choice of substrate, and feasibility of integration justify the interest and expectations based on this area of research. Abundant reports can be found in literature reporting the fabrication of waveguides in glass [30, 33] and crystals [6, 39], as well as passive devices such as X, Y or three-dimensional couplers or Mach-Zender interferometers [11, 50] with increasingly complex structures. Moreover, active devices based on waveguide inscription in gain substrates such as amplifiers in Nd-doped glass [12] and a laser in Er:Yb glass [35] have been reported.

The advantages of the method (versatility, direct inscription of three-dimensional structure, and simplicity) arise from the possibility of modifying a localised area in the bulk of the material by tight focusing in that region. By translating the substrate highly complex devices such as three dimensional couplers [51], or curved waveguides can be easily inscribed [52], with a set up such as the one proposed in figure 2.4. Another key advantage is that waveguides can be fabricated in materials such as laser crystals or nonlinear crystals in which previously it was not possible to inscribe waveguide structures. The same system can be used for inscription in the different materials just by adjusting the parameters of inscription.

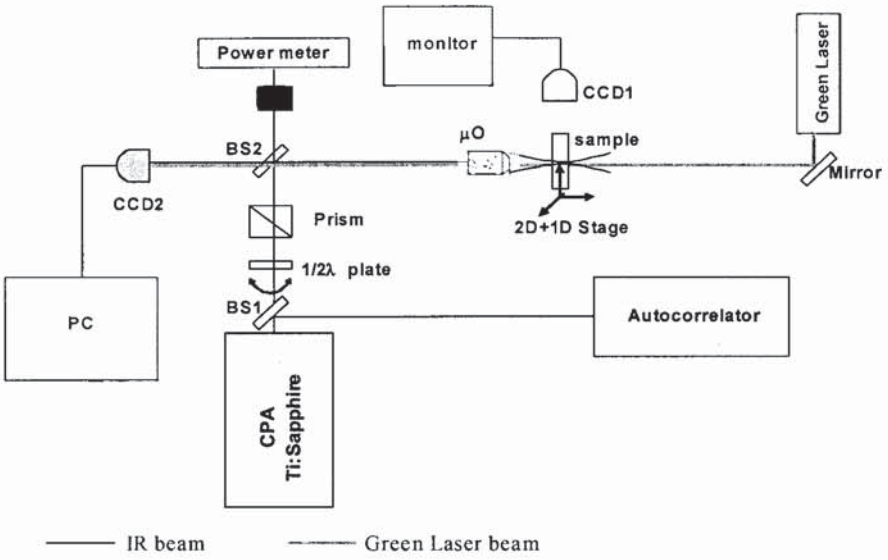

Figure 2.3: Experimental set-up for the inscription of waveguides, used at Aston University. The sample is illuminated using a probe laser beam and two cameras are used for alignment purposes.

Waveguide inscription relies on the formation of positive refractive index modifications. For glass this means that pulse energies must just exceed the threshold for refractive index changes. When energies significantly larger than the threshold energy are used, the modified region presents negative refractive index change [52]. This is generally undesirable for waveguide fabrication. Femtosecond inscription of waveguides can be categorised, as we mentioned in the previous section, depending on the pulse repetition rate. Therefore systems used for fabrication offer either a low repetition rate and high peak powers or high repetition rate and relatively lower peak powers. Systems with intermediate repetition rate (between 100kHz to 300kHz) produce structures similar to those observed for the low repetition rate system, with the advantage of a faster inscription process [4, 49].

In the systems with low repetition rate (lower than 1MHz, and typically between 1kHz and 5kHz) pulse energies are as high as 1mJ, and therefore peak powers of 10GW can be reached. Using this type of system the pulse energy dissipates prior to the arrival of the next pulse, and thus cumulative heating does not influence the properties of the waveguides. In this regime the features are inscribed in the focal region according to the intensity distribution in the area. Therefore the major complication for this technique rises from the geometrical considerations during inscription. In a tightly focused pulse the intensity will be different for the orthogonal and

parallel direction with respect to the axis of propagation. This leads to an ellipsoidal modified region, with the long axis of the ellipse in the direction of the propagation of the beam. In figure 2.5, different possible geometries for inscription are illustrated. Figure 2.5a represents the inscription geometry known as longitudinal where the sample is moved parallel to the direction of propagation of the beam. In this case, the cross-section of the waveguide is intrinsically symmetric; however the length of the waveguides and the flexibility of 3D inscription is severely restricted by the focal length of the objective used for focusing. An additional drawback is the spherical aberration which changes with the focusing depth, and therefore creates a non-uniform waveguide, for this reason the longitudinal geometry is seldom used.

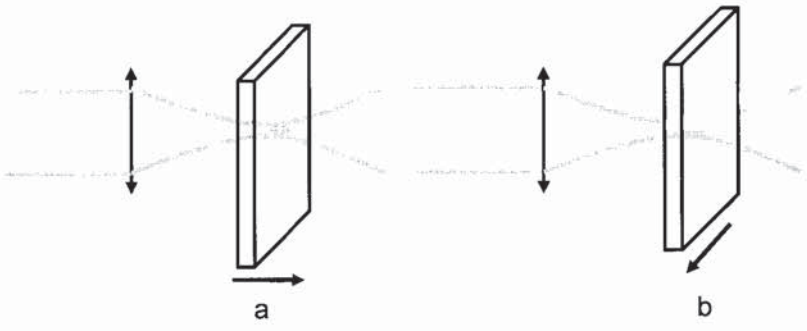

Figure 2.4: (a) longitudinal and (b) transverse geometries for the inscription of waveguides by tightly focused femtosecond lasers.

The perpendicular or transverse configuration is therefore more convenient in order to utilise the three dimensional capability of femtosecond inscription. This method has a major drawback in the ellipticity of the structures it creates as the affected length in the direction of propagation, which can be estimated by the Raleigh length (z_R), is always going to be larger than the affected length perpendicular to the axis of propagation of the beam which can be estimated by the focal radius (ω_o):

$$\omega_0 = \frac{0.61.\lambda}{NA} \tag{2.7}$$

$$z_r = \frac{\pi.\omega_0^2}{\lambda} \tag{2.8}$$

Where λ is the wavelength of the laser and NA is numerical aperture of the microscopic objective. Thus, the waveguides are intrinsically asymmetric, featuring an elliptical cross-

section. Tighter focusing reduces the asymmetry of the inscribed structure, but it does not grant the inscription of symmetric waveguides.

An elegant solution to this problem is using a cylindrical telescope before the microscopic objective [30]. In this method, the beam is astigmatically shaped by changing both the spot sizes in the tangential and sagittal planes and the relative positions of the beam waists. This method allows the inscription of waveguides with a circular cross-section and with arbitrary diameter. A similar solution uses a slit before the focusing lens to shape the beam near the focus and allowing the inscription of cylindrical waveguides [53].

An alternative method uses counteracting nonlinear effects to write waveguides. When a material 'sees' high intensity light, its refractive index changes as a function of the intensity due to the nonlinear refractive index coefficient. This is a well-known effect that can lead to self-focusing. On the other hand, when a material is radiated with high intensities plasma can be created, this has the effect of defocusing the incoming beams. These two effects can be balanced and the result is a filament of plasma, which will alter the refractive index of the area affected leading to narrow waveguides with a refractive index change in the order of 10^{-2} [54].

The shifted multiscan writing technique has been recently demonstrated for laser systems with a repetition rate of 150kHz. This technique produces waveguides with lower insertion losses and polarisation dependent losses by writing waveguide structures in multiple scans with inter-scan shifts of the order of 1.5μm [49, 55]. This technique is in principle applicable for systems with lower repetition rates, however this would lead to a significant increase in the fabrication process duration.

A number of reports illustrate the advantages of writing waveguides with high repetition rate lasers based on extended cavity Ti:Sapphire lasers with repetition rates as high as 25MHz and lower pulse energies [48]. Due to the cumulative effect mentioned in previous sections, the energy from the pulse is distributed in an isotropic manner away from the focal point, leading to the inscription of waveguides with a circular cross-section. The inscription of single-mode waveguides had been demonstrated using high repetition rate lasers. The flexibility of inscription using this type of lasers is lower due to the need for very tight focusing which does restrict flexibility, tight focusing also complicates the inscription process as it is, generally, achieved by oil-immerse microscopic objectives. It is generally accepted that inscription of waveguides by high (over 1MHz) and intermediate (100kHz to 300kHz) repetition rate lasers produces better quality waveguide than low repetition rate systems (up to 5kHz). A further boost to inscription based on cumulative heating, has been given by the recent development of novel femtosecond systems, offering a bridge between low and high repetition laser systems, as well as been more compact, economic and user friendly [33, 35].

Inscription of waveguides have been demonstrated in various glass substrates. Particularly abundant are the reports on fused silica and borosilicates, similar work has also been extended to active glasses such as Erbium-Ytterbium doped phosphate glass [35] and Nd-doped glass [12]. The mechanisms that lead to the refractive index change in these glass materials are similar and have been reported in section 2.3.

More complex is the analysis of the mechanisms that lead to refractive index changes in crystals. Nevertheless and despite initial reservations [11], recent studies on crystalline material such as Cr^{4+}:YAG [39], Ti:Sapphire [6] and Nd:YAG [56] indicate the feasibility of inducing structural changes leading to refractive index changes in crystals. Those reports generally indicate the presence of an area with a negative refractive index change at the focal position surrounded by an area with a positive refractive index change. Such structural changes are believed to rise from the relocation of electronic charges in the defects contained in the crystal [56]. Inscription of waveguides in crystals has been demonstrated by producing a depressed cladding [56]. The core of a waveguide requires higher refractive index than the cladding in order to allow total internal reflection. Depressed cladding waveguides are produced by modifying the area around the core so the negative refractive index induced acts as the cladding, and light propagates in the unmodified area.

Work in polymers has been also prolific and the possibility of creating positive refractive index changes in these materials has been reported in numerous occasions [5]. As in the case of glass materials, the processes that lead to the refractive index changes start with multiphoton absorption, which depending on the polymer can be a two-photon process, leading to reorganisation and densification of the material. In the case of polymers, we have observed that cumulative and thermal effects are relevant events even when low repetition rate laser systems are used for inscription.

Typical values for the propagation losses in waveguides photo-inscribed by femtosecond lasers were in excess of 1dB/cm [49, 55, 57]. As a result of using appropriate laser system and writing set-up this losses have been significantly reduced to levels low as 0.8dB/cm [49], 0.25dB/cm [30] and 0.1dB/cm [58] for different writing configurations. These losses are still higher than observed in waveguides fabricated by conventional technologies such as plasma-enhanced chemical vapour deposition and flame hydrolysis that produce propagation losses of less than 0.05dB/cm [33].

2.5.3 Applications for buried voids and micro-cracks

The properties of a structure inscribed by a tightly focused femtosecond laser are determined by the intensity level reached in the focal region of the laser. Three main regimes of femtosecond inscription can be distinguished, the first one leads to a smooth positive refractive index change structure and it is defined by the intensity threshold for structural changes, the second regime leads to an increased birefringence in the host material [44] and the third regime leads to micro-explosions and the formations of voids in the bulk of the material. The third regime is defined by a second threshold (damage threshold) higher than the threshold for structural changes. By fabricating voids in the bulk of the material numerous photonic devices can be implemented, in particular, the potential for fabricating data storage devices and photonic crystals has been receiving much attention.

Data storage

One of the first applications considered for buried structural modifications in glass photoinduced by a femtosecond laser was in data storage [14]. The discussion of three-dimensional optical storage is analogous to that of three-dimensional waveguide structures and based on the flexibility to produce buried structures in the bulk of transparent materials using infrared ultrafast inscription. Unlike for waveguide devices, the refractive index modification is not required to be positive. Thus, high refractive index contrast is possible by creating micro-voids within the material.

Optical inscription of three-dimensional optical data storage can be achieved by the use of volume holographic techniques [50] or point by point [14]. Femtosecond inscription offers, as well as three-dimensional capability, unique advantages regarding dimensions and refractive index contrast. Inscription with longer pulses offers focusing to micrometer spot sizes, using femtosecond inscription sub-wavelength dimensions are readily available, with such confined focusing bit concentrations as high as 0.8TBits/cm^3 have been demonstrated [50]. Furthermore femtosecond inscription provides a higher refractive index contrast than alternative techniques. This is particularly important considering that the limitations of data-storage technology are based on the data acquisition and reading rather than on the inscription process.

Currently volume data storage is inscribed in special materials such as photo-polymers and photorefractive materials. Using femtosecond inscription opens up the technology to a wide range of materials, including fused silica, quartz and polymers, which may be used as a storage medium allowing for more stable and inexpensive devices. Extensive work towards the

development of holographic techniques using femtosecond lasers both in glass [59] and polymers [5] is currently taking place. Results suggest the advantages previously mentioned of large refractive index contrast and also show the possibility to inscribe structures with periods in the range of tens to hundreds of nanometers [60].

Photonic crystals

Much expectation rests on the ability of photonic crystal technology to provide high levels of integration and performance in the photonics industry. Intense research concentrates on developing and optimising the fabrication of photonic crystals. The inscription of photonic crystals by a femtosecond laser is comparable to the point inscription of data storage devices, and it is in principle a simple and flexible method. However the requirements to create three dimensional structures with photonic band-gap at the required wavelengths are more exigent. As a result, the reservations from the scientific community towards the feasibility of producing photonic crystal fibres with such methods are significant. Concerns are based on whether true photonic band-gaps can be created by femtosecond inscription. Initial requirements include high refractive index contrasts, and high filling ratio (i.e. density of holes).

Despite doubts, initial results indicate weak photonic band gap effects in photonic crystals written in germanium doped silica [13]. Creating three-dimensional photonic crystal structures is an interesting proposition since the nature of the fabrication processes would allow great flexibility. Furthermore the inscription of embedded voids offers high refractive index contrast to produce photonic band gap structures.

2.5.4 Inscription of in-fibre structures

The technology for the inscription of fibre Bragg gratings based on UV inscription is well-established. Using the conventional methods complex devices of high quality can be created, hence there was not an obvious demand for a new method of inscription. Nevertheless, it was identified that femtosecond inscription proposes interesting advantages for the inscription of gratings in fibres.

The maximum refractive index changes achieved by the conventional UV photo-induced gratings are less than 10^{-3} [19], in contrast with changes higher than 10^{-2} for the femtosecond

inscription [9]. Other advantage is that the material in which the grating is going to be inscribed does not need to be photosensitive and therefore it can be written in standard silica fibre, unlike in UV inscription where gratings can only be inscribed in Ge-doped or alternative photosensitive cores. A final advantage is that the refractive index change is not based in the presence of colour centres but other structural changes in the lattice. Thus gratings inscribed by infrared femtosecond laser should be more robust and have longer lifetime than UV-inscribed gratings.

In-fibre inscription by femtosecond lasers was first proposed in 1999 [36]. A long period fibre grating (LPG) was written using infrared radiation. This result demonstrated the feasibility of using this technique, however this long period grating did not present a regular refractive index modulation in the fibre. Therefore it exhibited more complex transmission spectrum and excess losses when compared to conventionally written long period gratings.

Recently, research in the inscription of fibre structures has intensified. Various groups have proposed various fabrication schemes which exploit the characteristic of femtosecond interaction towards the fabrication of novel devices. Inscription of fibre Bragg gratings have been achieved by using various phase mask configurations [15, 37] and point by point configurations [38, 61]. Fibre Bragg gratings with improved or unique performance such as higher thermal stability [19, 62], ultra-low coupling to cladding modes [63] directional sensitivity [64], or inscribed through the coating [65] have been reported.

The main objective of this work was to develop a point by point method for the inscription of fibre Bragg gratings, study the properties of the inscribed devices and apply those properties to the fabrication of novel devices. Chapters 4 to 6 of this work describe the method, analyse the properties of the structures fabricated, and advantages and disadvantages over other techniques.

2.5 Conclusions

This chapter reviewed the most relevant milestones in femtosecond inscription and micromachining. The development of femtosecond lasers towards more cost efficient, simpler and more compact devices is an important factor and as such the latest developments were reviewed. Particularly interesting is the development of high repetition rate femtosecond fibre lasers with great tunability of the repetition rate to suit different requirements.

The interaction between ultrashort laser pulses and the material was described, starting from the highly nonlinear absorption processes and describing how these create localised plasma and a expanding pressure wave that produce the final structural changes. Cumulative heating effects observed in high repetition rates systems are also analysed.

The potential applications, advantages and shortcomings of inscription with such systems are discussed. The great potential of this technology and diversity of applications is a result of the efficient and fast energy deposition in a localised area of the bulk. This leads to minimal thermal and mechanical damage in the surrounding area and gives access to three-dimensional inscription, improved control of the inscribed structures, and applicability to a range of materials which include glasses, crystals and polymers. But despite the advances made since the first demonstrations in 1996, there are still questions to address both from a fundamental an a technological point of view before infrared femtosecond lasers are used to fabricate photonic devices such as waveguides, couplers, or gratings in a commercial environment.

This chapter highlights the great potential for integration and the versatility of ultrafast laser systems so the relevance of the research carried out during the course of this work can be put into context.

CHAPTER 3: Inscription and properties of fibre Bragg gratings

3.1 Introduction

The relevance of fibre optic technology in the telecommunication industry is well-known. It is reasonable to believe that the growth in market presence will consolidate as the technology develops [12]. Fibre Bragg gratings are a key component in this technology, as they have found applications such as selective wavelength filters, wavelength multiplexing or dispersion compensation [17]. Their inherent sensitivity to variations in parameters such as temperature or strain has led to a great deal of research interest [18], if not yet to significant presence in commercial applications as sensors. However, the number of applications is ever increasing with advances in the quality of grating inscription towards highly complex structures, which may be specifically designed to fulfil individual requirements for each application.

The various methods of inscription can be categorised in three major techniques; Interferometric [66], by phase mask [67], and point-by-point [21]. In this chapter, these methods will be described and their merits on flexibility, quality of the device, and stability will be considered. Most methods are based on the photosensitivity of the subject fibre to UV light in order to create a periodic modulation in the refractive index along the fibre core. Unfortunately, the standard fibre preferred for most telecommunication applications is not sufficiently photosensitive to UV light and therefore inscription of strong gratings is not possible. Fibres with higher doping concentrations, or previously photosensitised are used to overcome the low photosensitivity of the standard fibre [68].

As it has been thoroughly detailed in the previous chapter, during the last decade considerable advances have been made in the use of infrared femtosecond light to manufacture photonic devices in materials similar to those of an optical fibre. Femtosecond inscription has been recently applied to fibre Bragg grating fabrication using analogous techniques to those previously applied to UV sources. The advantages and disadvantages of applying infrared femtosecond inscription will be only briefly introduced in this chapter since it will be the sole subject of investigation in chapters 4 to 6.

3.2 Bragg Grating Characteristics

The characteristics of fibre Bragg gratings have been thoroughly explored in literature [19], the intention of this section is to provide a broad understanding of the physics involved in the operation of these devices and to introduce the most relevant properties of standard gratings considering the scope of this work.

3.2.1 Basic Bragg grating theory

A fibre Bragg grating consists of a periodic modulation of the refractive index in the core of an optical fibre. Light guided along the core is scattered by each grating plane, should the Bragg condition not be satisfy the reflected light will progressively be out of phase until it is cancelled out. When the Bragg condition is satisfied, the reflected light from each grating plane experiences a constructive interference in the backward direction with the reflected light from other grating planes. This forms a back-reflected peak with a central wavelength determined by the grating parameters. The working concept of a fibre Bragg grating is illustrated in figure 3.1.

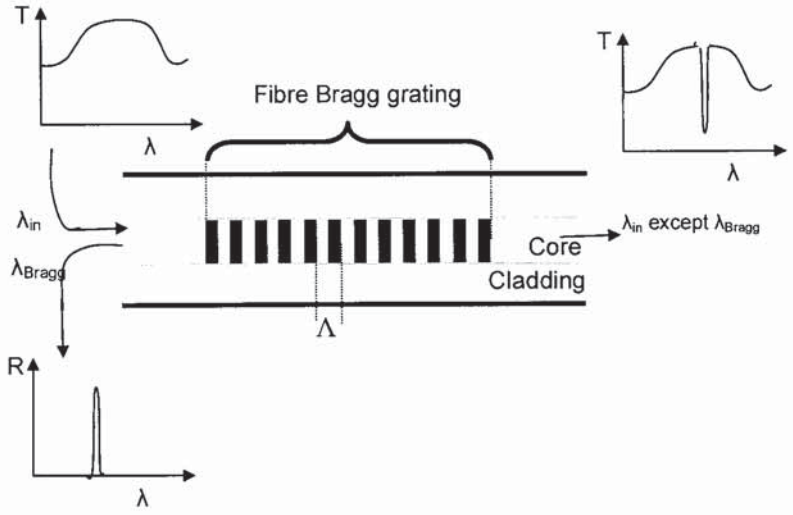

Figure 3.1: Structure of a uniform fibre Bragg grating inscribed in the core of the fibre. T stands for Transmission, R for reflection, λ_{Bragg} is the resonant wavelength and Λ is the pitch of the grating.

A detailed description of the coupling of counter propagating modes in fibre Bragg gratings is not given in this work, various highly effective models have been proposed for the quantitative study of Bragg gratings, with the coupled mode theory been the most widely used [69]. In this section, a brief qualitative explanation of the concepts involved in the fibre Bragg grating operation is given, leading to the basic Bragg condition [70]. A fibre grating is simply an optical diffraction grating, it is therefore possible to describe its effect over the incident light following the standard grating equation [71], equation 3.1;

$$n \sin \theta_2 = n \sin \theta_1 + N \frac{\lambda}{\Lambda} \tag{3.1}$$

where θ_2 is the angle of the diffracted wave, θ_1 is the incident angle, n is the refractive index of the propagating media, λ is the wavelength of the light source, Λ is the pitch of the grating and N is an integer that determines the diffraction order. We shall consider the case in which the diffracted wave has the same angle but opposite direction of propagation than the incident wave. These conditions lead to constructive interference between the incident and diffracted waves, $\theta_2 = -\theta_1$.

In order to simplify equation 3.1, we will introduce the mode propagation constant, β for a wave travelling through a fibre grating as equation 3.2;

$$\beta = \frac{2\pi}{\lambda} n_{eff}$$

where

$$n_{eff} = n_{co} \sin \theta \tag{3.2}$$

It is therefore possible for this case to rewrite equation 3.1 as follows in equation 3.3;

$$\beta_2 = \beta_1 + N \frac{2\pi}{\Lambda} \tag{3.3}$$

Since we are assuming that both modes propagate in opposite direction, it is evident that their mode propagation constants would be of opposite sign, using equation 3.3, it is possible to calculate that the resonant wavelength for reflection from a mode of index $n_{eff,1}$ into a mode of index $n_{eff,2}$ in a grating with a pitch Λ as described by equation 3.4;

$$\lambda = (n_{eff,1} + n_{eff,2}) \frac{\Lambda}{N} \tag{3.4}$$

We are considering the case for fibre Bragg gratings with both modes propagating through the core, and thus $n_{eff,1}=n_{eff,2}$. This further simplifies equation 3.4 to leave the Nth order Bragg condition, equation 3.5;

$$\lambda_B = 2n_{eff}\frac{\Lambda_N}{N} \tag{3.5}$$

Where λ_B, stands for resonant wavelength, n_{eff} is the effective refractive index of the fibre core, N is the Bragg order and Λ_N is the grating pitch. Standard fabrication techniques commonly inscribe first order grating, since it does not propose significant technological complications, and generates stronger reflections for gratings of equal lengths. This is so not only because the number of grating pitches is higher but also because the coherence between counter-propagating modes is higher.

Since the ultimate purpose of this work is not to embark into a fundamental discussion on fibre grating theory, but to highlight the advantages and applications of a novel method of inscription, the relevant parameters in reflectivity and linewidth of standard uniform gratings will be mentioned without further analysis.

At the Bragg grating resonant wavelength, the reflectivity, R, is dependent primarily in two parameters, the length of the grating, l, and its refractive index modulation, Δn, as either of these parameters increases, the reflectivity at the resonant wavelength increases. The complete expression is described by equation 3.6 [69];

$$R(l,\lambda) = \tanh^2\left(\frac{\pi\Delta n\eta(V)}{\lambda}l\right) \tag{3.6}$$

where $\eta(V)$ is a function of the fibre that indicates the level of confinement of the fundamental mode within the core.

An expression indicating the full width at half maximum bandwidth, $\Delta\lambda$, is given in equation 3.7, indicating that the linewidth of the reflection broadens with increasing refractive index modulation, Δn, and narrows down with an increasing number of grating planes, M, and hence grating length [69];

$$\Delta\lambda = \lambda_B\,\alpha\sqrt{\left(\frac{\Delta n}{2n_o}\right)^2 + \left(\frac{1}{M}\right)^2} \tag{3.7}$$

where the parameter α is ~1 for strong gratings and ~0.5 for weak gratings.

From equation 3.7, it is evident, that for high refractive index modulation the resonant wavelength is strongly reflected in the first few grating planes, and even if the grating is long the latter part of the grating does not contribute to the reflection, leading to a broader spectrum. Narrow strong gratings must be inscribed by longer gratings with lower refractive index modulations. The transmission and reflection spectrum profile of a standard uniform grating is shown in figure 3.2 for illustration. This grating was inscribed by a continuous wave (CW) UV laser in hydrogenated fibre by a phase mask[1]. The spectral profile for gratings inscribed by other UV methods or in doped fibres does not differ significantly from the one shown in figure 3.2.

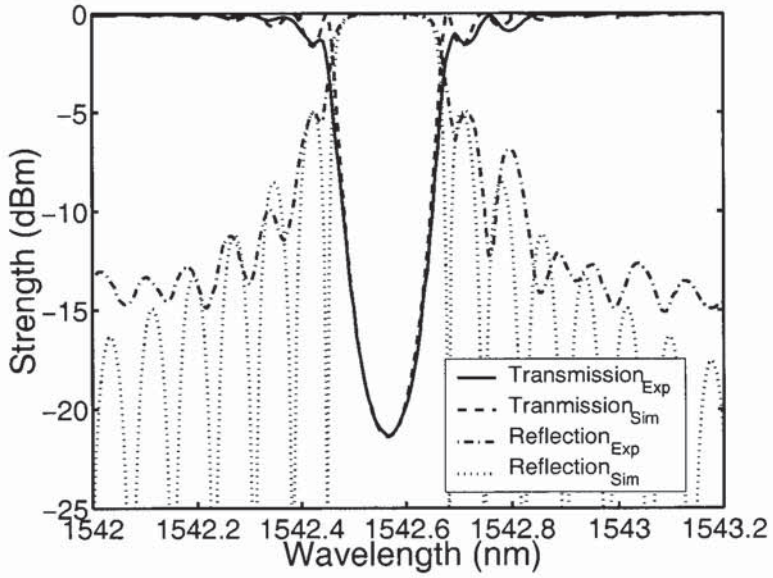

Figure 3.2 Transmission and reflection spectrum of a standard uniform grating, simulated and experimental result [courtesy of PC Won].

3.2.2 Types of UV inscribed fibre Bragg gratings

Gratings inscribed by UV light can be classified according to the physical properties of the structural changes induced in the fibre. Therefore, UV inscribed gratings may be classified in three major types of gratings [19, 68]; type I gratings which consist of positive refractive index changes induced by a pulsed or CW laser and grow linearly until saturation, type IIA which present a negative refractive index change and appear after overexposing for a certain amount of time a type I grating, and a third type of fibre Bragg grating, known as type II, appears after

[1] UV- inscribed fibre Bragg gratings were fabricated by Rachel Won at the Photonics Research Group, Aston University.

irradiation by a high power, pulsed UV laser, such as an excimer laser. These gratings, also known as damage gratings, produce very large refractive index modifications of up to 10^{-2}. Their spectral behaviour is significantly different from the other two types of gratings, with a very broad reflection band, and a transmission band in which the wavelengths lower than the resonant wavelengths are coupled to the cladding and greatly attenuated [72].

Type I gratings are commonly inscribed in germanium doped gratings with concentration levels in the order of 10mol%, although they can be also inscribed in highly doped fibres. Hydrogenation is a technique often used to increase the photosensitivity of fibres with low or no dopants [19, 68]. This technique, briefly introduced in the following section, allows the possibility of inscribing type I gratings in fibres with low concentrations of dopants. Type IIA gratings are inscribed in highly doped fibre (~30mol%) and appear after overexposing a type I grating. The initial grating is photo-annealed and disappears, a second reflection peak appears product of the negative refractive index modulation. Hydrogenated fibre prevents the formation of type IIA gratings [73]. A fourth type of gratings, known as type IA grating has been recently demonstrated [74], which raises from the overexposure of hydrogenated type I gratings. Despite the similarities in the method of inscription with type IIA gratings, their behaviour during fabrication and thermal stability indicates that the mechanisms that lead to the creation of type IA and type IIA are fundamentally different.

3.2.3 Photosensitivity of fibres to UV sources

The discussion on photosensitivity and the processes that lead to refractive index changes is complex due to the number of parameters that must be taken into consideration. The characteristics of the region modified by UV light are different depending on the composition of the fibre, photosensitisation treatments and laser parameters such as the wavelength, energy of the source, and whether the laser emits CW or pulsed radiation.

Photosensitivity of fibres has been studied for a number of dopants and concentration levels. Reports evidence that undoped, pure silica core fibre and lightly doped, standard fibre for telecom applications (~3mol% Germanium doped) are not sufficiently photosensitive to allow the inscription of gratings, refractive index changes induced in such fibres do not exceed 10^{-6}. Doping with various elements has proved to increase the photosensitivity of the fibre, particularly relevant due to the wide use of this type of fibres and their compatibility with telecommunication and sensing systems are the Ge-doped fibres.

Fibres with concentrations of Germanium over 10mol% are efficient hosts for the inscription of fibre gratings, various other doping combinations have been proposed which will not be

discussed here [19]. A widely used alternative method to increase the photosensitive of fibres is hydrogenation. By immersing a fibre in a hydrogen gas at pressures from 20atm to more than 750atm, but typically around 150atm, hydrogen molecules diffuse into the fibre core. Hydrogen loading increases the photosensitivity of the fibre to the level of allowing refractive index changes of up to 0.01. After inscription the hydrogen diffuses out of the fibre, leaving negligible absorption losses.

Two mechanisms are generally considered to be responsible for the refractive index change of the material, colour centre formation and compaction. Colour centre formation is generally considered the main contributor for refractive index changes in doped fibres and hydrogenated fibres. In Germanium doped fibres the process is photochemical and relies on the presence of defects such as the so-called Ge-Si and Ge-Ge wrong bonds. These defects have an absorption band at approximately 240nm, the UV light therefore easily ionises the bonds to form Ge(1), Ge(2) and GeE' centres. The presence of these colour centres leads to a higher refractive index.

Introducing hydrogen in the fibre leads to the formation of OH absorbing species and this improves the absorption of UV light. The mechanism responsible for the refractive index change is believed to be a result of thermally driven reactions which create germanium-oxygen deficiency centres Ge-O, Si-O and Ge-OH defects [19].

The compaction model postulates that the refractive index change is a product of densification after prolonged exposure of the fibre to UV light. Densification may rise from a number of microscopic mechanism in which the structure of the glass is modified, such as a phase transformation, a change in polymerisation of the glass or a change of coordination, depending on the wavelength and intensity of the laser used for inscription of the grating [69].

The process that leads to the creation of type II gratings starts by high single photon absorption of the UV light. Absorption excites the electrons into the conduction band of silica, this leads to the formation of a highly absorbent electron plasma which leads to mechanical damage in the structure [69], similar in nature to the process for long pulse micro-structuring described in chapter 2.

3.2.4 Thermal properties of fibre Bragg gratings

One of the major drawbacks of fibre Bragg gratings is their low thermal stability. Some of the species responsible for the refractive index modification, such as colour centres, tend to

recombine at relatively low temperatures. This annealing process must be understood and controlled in order to ensure a stable performance through the work life of the device.

Thermal stability depends largely on the type of grating and on the fibre in which it has been inscribed. Type I gratings exhibit the lowest thermal stability, while type II gratings are the most thermally robust, type IIA gratings decay at a temperature between the erasure temperatures of type I and type II.

Reports indicate that type I Bragg gratings are more thermally stable when inscribed in unloaded fibre, this is the case particularly for temperatures below 400°C. For temperatures above 400°C the decay tends to be equivalent for both types of grating. The difference in thermal stability evidently rises from the different properties of the species that lead to the index change for hydrogenated and unloaded fibre. This point will not be discussed in this work [75].

Reports in literature indicate that type IIA gratings are stable up to 300°C. They are completely annealed at temperatures of the order of 500°C in less than 20 hours [76]. This indicates a slight improvement in the thermal stability of the type IIA gratings with respect to type I. Type II gratings [72] are stable at 800°C and are at 1000°C erased completely in less than 5 hours. The stability of these gratings offers evidently a significant improvement over the other types. However, these gratings do not have the required spectral properties to replace standard gratings in most applications. Type IA gratings are fabricated in a similar way than type IIA gratings, with the exception of been inscribed in hydrogenated fibre. Unlike type IIA gratings, their thermal stability is lower than type I gratings, their thermal behaviour is also fundamentally different to type I gratings, and this property has been used to produce dual thermal-strain sensors [77]. It must be pointed out that reports in literature agree in general terms on the behaviour of the different types of gratings but discrepancies are found on the actual limiting temperatures for stability and erasure.

Plausible methods have been proposed to improve the thermal stability of type I or IIA gratings. Those include the inscription in Sb-Ge codoped photosensitive fibre which allows the inscription of gratings stable up to temperatures of 400°C, and it is only fully erased at temperatures over 800°C [78], Tin doped fibre [79] or antimony-erbium-germanium (Sb-Er-Ge) codoped fibres, which are stable up to 800°C.

Fast decay at high temperatures is not the only issue to consider when inscribing a grating. Thermal stability is fundamental to the reliability of the device since UV-inscribed gratings slowly decay at low temperatures even at room temperature. This leads to a constant change in the properties of the gratings that lead to inaccurate performance particularly in telecommunication and fibre laser applications. Pre-annealing has been proposed and it is wide used as a solution for decay at low temperatures. The process, also referred as accelerated aging consists on subjecting the grating for a limited period of time to a temperature higher than it is expected to

be operating through its lifetime. The annealing process erase the features responsible for the refractive index change that would decay over the life time of the device, leaving out only the very stable part of the refractive index change. Pre-annealing allows an improved performance of the device but in no way improves the thermal stability at higher temperatures [20].

As it will be extensively cover in this work, stability of gratings inscribed by femtosecond lasers offer a thermal stability superior to that reported in any type of UV inscribed grating, whether type I, type IIA or type II.

3.3 Methods of inscription

The inscription of fibre Bragg gratings, was first demonstrated after launching a laser beam of high intensity with central emission at 488nm into a Ge-doped fibre [80]. A periodic structure was formed in the glass because the back-reflections from the cleaved end-facet generated a standing wave pattern that created a permanent refractive index modulation along the fibre. Despite the potential of such devices, it was the development of the side exposure techniques [66, 81] that truly incited the interest of the research community in this type of devices. Side-exposure provided greater flexibility and hence applicability to the technology.

Side exposure fabrication techniques can be categorised into three major groups; holographic [66], those using phase mask [67] and a third method consisting on inscribing the periodic structure point by point [21]. The use of the point by point inscription with UV light has been mainly restricted to the inscription of long period gratings since this method has been unable to deliver high quality gratings.

3.3.1 Interferometric fabrication techniques

First introduced in 1989 [66], the holographic technique was the first proposed method for side-inscription of gratings. The beam of a UV source is separated in two beams of equal intensities, which later are made to interfere in the fibre as illustrated in figure 3.2. The interference fringe pattern produces a refractive index modulation confined to the core, since it is the only photosensitive part of the fibre. The resonant frequency is a function of the wavelength of the UV source used for inscription, λ_{UV}, and the angle between the two interfering beams, θ, and described by equation 3.8;

$$\lambda_{FBG} = \frac{n \cdot \lambda_{UV}}{\sin\theta} \tag{3.8}$$

As it is implied by equation 3.8, resonant wavelengths can be selected by adjusting the angle of incidence, this is an important advantage compared to the phase-mask techniques which will be introduced later in this section.

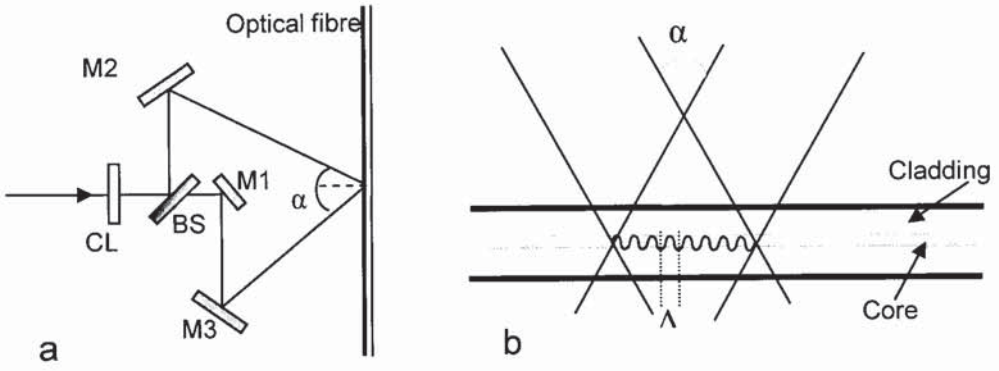

Figure 3.3: (a) Illustration of the basic holographic set-up for the inscription of fibre Bragg gratings, where CL stands for cylindrical lens, BS for beam splitter and M stands for mirror. (b) Close up at the interference pattern in the core of the fibre where Λ is the grating pitch and α is the interference angle, adapted from [16].

The configuration in figure 3.3, represents the basic holographic set-up, a third mirror is included to allow both beams to experience the same number of reflections prior to their interference, and therefore avoiding lateral inversion of the wavefronts, which would results in a reduction of the fringe visibility and therefore in the performance of the grating. This mirror is not required for UV sources with high wavefront symmetry.

Despite the flexibility that this method offers to select parameters such as length or resonant frequency of the grating, its set up is highly sensitive to the surrounding environment. Vibrations, submicron displacements in any of the optical components, air flows and poor laser stability, can significantly reduce the quality of the grating by affecting the fringe pattern. Thus, technical requirements to produce high quality gratings with this technique are very high. Other interferometric approaches such as prism [82] or Lloyd interferometers [83] have lower susceptibility to environmental variations; this however comes at a cost in allowed grating lengths and wavelength tunability.

A holographic set-up using an infrared femtosecond laser presents additional difficulties due to the low temporal coherence of femtosecond pulses. Nevertheless, and thus there are no reports of in-fibre inscription of gratings with a holographic set-up and infrared femtosecond lasers, interferometric inscription of gratings in planar substrates has been demonstrated in numerous occasions [5, 42, 60].

3.3.2 Phase-mask techniques

Diffractive methods using a phase mask have been the preferred method for inscription since they were first introduced in 1993 [67]. This is due to the stability requirements for the inscription of gratings, which are lower for phase mask techniques than for holographic methods. The diffractive method uses a phase mask to diffract the incident beam into several orders, a phase-mask is a periodic relief grating etched in a fused silica plate, ideally this grating diffracts the incident beam suppressing the zeroth order and transmitting most of the power through the +1 and -1 order beams only. The grating is inscribed by placing the fibre in the near field pattern created by the interference of +1 and -1 diffraction orders as it can be seen in figure 3.4.

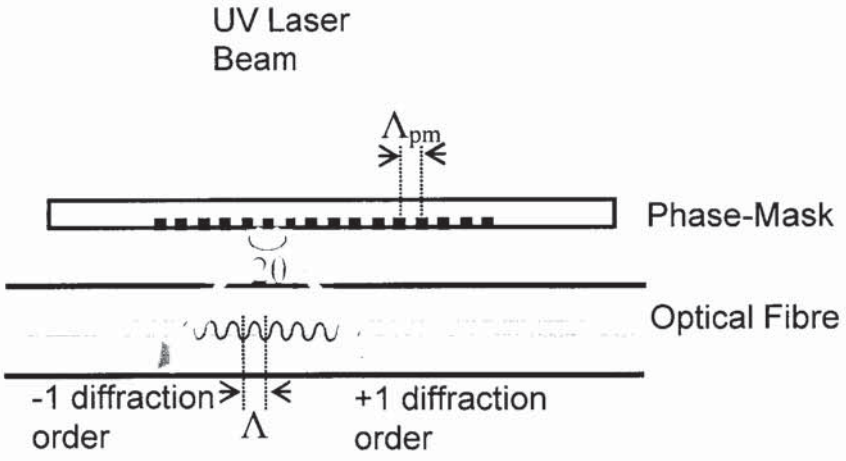

Figure 3.4: Diffractive technique for the inscription of fibre Bragg gratings. Λ_{PM} correspond to the period of the phase mask and Λ is the period of the inscribed grating.

The grating pitch inscribed in the fibre core is given by equation 3.9;

$$\Lambda_{FBG} = \frac{\lambda_{UV}}{2\sin(\theta)} = \frac{\Lambda_{pm}}{2} \tag{3.9}$$

Where Λ_{FBG} is the pitch of the grating inscribed in the core, λ_{UV} is the wavelength of the laser source used for inscription, θ is the angle of first order diffraction, and Λ_{pm} is the phase-mask period.

A further relevant parameter for phase mask fabrication is the corrugation depth, d, given by equation 3.10;

$$d = \frac{\lambda_{UV}}{2(n_{s(UV)} - 1)} \tag{3.10}$$

where λ_{UV} is the wavelength of emission of the laser used for inscription, and $n_{s(UV)}$ is the refractive index of the phase mask. The level of suppression of the 0^{th} diffracted order and the percentage of transmitted power into the first diffraction orders depend on this parameter.

Phase mask inscription offers a number of advantages, such as low system requirements, great reproducibility, and the possibility of introducing special periodic structures by changing the periodicity of the phase-mask. Demonstration of long Bragg grating inscription has also been reported using phase-mask, by translating the UV beam along the fixed phase mask and fibre or translating the fibre and phase-mask across the fixed beam, allowing therefore the inscription of gratings of lengths proportional to the length of the phase mask used [84-85]. The most significant disadvantage of the diffractive techniques rises from the need of a separate phase mask for each Bragg wavelength. Methods such as using a lens before the phase-mask [86] or stretching the fibre [87] partly reduce the problem by allowing a tuning range of approximately 2.5nm.

Phase-mask methods have been used in conjunction with femtosecond laser to fabricate Bragg gratings. One method uses an infrared source and a specially designed phase-mask for infrared light [15] while the other uses a standard phase-mask with an ultrafast UV laser emitting 220fs-long pulses at a central wavelength of 264nm [37].

The nature of femtosecond pulses presents a problem for phase-mask inscription since high angular dispersion may be induced by the mask due to the broad spectrum of the pulse, reducing the fringe visibility and consequently the quality of the grating. A solution for angular dispersion is using higher order phase masks [15]. Both the mask and the fibre are made out of similar materials, and thus, have similar threshold levels. Thus, focusing in the phase mask must be avoided as this would damage it. In addition to allowing inscription in non-photosensitive materials and producing high quality gratings, devices inscribed by this method have shown high resistance under hostile environments, desirable for sensing applications [15, 62].

3.3.3 Point-by-point techniques

Point-by-point fabrication is based on the inscription of one grating pitch at a time. Therefore it offers a number of distinctive advantages such as great flexibility to inscribe gratings with any periodicity and length. In principle, it is also possible to inscribe highly complex structures, since the induce refractive index modification and pitch period can be altered for each grating pitch. This level of control is unattainable by either the diffractive or the holographic method.

Despite its potential advantages, the point by point method is rarely used in UV inscription, mainly considered only for the inscription of long period gratings. Very long process times, complex alignment and errors in the grating periodicity due to thermal and strain changes in the fibre have allowed only the inscription of weak gratings of low quality [21].

Inscription by femtosecond radiation offers distinctive advantages when using the point-by-point method, since the high nonlinearity of the absorption process leads to highly localised modified regions and small features allow the inscription of gratings with lower periods. Chapter 4 introduces a novel point-by-point inscription method based on tightly focused infrared femtosecond pulses that contrary to previously reported methods allows fast inscription of high quality gratings while preserving the advantages previously mention for this type of inscription. Another point-by-point method for the inscription of gratings has been proposed in literature based on an infrared femtosecond laser [61], using this method maximum reflections achieved were around 30%, low reflection was due to; the use of higher order gratings with a 2.1μm pitch, and long processing times with low grating lengths.

3.4 Types of grating structures

The standard fibre Bragg grating consists on a uniform periodic modification along the fibre core. This type of grating has a spectral reflection centre at a resonant wavelength given by equation 3.5, the peak reflectivity and linewidth are given by equations 3.6 and 3.7. The presence of side lobs in the reflection spectra is a feature of uniform gratings. This may be detrimental for the performance of the device for some applications. Modifications in the structure of the grating to reduce the side lobs or to pattern the spectral profile are often used to fulfil the particular requirements for each application.

Apodised gratings are non-uniform grating structures produced in order to reduce or suppress the side-lobs. An apodised grating consist of a grating with constant pitch periodicity and a refractive index modulation which gradually increases towards the centre of the grating. This technique allows reducing the side-lobs below -30dB from resonant reflection. Apodisation is more effective if the effective refractive index along the grating is constant and only the refractive modulation varies.

Chirped Bragg gratings are devices with a non-uniform period along their length. The spectral reflection and transmission of these gratings present broad bandwidths which can be over 10 nm depending on length and chirp rate. These gratings have found multiple applications in areas such as dispersion compensation in telecommunications [88] and distributed sensing [89].

In figure 3.5, the typical transmission and reflection spectra of an apodised and chirped gratings are illustrated.

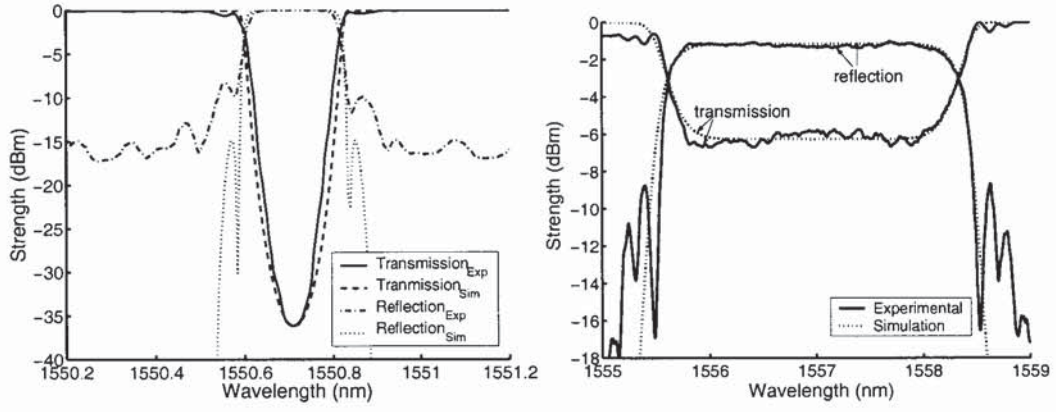

Figure 3.5: Spectral characteristics of various grating structures, (a) apodised and (b) chirped.

By introducing a phase shift across the fibre grating, two gratings out of phase with each other are in effect produced. These two gratings create a narrow resonator that is characterised by a very narrow transmission band. Phase shift gratings are particularly relevant in the field of fibre lasers, in particular, distributed feedback (DFB) lasers which consist of a phase shift grating inscribed in active fibre. DFB lasers are for many applications the preferred fibre laser configuration due to their very narrow single-mode lasing, tunability, and compactness [90]. Phase shift gratings are also commonly used as very narrow transmission filters, which consist essentially on a narrow band-pass filter with a relatively narrow stop-band outside, concatenate phase shifts lead to the creation of a multiple band-pass filter [91].

In a blazed or tilted grating, the grating planes are at an angle with respect to the fibre axes this leads to coupling out of the fibre the propagating mode. The angle at which light emerge from the core is dependent on the wavelength and mode. These devices have been used in applications such as; gain flattening of erbium doped amplifiers (EDFA) [92], as mode-converters and for interrogation schemes in sensing [93]

3.5 Applications of fibre Bragg grating

Fibre Bragg gratings have become rapidly a key component in a wide variety of components particularly in the fields of communications and sensing. Chapters 5 and 6 will look in detail to a number of these applications, particularly in sensing and the fabrication of fibre lasers. This section offers a brief summary of the possibilities and applications of fibre Bragg gratings.

3.5.1 Applications in communications

Fibre Bragg gratings offer a number of unique advantages for optical communications. Their filtering capability and intrinsic integration in the fibre system has lead to its use as an integral part in fibre lasers, optical amplifiers, wavelength division multiplexing, add-drop filters, gain flatteners and dispersion compensators [19].

Filtering is one of the most natural applications for fibre Bragg gratings, numerous configurations have been proposed to suit different requirements, particularly relevant are the interferometric band-pass filter and filters based in bulk optics circulators both made by uniform or apodised gratings and used as add-drop filters. The importance of these configurations rises from their suitability to perform as wavelength division multiplexers/demultiplexers [94]. Demonstration of dense wavelength division multiplexing has been achieved using a combination of the two configurations [95]. Various other grating devices such as Moiré gratings, phase shifted gratings, grating-based Fabry-Perot filters or long period grating also operate as filters and will be introduced in the context of this work.

Optical amplifiers are a key component for long-haul optical communications, two configurations are generally considered either based on amplification by erbium-doped fibre or by Raman amplification. The efficiency of erbium doped fibre amplifiers can be significantly improved by adding a highly reflective grating after the erbium-doped fibre [17]. Various amplifier configurations have been proposed, either reflecting the pump, the signal or both in order to enhance the performance of the device. Fibre Bragg gratings have also been used as gain flatteners, this is a key function in fibre communications since erbium-doped fibre amplifiers present an uneven gain profile, by introducing a long period grating or a blazed grating the uneven gain can be corrected.

Dispersion is a key limiting factor for long-haul optical communications, evermore pressing as the bit rate demand increases. Dispersion compensation is achieved by using linearly chirped gratings which reflect the different wavelengths that constitute the pulse at different positions. By using a chirped grating with the required chirp and direction broadening of the pulse is compensated [96]. This technique can also be used to stretch and compress the pulse for in-fibre chirped pulse amplification, which may be applicable to the fabrication of short-pulse fibre lasers.

3.5.2 Applications in sensing

Fibre Bragg gratings are excellent sensors. The principal advantage is that the measurand information is acquired from the analysis of the shift on the resonant wavelength. Fibre Bragg gratings are therefore self-referencing and independent on fluctuation in the light source levels or losses within the system. Fibre sensors also offer distinct advantages such as truly remote and distributed sensing, electrically passive operation, electromagnetic interference (EMI) immunity, high sensitivity, and multiplexing capabilities, allowing real-time sensing with improved safety conditions [18]. Smart materials are structures in which distributed gratings have been embedded. With these structures, various parameters such as load, strain, temperature and vibration can be monitored in real-time.

A wide variety of parameters can be measured by grating structures; including temperature, strain, pressure, refractive index of the surrounding area or bending. A general overview of sensing applications for fibre Bragg gratings is given here, whereas chapter 5 offers an in-depth look at various sensing devices related to this work. Sensing applications based on Bragg gratings generally operate by the simple concept of monitoring a wavelength shift dependent on a given parameter. Sensing has been targeted as one of the key commercial applications in fibre technology despite competing with more established technologies such as electromechanical sensor systems [18]. To date they are still only a very small market compared to that of fibres in communications.

As we mentioned above, fibre gratings are intrinsically sensing elements, changes in the properties of the fibre such as; effective index of refraction and spacing between grating planes give rise to shifts in the resonant wavelength. These changes may rise from variations in temperature, pressure or strain causing a quantitative shift independent on any other parameter of the system.

The flexibility of inscription allows tailoring the structures in accordance to the parameters and geometries of interest. It is therefore possible to apply the same concepts to measure a range of

parameters from chemical composition to pressure. The main drawback for grating sensors is the ambiguity of the wavelength changes that may have arisen from variations from different parameters. A number of configurations have been proposed in order to discern between measurands, long period gratings, which are discussed in the following section, have demonstrated to be particularly effective for this purpose [18]. A further disadvantage is that despite the inexpensive nature of fibre gratings, the interrogation system for sensing applications have often increased the cost of the system and reduced their applicability.

Configurations such as chirped gratings for distributed sensing [89], long period gratings for bending and simultaneous measurements of various parameters [97-99], fibre lasers for increased resolution or Blazed gratings used for interrogation [99] are commonly applied to suit the requirements of the application.

3.6 Long Period Gratings

Fibre Bragg grating operate by creating a refractive index modulation that leads to constructive interference between counter propagating core modes, Long period gratings on the other hand operate by promoting coupling between the co-propagating core and cladding modes. An alternative to fibre Bragg gratings for a number of applications, the first report of long period gratings appeared in 1995. The spectral characteristic of these devices has lead to their use in a number of applications such as band rejection filters [100], gain flatteners in fibre amplifiers [101] and fibre sensing [97]. Light propagating in the cladding suffers high attenuation, the spectral profile at transmission of a long period grating presents a series of attenuation bands at discrete wavelengths, each attenuation corresponds to the coupling to a different cladding mode. Unlike fibre Bragg gratings this type of devices do not reflect any component of the incident signal. The light from the attenuation bands dissipates through the cladding boundaries. The typical spectral characteristics at transmission of a long period grating are illustrated in figure 3.6.

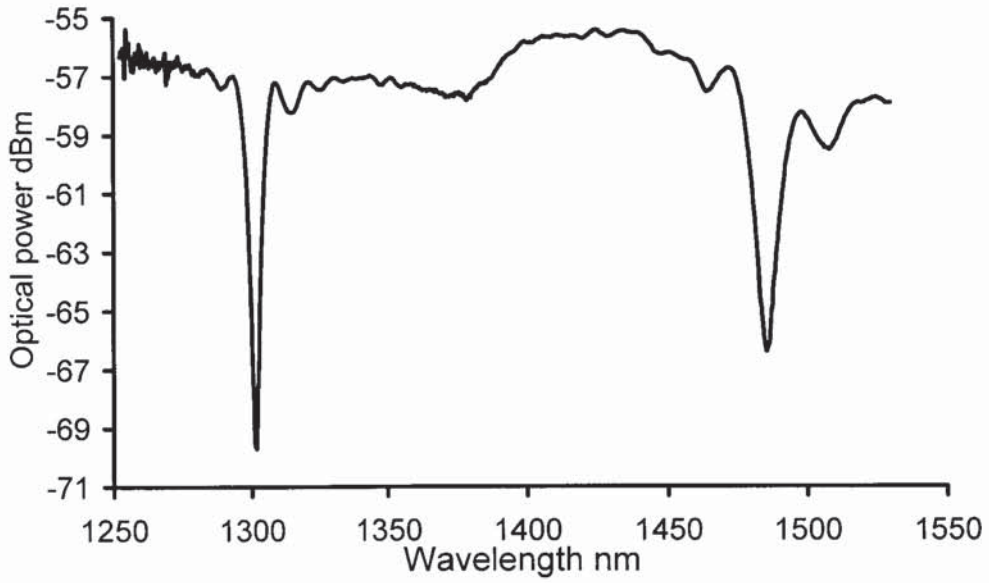

Figure 3.6: Spectral characteristics at transmission of a long period grating.

3.6.1 Basic concept of long period theory

In order to give an equivalent analysis to long period grating to that given in section 3.2.1 to fibre Bragg grating [69], we can reconsider, equation 3.11;

$$\beta_2 = \beta_1 + \frac{2\pi}{\Lambda} \tag{3.11}$$

In this case, β_2 is the mode propagation constant for a given mode confined in the cladding, and β_1 is the mode propagation constant of the wave travelling through the core unlike the case considered in section 3.2.1, both modes are travelling in identical direction and therefore they have equal sign, leading to equation 3.12;

$$\lambda = (n_{eff,1} - n^{i}_{eff,2})\Lambda \tag{3.12}$$

The interaction in this case is between two modes propagating in different media, therefore $n_{eff,1}<n_{eff,2}$. Comparing equation 3.4, and 3.10 it is possible to conclude that for coupling to the cladding the grating pitch required must be much larger.

The cladding is large compared to the core; it therefore supports a large number of modes with different propagation constants, many of which may meet the condition of equation 3.10. In order to have efficient coupling between modes it is also important for their electric field profiles to overlap, this means that coupling is only efficient between the core modes and circularly symmetric odd order modes [97].

Long period gratings have periods typically in the range between 100μm and 1mm. The spectral characteristics of a given grating depend on the length, period and refractive index modification of the device as well as on the local environment. Properties that affect the spectral characteristics include temperature, strain, bend radius, and refractive index of the surrounding medium.

The fabrication of long period gratings is less demanding that the fabrication of fibre Bragg grating. The larger periodicity allows for the inscription of these devices using many alternative methods to the standard UV lasers. Reported alternative methods include irradiation by CO_2 lasers [102] diffusion of dopands in the core [103], relaxation of mechanical stress [104] and electrical discharges [105].

3.6.2 Applications of long period grating

Long period gratings have found numerous applications in the field of sensing. The use of these devices is advantageous over the use of fibre Bragg gratings in various ways. Long period gratings present improved sensitivity compared to Bragg gratings to variations in parameters such as temperature or strain. Other parameters to which Bragg gratings are insensitive can be monitor with long period gratings such as bend radius or refractive index of the surrounding material. A further advantage is the possibility of tailoring the sensitivity to a given parameter during fabrication by appropriate choice of period, refractive index change and length; this solves the ambiguities that rise when analysing the wavelength shifts in fibre Bragg gratings.

A long period grating has different sensitivity depending on the attenuation band. It is therefore suitable as multi-parameter sensor, where different attenuation bands are sensitive to a given parameter but not to other parameters. Chirped long period gratings are also extensively used as band rejection filters [100], due to their large spectral profile and transmission characteristics, and as gain flatteners in erbium doped amplifiers [101].

3.7 Conclusions

This chapter outlined the principal characteristics of fibre Bragg gratings and long period gratings inscribed by UV methods. Priority was given to those characteristics which will be studied in this work and will be compared to gratings inscribed by femtosecond lasers in the following chapters; such as the thermal properties of the different types of grating structures and the mechanisms that lead to refractive index change. The inscription methods most commonly adopted were described and their relative merits compared.

The major applications of both types of fibre gratings were introduced in order to highlight the importance of this type of devices in the context of optical fibre technology, both for sensing applications and for telecommunications. The following chapters will concentrate on the properties of femtosecond inscribed gratings; particularly those inscribed point-by-point. We will also introduce applications in which the use of these gratings may be advantageous and novel applications which are only feasible using gratings inscribed point by point by an infrared femtosecond laser.

CHAPTER 4: Point-by-point inscription of fibre Bragg gratings using an infrared femtosecond laser

4.1 Introduction

The basic properties and main applications of fibre Bragg gratings have been outlined in chapter 3. Most inscription methods are based on refractive index modulations induced by UV sources. Judging by the wide range of commercial applications based on UV-based inscription and the high quality of structures inscribed, there is not clear indication of the need for a novel method of inscription. Nevertheless, infrared femtosecond inscription has been identified as a method to overcome the major disadvantages inherent to UV inscription. In particular, UV inscribed structures present low thermal stability and they can only be inscribed in photosensitive fibres.

The thermal stability of fibre Bragg gratings is, in most cases, very low and degradation of the device is significant even at modestly high temperatures, thus annealing after the inscription is required in order to reduce the rate of degradation at room temperature. By inscribing gratings using femtosecond inscription thermal stability is greatly enhanced. In addition, the post-process of thermal annealing is not required, simplifying the fabrication procedure.

For UV light to be efficiently absorbed in the core, photosensitivity of the material is required, standard fibre used for telecommunications is not sufficiently photosensitive and therefore gratings inscribed by standard UV methods in such fibres only present a refractive index change of the order of 10^{-6}, which is not sufficient for most applications. Photosensitisation is achieved by different methods, such as hydrogenation, or using fibre with higher dope concentrations (mainly Germanium). Both methods of photosensitisation are efficient and allow the inscription of high quality gratings; they do nevertheless also increase the complexity, cost and time consumption of the fabrication process.

Inscription of buried structures using infrared femtosecond lasers has been widely reported in a variety of transparent dielectric materials, and thoroughly described in chapter 2. Inscription in glasses similar to those that compose standard fibres is well known. The main initial motivations for the inscription of fibre Bragg gratings using infrared femtosecond lasers raised from the expected improved thermal stability of such devices and from the possibility of inscribing gratings in fibres which are not photosensitive to UV light. Furthermore the refractive index modifications that may be induced in the glass are expected to be higher than those observed in gratings inscribed by UV light.

In this chapter, the fabrication of gratings using a point by point method is reported. This method consists on tightly focusing infrared femtosecond pulses inside the core of the fibre to inscribe, point by point, a periodic refractive index modulation which will lead to the creation of highly reflective gratings. Unlike other point by point methods, the process of inscription only takes a few seconds and is capable of producing highly reflective devices.

The main properties of these gratings are studied including the induced refractive index changes, spectral properties and polarisation sensitivity. Chapters 5 and 6 will look at the applicability of the unique characteristics of fibre Bragg gratings inscribed by this method in various sensing and fibre laser configurations.

4.2 Inscription Method

A point-by-point technique was developed for the inscription of fibre Bragg gratings, similar methods have been previously used to inscribed FBG and LPG using UV light sources [21]. The reasons that led to adopting this approach were the flexibility of the method and the simplicity of the set-up compared to more complex interferometric and diffractive techniques. Despite the demonstration of inscription of high quality gratings by an infrared femtosecond laser using diffractive methods [15], this method requires a specially designed phase-mask, which only produces gratings for a pre-determined resonant wavelength. Using a point by point technique, it is possible to alter grating parameters in a simple way, allowing in principle the fabrication of highly complex structures by programming the stage motion accordingly. Nevertheless until now the use of this technique has been very limited, mainly confined to the inscription of long period gratings. The reduced interest for this method of inscription is a result of major shortcomings, such as; complex and inaccurate alignment procedures, long processing times, low reflectivity and short grating lengths. The method here proposed utilise the unique specific characteristics of femtosecond lasers to overcome the above mention disadvantages of the point by point inscription and allows fast, accurate alignment and inscription of highly reflective fibre Bragg grating using a point-by-point technique for the first time.

4.2.1 Focusing considerations

The writing process involves focusing very tightly the femtosecond pulse into an area of the core. Since the photo-absorption process is highly nonlinear [7], the beam energy is only absorbed at the focal region of the beam through the highly non-linear ionization processes of multiphoton absorption, tunnelling and avalanche as described in chapter 2. The dimensions of the inscribed structures are therefore intimately related to the focusing conditions. In this section, we analyse the requirement for microscopic objectives and the effect of self-focusing in the inscription of fibre Bragg gratings.

Assuming optimum focusing conditions the diffraction limited dimensions of the focused beam radius is given by equation 4.1 [71];

$$\omega_o = \frac{0.61\lambda}{NA} \tag{4.1}$$

where ω_o stands for beam waist after focusing, λ is the wavelength of the laser and NA is numerical aperture of the microscopic objective used for focusing. The Rayleigh length, z_r, relates to the dimensions of the inscribed structure in the direction of propagation of the beam, and it is also a function of the refractive index of the material, n, as shown in equation 4.2 [71];

$$z_r = \frac{\pi \omega_o^2 n}{\lambda} \tag{4.2}$$

The size of the structure inscribed in the core is proportional to the Rayleigh length and the beam waist. This indicates that the dimensions of the structure inscribed depend on two parameters, the numerical aperture (NA) and the wavelength of emission of the laser (λ). Figure 4.1 illustrates how the beam focuses in the beam and modifies the material. In practice a number of factors prevent from optimum focusing inside the core of the fibre, particularly important are the effect of focusing inside an optical fibre (and thus focusing through a cylindrical surface) and the effect of self-focusing [7].

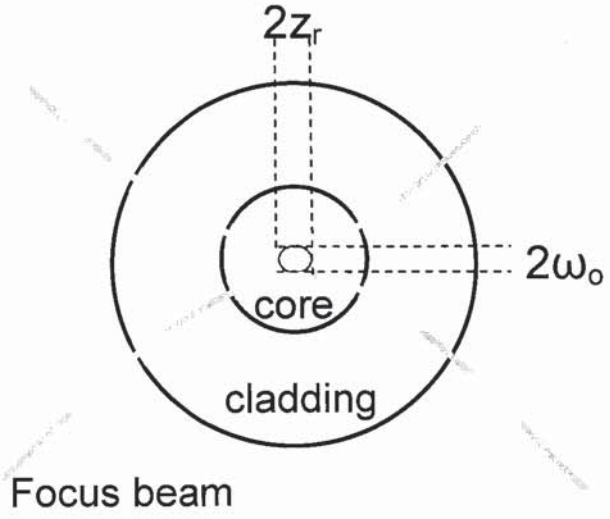

Figure 4.1: Illustration of the beam focusing inside the core, during point-by-point inscription by a femtosecond laser.

The nature of the point-by-point method, in which each laser pulse produces a grating pitch leads to constringent requirements regarding the size of the structures inscribed and the size of the focused beam. It is evident that to produce high quality gratings it is desirable for the beam waist to be smaller than the grating pitch ($\omega < \Lambda$). Tight focusing of the beam into the fibre becomes therefore critical in order to produce high quality gratings.

To estimate the size of the inscribed structures needed for inscription of good gratings, and thus estimate the required focusing, we may look at the condition for N order Bragg reflection;

$$\lambda_B = 2n_{eff} \Lambda_N / N \tag{4.3}$$

Where λ_B is the resonant wavelength, n_{eff} is the effective refractive index of the core, Λ_N is the grating pitch for a N^{th} order grating, and N is an integer number. The grating pitch required for a resonant wavelength of 1550nm, the preferred wavelength for most fibre optic applications, is approximately 0.535μm, less than the wavelength of the laser at 0.8μm.

During this work, two different objectives were used, a 40X microscopic objective with a numerical aperture of 0.65 and a 100X objective with long working distance, and a numerical aperture of 0.55. Tighter focusing may be considered for the inscription of special structures for specific applications. The 100X objective presented significant advantages over the 40X objective. First, it is a long working distance objective. Inscription is carried out with 13 mm separation between the surface of the lens and the fibre unlike the 40X objective which has a working distance of 600μm. Short working distances increase the difficulty of the alignment and also increase the risks to damage the end surface of the lens. Furthermore, as it will be shown in section 4.2.2 the quality of the gratings is significantly improved with the tighter focusing achieved by the 100X objective. Using equation 4.1 and 4.2, the focusing dimensions using the 100X objective are ω_o~0.9μm and z_r~3.6μm.

The cylindrical surface of the fibre represents an obstacle in order to achieve optimum focusing condition. In the case of the 40X objective, the objective is corrected in order to achieve optimum focusing through a plane surface of fused silica at a depth of 0.17mm (This is the thickness of the cover plates used in standard microscopy). It is known that any departure from such focusing conditions leads to a significant increase in the size of the focused beam [7]. If we consider the horizontal direction, i.e. parallel to the fibre axis, the focusing is through a plane surface, but the depth of focusing is 62μm rather than 170μm, leading to a larger affected area in parallel to the axis of the fibre. Focusing in the vertical direction is characterised by the beam propagating through a cylindrical lens leading to distorted focusing in that direction.

In the case of the 100X objective the focusing conditions improve significantly. This objective, unlike the 40X objective, has not been corrected for optimum focusing through a cover plate, therefore optimum focusing is achieved in air. By focusing in the centre of the fibre, in the vertical plane, we can assume that the beam does not change its trajectory in the air-cladding interface, since the wavefront would be perpendicular to the surface. This is valid both for geometrical and Gaussian considerations, since the curvature of the beam, at lengths much larger than the Rayleigh length can be considered linear. The focusing in the horizontal plane on the other hand, presents a large spherical aberration of the order of 20μm in its longitudinal

component (i.e. distance between the axial intersection of a ray and the paraxial focus) as shown in figure 4.2;

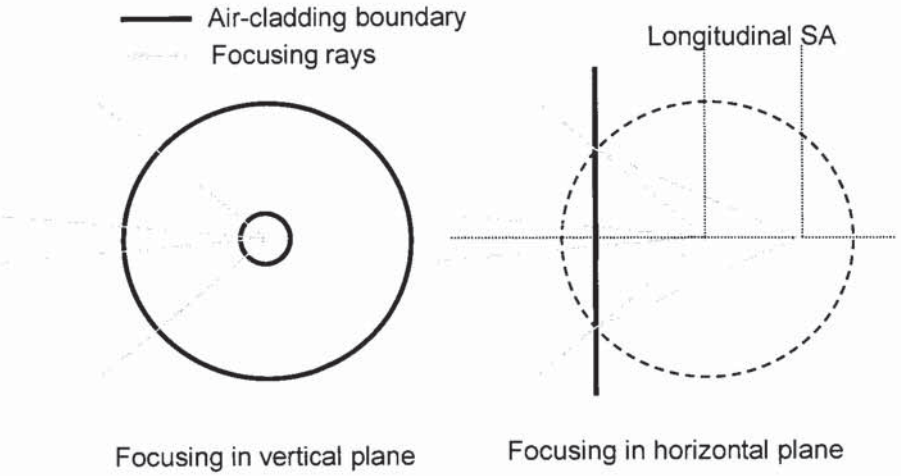

Figure 4.2: Conditions of focusing by the 100X microscopic objective in an optical fibre. While the focusing in the vertical plane can be considered optimum, spherical aberrations are important in the horizontal plane.

From the above analysis, we can conclude that while the quality of the focusing is affected by focusing through a cylindrical surface for the 100X objective, it does not affect the confinement of the beam in the longitudinal direction, as drastically as in the case of the 40X microscopic objective. Confinement in this direction determines the potential for the inscription of Bragg grating.

Self-focusing is also likely to have an important effect in the size of the focused spot size. Self-focusing results from the intensity dependence of the refractive index. This relationship, known as the Kerr effect, is stated in equation 4.4;

$$n = n_o + n_2 I \tag{4.4}$$

At high intensities, and since n_2 is positive in most materials, a variation in the refractive index acts as a lens which focuses the beam further. Self-focusing is dependent on the peak power, and as the peak power increases, the focusing becomes stronger up to a critical power after which self-focusing leads to a catastrophic collapse of the laser pulse, leads to a micro-explosion in the material. The critical power is given by equation 4.5;

$$P_{cr} = \frac{3.77\,\lambda^2}{8\pi\, n_o\, n_2} \tag{4.5}$$

It is unlikely that the critical power for self-focusing is reached during inscription. However, we believe this effect contributes towards the confinement to a smaller spot size and higher intensities. This effect counteracts partially the defocusing that rises from the non-optimal focusing conditions.

4.2.2 Experimental set up

The experimental set up used to inscribe gratings in this work is shown in figure 4.3. An amplified laser system, operating at a wavelength of 800nm, is used in the inscription procedure. This laser system produces 150fs-long pulses at a repetition rate of 1 kHz, reaching a maximum average power of 1W. Pulse energy was adjusted by a half-wave plate that rotated the direction of the linearly polarised laser beam and a Glan prism that transmitted only the vertically polarised component, thus reducing the laser energy without modifying the direction of polarisation of the beam. The fibre is placed on a computer controlled XY stage with 10nm resolution, and fixed at two points at each end of the region that is going to be processed on two XYZ manual translation stages. During inscription the stage is moved at a constant speed along the fibre axis, translating the fibre with respect to the focal point of the beam. Each grating pitch is produced by a single, tightly focused laser pulse. The grating period is set by changing the ratio of the translation speed to the pulse repetition rate (1kHz). Therefore writing speeds ranged between 0.535mm/s to 1.605mm/s, for gratings of first to third order as described by equation 4.3. The fast inscription process represent a significant advantage, with respect to other point by point inscription methods based on the 'stop and shoot' approach, in which each grating pitch is inscribed individually and then the fibre is translated the distance of the grating pitch that is to be inscribed. The 'stop and shoot' methods have major disadvantages, such as long processing times, short grating lengths and low reflectivity [60, 67]. In the approach presented in this work, these disadvantages are overcome and highly reflective gratings as long as 50mm are inscribed in tens of seconds.

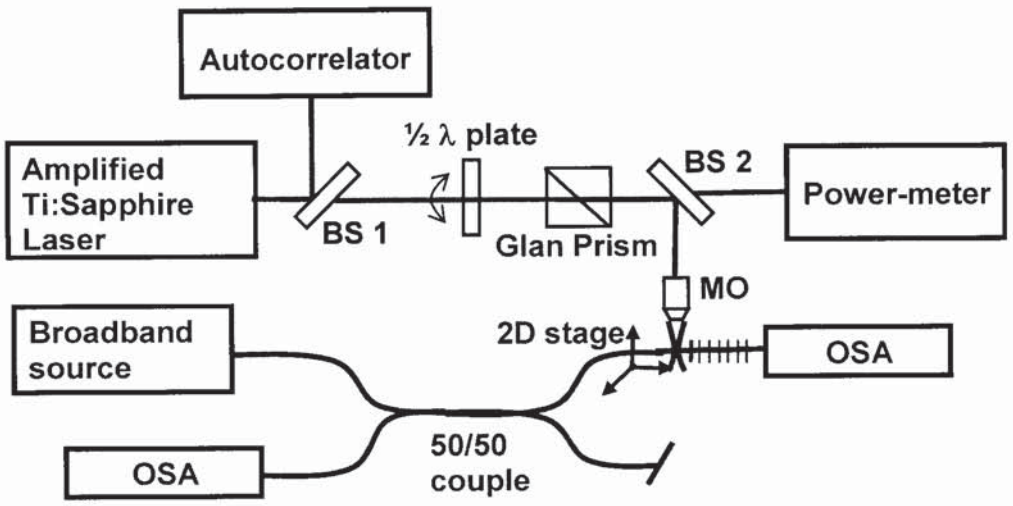

Figure 4.3: Experimental set-up for the inscription of fibre Bragg gratings using a point by point technique and an infrared femtosecond laser. MO stands for microscopic objective, ½λ for half-wave plate and BS for beam splitter.

The laser power was measured using a thermal power-meter. The amplified spontaneous emission from an EDFA was coupled into the fibre and used as reference to monitor the inscription in real time. Reflection and transmission spectra were captured using two optical spectrum analysers. After the inscription, the gratings were characterised using a tuneable laser with a linewidth of 1pm and a high-performance spectrum analyser with a resolution of 5pm.

An autocorrelator was built to measure the duration of the pulse. It consisted of a basic Michelson interferometer configuration, as illustrated in figure 4.4. One of the mirrors moves with a frequency of 0.5Hz to 2 Hz. The two beams are focused using a spherical lens (f=50mm) inside a nonlinear crystal ($LiNbO_3$) where they collide. The non-collinear second-harmonic, product of the combinations of one photon from each beam is collected and measured in a photodiode. Thus, there is only a second harmonic signal when the two beams coincide in the nonlinear crystals.

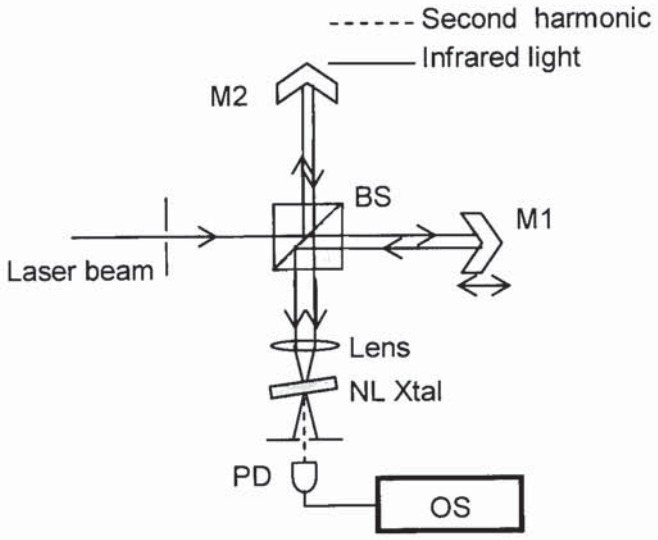

Figure 4.4: Design of the autocorrelator used in the writing set-up. BS stands for beam splitter, M for mirror, NL Xtal for nonlinear crystal, PD for photodiode and OS for oscilloscope.

4.2.3 Alignment of the fibre

Aligning the fibre with respect to the laser beam is arguably the most critical factor in the point by point inscription process. The alignment in other point by point methods lacks sufficient accuracy and is tedious and complex. The method developed in this project is not only fast, but it also permits very accurate alignment yielding a positional error better than ±1μm.

During alignment, blue light from an Ar^+ Laser is coupled into the fibre to improve the visibility of the core. Two CCD cameras are used to view the fibre from directions parallel and perpendicular to the beam, as illustrated in figure 4.5.

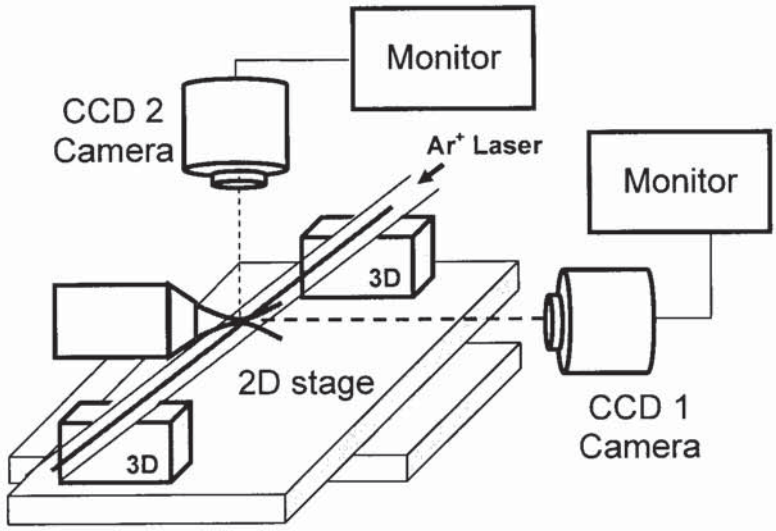

Figure 4.5: Illustration of the set-up used to align the position of the beam waist of the laser to the core of the fibre. An Ar^+ laser is used to visualise the core. CCD cameras allow parallel and perpendicular alignment of the fibre with respect to the focal point of the beam.

The position of the focal point of the beam in the horizontal plane is recorded by using laser power high enough to provoke plasma on air. In the vertical plane, the focal position can be adjusted by monitoring the position of the beam using energies well below the energy used for inscription using a CCD camera (CCD1 in figure 4.5). Using the power control of the system, the laser energy can then be reduced to a level in which the fibre is not affected by the focused pulses, but the focal position can still be visualised by the CCD camera and the fibre can be accurately aligned in the vertical direction. The fibre is aligned with respect to the beam at two points at either end of the region that is going to be processed, and the alignment through the fibre is assessed by scanning the position along the fibre. Careful alignment provides accuracy better than ±1μm over 60 mm translation.

4.3 Photoinduced refractive index change by infrared femtosecond lasers

Before analysing the spectral characteristics of the gratings inscribed by this method, it is convenient to study the structural changes inscribed inside the fibre, particularly, in terms of the dimensions of the structure and the refractive index change. This is important since the spectral behaviour of the grating is intrinsically linked to these characteristics, and posterior analysis is simplified when these characteristics are acknowledged.

4.3.1 Photosensitivity to femtosecond infrared radiation

Grating inscription by UV light relies on the photosensitivity of the fibre to the wavelength used for inscription. The energy from a photon of UV light is not sufficient to promote an electron to the conduction band of germanium doped fused silica (E_g~7.1eV [106,107]). UV inscription relies on the presence of germanium. Different germanium defects are absorbent of wavelengths from 213nm to 280nm (5.8eV to 4.4eV) by one photon absorption [68]. Standard single-mode fibre only has 3mol% concentration of germanium, as a result its photosensitivity is low and only gratings with low reflections can be inscribed in these fibres by standard UV methods [19]. Photo-sensitisation of the fibre is therefore required. This is achieved either by using highly doped fibre, commonly germanium with concentrations between 10mol% and 20mol% or by hydrogenation of a standard fibre, increasing the absorption characteristics of UV photons and the creation of defects [19, 68].

One of the most appealing reasons for the fabrication of fibre Bragg grating with a femtosecond laser is the capacity to write gratings in non-photosensitive fibre. Inscription of structures by changing the refractive index of the material using femtosecond laser processing is well documented in a variety of transparent materials such as, non-photosensitive glasses [30, 33-35], polymers [42, 43] or crystals [6, 39, 40]. Most of that work has been carried out in planar substrates and it is extensively reported in chapter 2.

Recently femtosecond inscription in non-sensitive fibre has been reported in a variety of materials including standard telecom fibre, 3 mol% Germanium [38], pure silica core fibre [15], co-doped Er:Yb fibre [108], and sapphire fibre [62]. Since photosensitivity is not necessary, it is also possible to produce structures in the core or in the cladding, as required depending on the application. Writing in the cladding has been applied to minimise the cladding modes [63], or to fabricate direction sensitive bending sensors [64, 109]. All the gratings presented in this chapter,

unless otherwise stated, were fabricated in non-photosensitive fibre, with 3mol% concentration of germanium in the core.

Inscription by infrared femtosecond radiation relies on multiphoton ionisation followed by avalanche ionisation. The presence of defects is not required for this type of inscription despite reports indicating that doping with germanium may reduce the threshold for inscription of gratings with a phase-mask [15], while hydrogenation in Ge-doped fibre significantly reduces the required pulse energy for femtosecond inscription using a phase mask [110].

The properties of gratings written point by point are defined, not only by the magnitude of the refractive index change, but also by the particular geometry of the structures inscribed. In a UV inscribed grating by a phase mask the photo-induced modified area is homogeneously distributed across the core. Point-by-point fabrication leads to a modified region that is confined to the area where the laser beam is focused. The size of the affected area represents a significant difference with respect to the gratings inscribed by alternative method where the whole cross section of the core is modified during inscription. These small structures are enough to create highly reflective gratings; as well as allowing the inscription of novel grating structures that will be introduced later in this work.

The dimensions of the structure and the refractive index changes were studied by imaging the structure with a microscope. This type of grating can easily be visualised using a standard microscope. The refractive index modification was studied using Quantitative Phase Microscopy (QPM) a novel technique which is briefly described in the following section.

4.3.2 Method used for refractive index investigation: Quantitative Phase Microscopy

Imaging a sample by a microscope is based on monitoring the variation of transmission of the illuminating light due to the presence of the object to be studied. These changes can be categorised into amplitude changes, due to absorption and reflection in the sample, and phase changes, due to refraction through the sample [111]. In this work, the interest resides in the phase change, since refractive index and dimensions of the inscribed structures are encrypted in the phase changes.

The most commonly adopted techniques used for the microscopic study of structures inscribed by femtosecond lasers are interferometric, such as the Differential Interference Contrast (DIC) or Nomarski microscopy and phase-contrast microscopy, which makes use of spatial filtering. Both of these methods offer high resolution images, nevertheless neither is quantitative, thus an

accurate value of the refractive index modification cannot be calculated with these techniques. Algorithms have been developed in order to acquire quantitative information on the phase profile. However, they neglect the amplitude component in the image recorded [112].

Phase visualisation techniques provide phase information, but any absorption and reflection is entangled with the phase image. Another disadvantage of Nomarski microscopy is its highly nonlinear response to phase information. Phase contrast microscopy, on the other hand, offers a linear response but only on small phase variations and negligible absorption. On top of previously mention disadvantages, both of these methods are complex and require specialised optics.

The method of Quantitative Phase Microscopy (QPM) was used in this work for the calculation of the refractive index changes introduced in the fibre. With this method, which was developed in 1998 [113] the phase information is separated from the amplitude information. Using a non-interferometric technique and bright-field microscopy, an accurate phase map can then be used to measure the refractive index change in the structure. It was known that using bright-field microscopy and partially coherent illumination, it is possible to see the phase structure by slightly defocusing the sample. This reduces the resolution in the image making the method undesirable for most applications. Advances in the theoretical understanding of the propagation of light through transparent materials, led to the development of the QPM technique which computes the bright field images of the sample at three positions, one in-focus, and two slightly defocused at either size of the focal image. This technique offers a complete phase map of the sample, which can be processed using the in-focus image to produce an analogue image of the phase contrast. In this work, the QPM software (from Iatia imaging ltd) was used in conjunction with a Axion microscope, since it offered an automated imaging and computational process.

4.3.3 Analysis of induced refractive index change

The refractive index modulation of the gratings fabricated in this work was studied using the method of quantitative phase microscopy. In order to take well-defined images of the core and grating, the fibre was immerse in index match fluid, as illustrated in figure 4.6, this was necessary in order to reduce the effect of the curvature of the fibre.

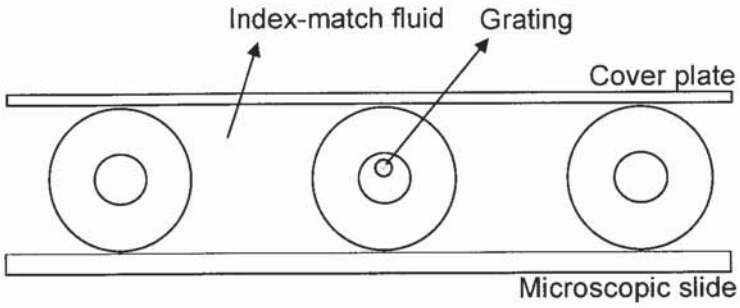

Figure 4.6: Scheme for the measurement of refractive index change. The fibre is immersed in index match fluid and covered with a cover plate to cancel the effect of the curvature of the fibre.

An example of a second order grating with a 1.07μm period inscribed in DSF fibre is shown in figure 4.7. The dimensions of the inscribed structures are visibly different to those of gratings inscribed by the standard UV methods. Such reduced modified area is a unique feature of this method of inscription and the strong focusing conditions used. Each grating pitch is inscribed by an individual laser pulse and corresponds to one grating pitch. The pulse energy was in all cases approximately 0.5μJ. The modified area is slightly ellipsoidal with a maximum cross-section length of approximately 1μm.

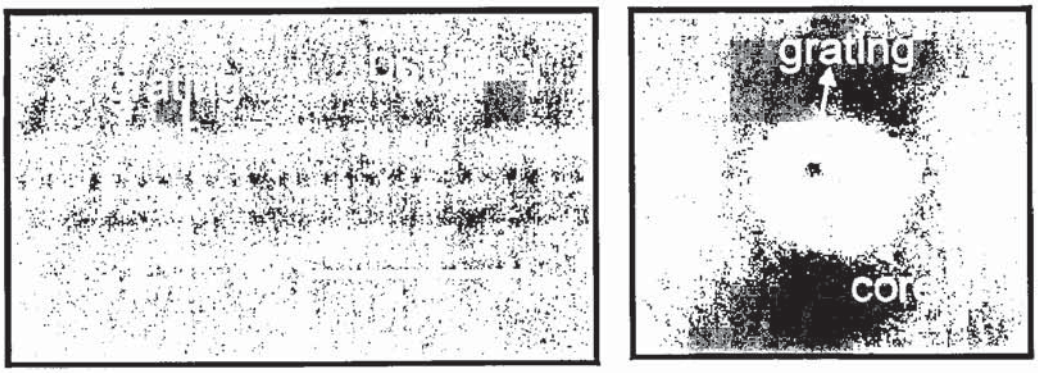

Figure 4.7: Microscopic images of a second order grating with the pitch size of 1.07μm pitch, inscribed in dispersion shifted fibre (core diameter of 6μm). (a) side view, (b) cross-section view.

To measure the refractive index modification, after a focused image of the core such as that in figure 4.7 (a) is recorded, the QPM Iatia imaging software takes images from the microscope at different depths with 1 μm separation, a filter is used in the microscope in order to have a monochromatic light source at 0.55μm, the resolution of the microscopic objective is better than 0.5μm, these images are processed to give a phase map of the image. The phase change, Δø, relates to refractive index changes, Δn, as given by equation 4.6;

$$\Delta\phi = \frac{2\pi L \Delta n}{\lambda} \tag{4.6}$$

where L is the length of the feature with a different refractive index change and λ is the wavelength of the light source.

In figure 4.8, the refractive index modification along the grating structure is presented. The refractive index modulations measured were in the order of 10^{-4}, with evidence of areas with a positive refractive index and areas with a negative change.

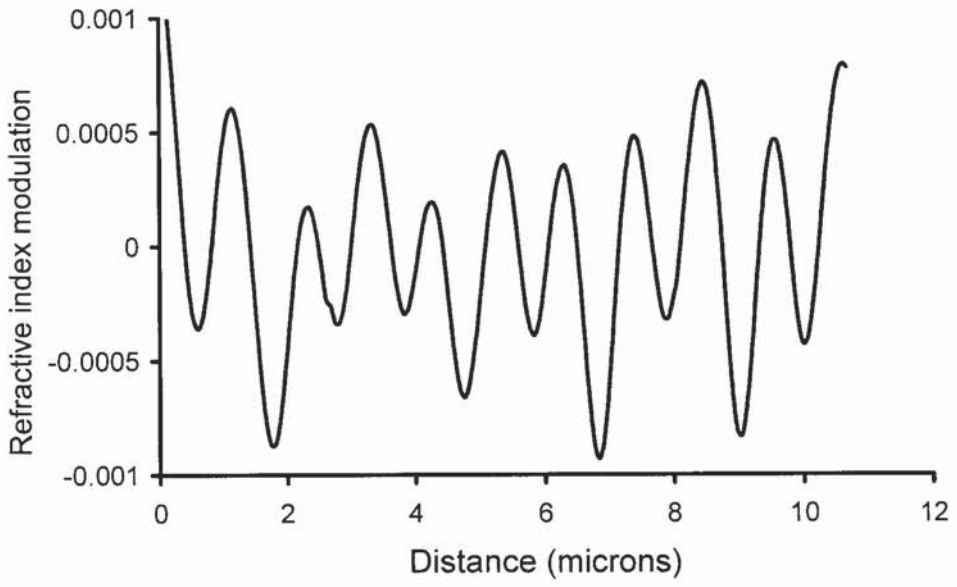

Figure 4.8: Refractive index modulation in a femtosecond inscribed fibre Bragg grating along the core of the fibre.

From figure 4.8, we can observe the periodic modification required for Bragg reflection, the absolute refractive index changes and whether it is positive or negative are difficult to determine. This is due to overlapping between the pulses which leaves a modified region comprised of positive and negative changes in the refractive index which are difficult to evaluate in absolute terms.

Since it was not possible to determine clearly the features inscribed by the individual pulses due to overlapping, structures with larger separation between the inscribed structures were made. The writing speed for the gratings was set at 5mm/s so the separation between individual structures was 5μm. This is sufficient to consider the effect of each pulse independently. In order to assure that the inscription conditions were identical to the conditions when gratings are inscribed, second order gratings were inscribed with lengths of a few millimetres. The remaining part of the fibre was inscribed in identical conditions but with a writing speed of 5mm/s.

A microscope image of such structure with 5μm period shows that each structure is independent from each other. Using the method previously mention of phase microscopy a phase map was acquired for each of the structures inscribed. The phase data can then be conveyed to refractive index information. In this study, interest was focused on the changes across and along the fibre. In figure 4.9, the phase change across the core of a single mode fibre is measured; we can observe a negative change in the region where the grating was inscribed. This area has been circled for clarity.

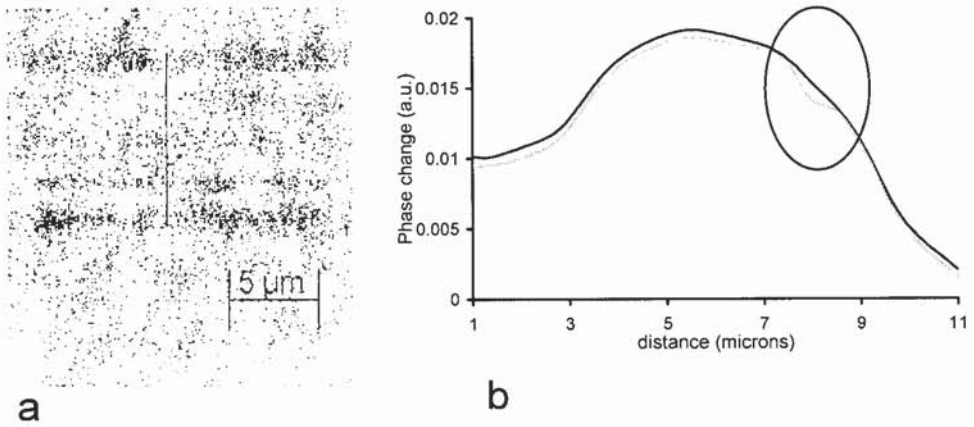

Figure 4.9: (a) Single mode fibre with a period structure with a 5 microns period. (b) Phase change across the core in a region in which the grating was inscribed, and an unmodified area.

In figure 4.10, the typical phase changes across the fibre rising exclusively from the area modified by the tightly focused femtosecond laser are shown. This was done by subtracting the phase changes through the core in two lines across the core that were in close proximity, but one crosses through a region with an structure inscribed by femtosecond radiation, and one crosses through an unmodified region, such as shown in figure 4.9. The curvature observed in the phase in figure 4.9(b) is a result of the dimension and refractive index of the core in the phase map. Since the parameters of the core are well-known both in dimensions and in

refractive index, the refractive index change induced by the femtosecond pulse can be estimated.

The result presented in figure 4.10 supports previous evidence that the topography of the modification consists of a region with a negative refractive index change surrounded by a "ring-like" region with a positive refractive index change. Such structures have been reported in numerous occasions after inscription with high intensities [52, 56].

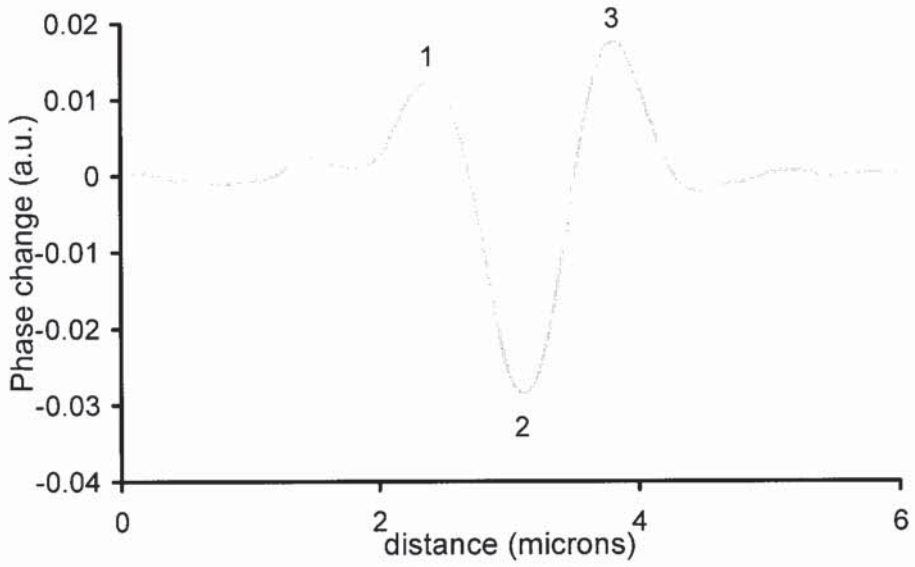

Figure 4.10: Phase change across a feature inscribed by a single femtosecond laser pulse with energy of 0.5μJ and focused by a 100X objective. Points marked as 1, 2 and 3 correspond to the position across the grating that are later investigated along the fibre in figure 4.11 and are label as a, b and c respectively.

The diameter of the region with a negative refractive index change was in a range between 0.8μm to 0.9μm measured from the points were the phase change is zero, while the diameter of the total modified region including the positive and negative refractive index change regions ranged between 2.5μm and 3.5μm approximately. Despite numerous reports of the inscription by infrared femtosecond lasers of structures with exclusively a positive refractive index change, none of the gratings inscribed by this method and pulse energy of 0.5μJ presented only a positive change. If the pulse energy was further reduced, it would be in principle possible to produce positive changes in the refractive index. However at those energy levels, no Bragg reflection was observed. These could be a result of the large area of the positive change

compared to the grating pitch. At higher pulse energies, the higher intensities may lead to narrower beam dimensions due to self-focusing.

The phase changes along the fibre in three different positions within the fibre core were examined. The first one in the centre of the inscribed structure (this position is marked in figure 4.10 as number 2), and the other two at either side of the structure, at the points in which the positive refractive index change was maximum (marked in figure 4.10 as 1 and 3), which was at distances of ~0.6μm from the point of maximum negative index change. The resulting phase changes can be seen in figure 4.11. It confirms that the induced modification leaves a central part with a negative refractive index change, and the outer part of the modified region presents a positive index change, with the maximum positive index change at the previously stated approximate distances of 0.6μm from the centre of the modified region.

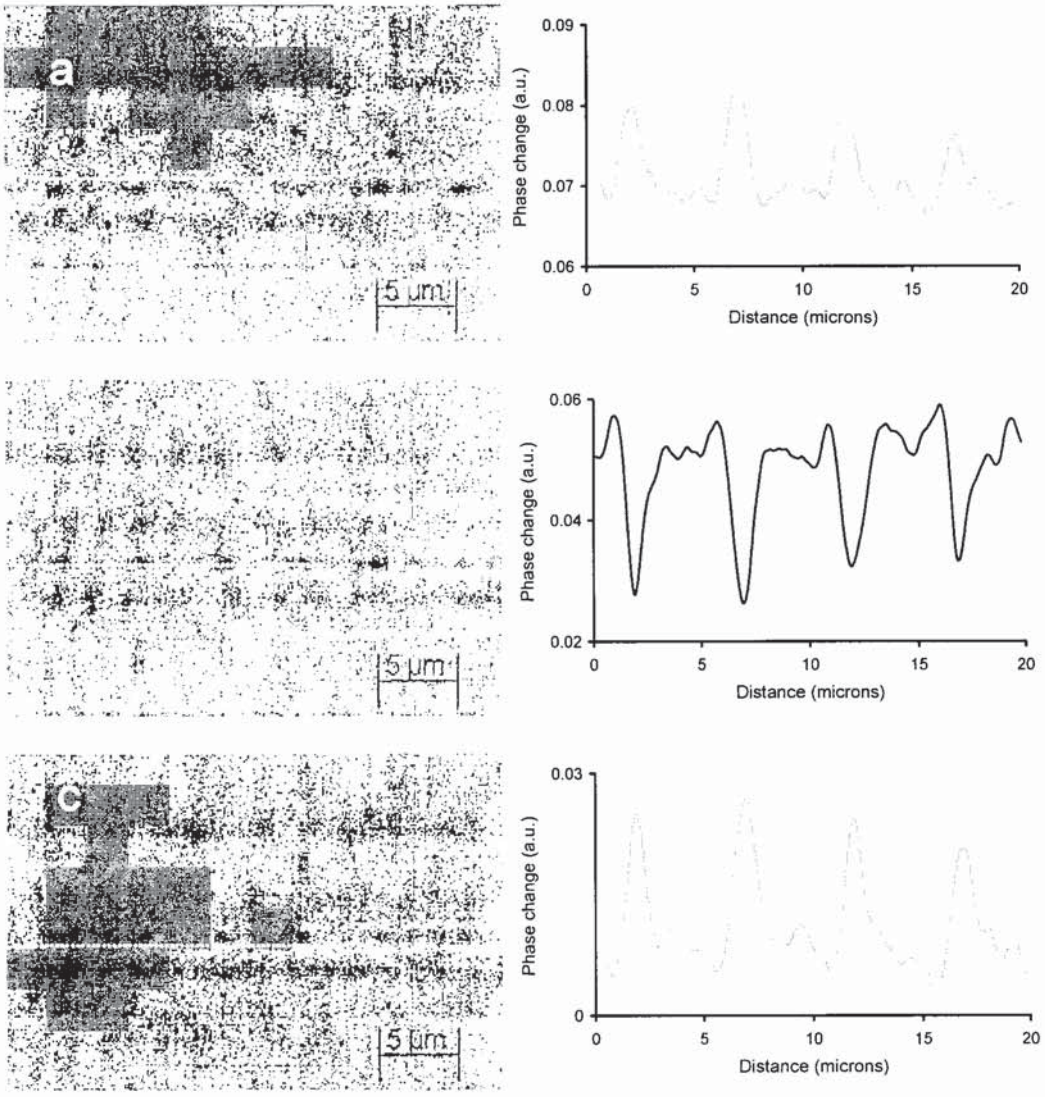

Figure 4.11: Induced phase changes across the fibre at three different positions in the core demonstrating the presence of positive and negative refractive index change.

A number of assumptions were made in order to estimate the refractive index change. The estimation is based on the complete knowledge of the refractive index step and dimensions of the fibre. Comparing the phase change caused by the difference of refractive index between core and cladding to the phase difference cause by the grating. Measurements were done from image when the grating structure is on focus. It was assumed that the core was equally on focus, which means we are focusing in the central plane of the core. The structures inscribed are assumed to be a sphere with 1micron diameter.

Finally, and considering all the assumptions mention above, In figure 4.12, the refractive index change induced by a single infrared femtosecond pulse which was tightly focused with a 100X microscopic objective is presented.

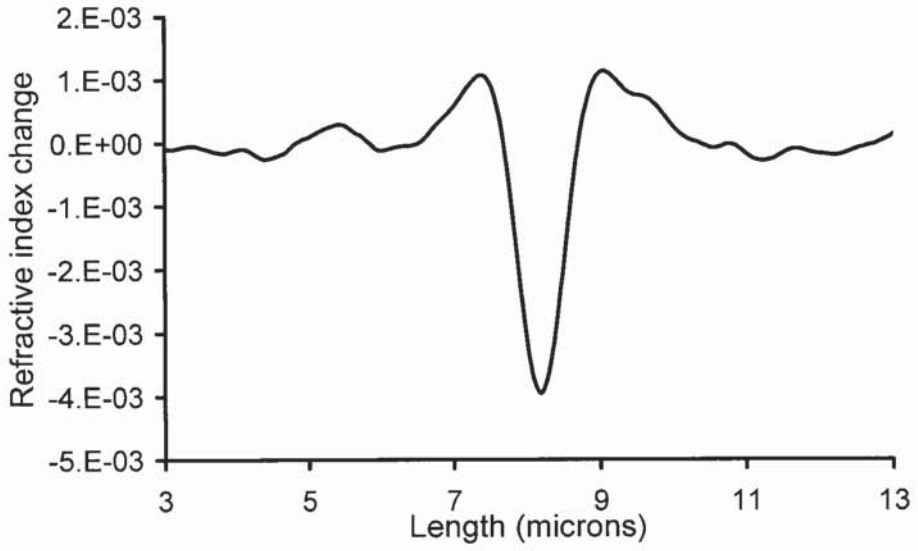

Figure 4.12: Refractive index change induced by femtosecond laser inscription, at the energies used for fibre Bragg grating inscription.

The refractive index was measured for a number of gratings. The features observed were in all cases analogous to the ones presented in this work. The refractive index changes measured vary from approximately $2x10^{-3}$ to $6x10^{-3}$ for different gratings, these values are estimates based on the above mention assumptions. The dimensions were between 0.8μm to 1.0μm for the negative refractive index change area and a ring with a ~3μm diameter with a positive refractive index change. This means that when gratings with a 1.07μm period, are inscribed, there is significant overlapping of the grating pitches and this reduces the visibility of the periodic structure.

Induced refractive index change can be higher for femtosecond inscribed gratings than for UV inscribed gratings. Inscription by a femtosecond laser induces areas with negative refractive index change and areas with positive change. This has been observed in phase mask inscription and it is also present in point by point inscription as it was shown in this section. The structure inscribed is similar to a frozen pressure wave in a solid. The central part where photo-ionisation first occurs presents lower refractive index after inscription while the area surrounding this point has a higher refractive index. Indicating that while density at the focal point is reduced the density in the surrounding area increases. A possible explanation for such structure is that when pulse is absorbed by the glass, it creates an electron-plasma. The pulse energy is such that this plasma begins to expand into the surrounding areas creating an acoustic wave. This result indicates that we are operating at intensities in the level of micro-explosions, and not of exclusively positive refractive index modifications, thus it is possible that voids of dimensions in the order of 100s of nm that cannot be resolved using this method. Future work will investigate the presence of such holes.

4.4 Spectral characteristics of fibre Bragg gratings inscribed directly by a infrared femtosecond laser

In this section, the properties of gratings inscribed point-by-point using an infrared femtosecond laser are analysed. We will compare the characteristics of these gratings with gratings inscribed with UV sources and gratings inscribed by other methods using femtosecond sources. The effect of varying parameters such as the focusing conditions or the order of the grating pitch in the performance of the gratings will also be investigated.

In particular, we will concentrate on those characteristics that differentiate gratings inscribed point by point from gratings inscribed by other methods, such as the coupling between cladding and radiation modes or the polarisation sensitivity. The shortcomings of the set up will be pointed out and ways to improve the quality of the gratings inscribed by this method will be proposed.

4.4.1 Effect of focusing conditions on the quality of the grating

The focusing conditions inside a fibre for the two objectives used in this work were considered earlier in this chapter in section 4.2.1. In figure 4.13, the modified regions in the cross section of the fibre for each objective are compared. The dimensions of the modified region created by the 40X objective is larger than the modified region created by the 100X objective, even though the former has a higher numerical aperture.

Figure 4.13: Cross-section of fibre Bragg gratings inscribed by focusing infrared femtosecond pulses with a (a) 40X objective, NA-0.65 and (b) 100X objective NA-0.55.

Figure 4.13 indicates that the 40X objective presents a larger modified area. This contradicts the expected behaviour from equation 4.1. Reports in literature indicates that for microscope objectives with a numerical aperture greater than about 0.5, the threshold for optical damage increases considerably when the laser is not focused at the optimal depth in the material [7]. This effect is more pronounce for objectives with higher numerical aperture. This increase in the threshold is a result of a larger spot size that takes place when the optimum focusing conditions are not met [7]. By focusing in the centre of the fibre we are focusing at a depth of approximately 63μm inside the silica fibre. Optimum focusing for the 40X objective is obtained at a depth of 170μm. This leads to a large modified area observed in the gratings inscribed by the 40X objective and, as we will see in this section, it affects the performance of the gratings inscribed using this objective.

Less tight conditions produce a more elliptical and larger structure in a cross-sectional plane of the core, in principle this leads to a higher average refractive index modification of this plane compared to an unmodified plane. However, along the fibre the modified region for such focusing conditions is larger than the required grating pitch; therefore the index modulation experienced by the propagating light is expected to be lower.

Results obtained in this work indicate the convenience of using tight focusing. Figure 4.14 shows the second order gratings (1.07μm pitch) for a resonant wavelength of 1550nm, after focusing with both objectives. The gratings inscribed with a 100X objective not only exhibit significantly stronger resonant reflections, but also generally induce lower out of band losses than those gratings inscribed using the 40X objective.

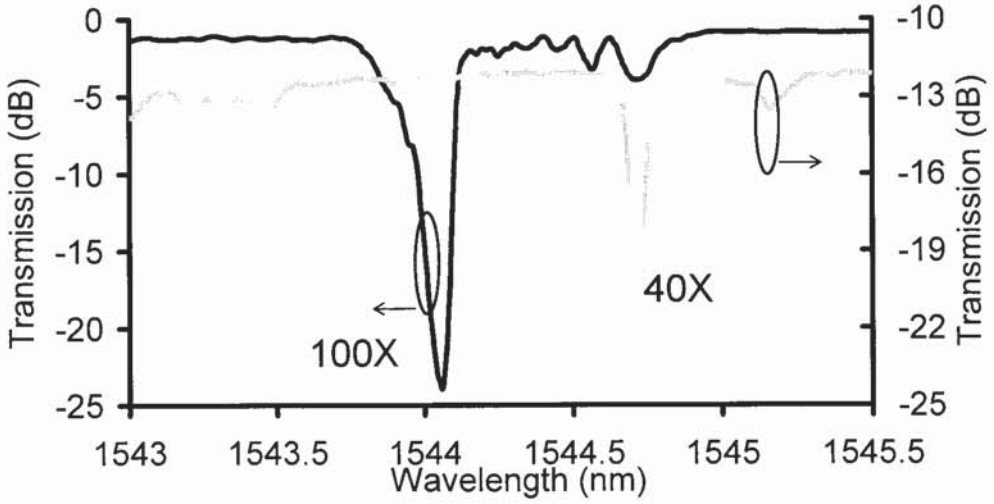

Figure 4.14: Comparison between gratings inscribed with a 40X objective and a 100X objective with pitches of 1.07μm, corresponding to second order Bragg reflection at 1550nm.

The advantage of using tighter focusing with the 100X objective is further illustrated by the fact that it is possible to inscribe first order gratings (gratings with a pitch of 0.535μm). This represents the first time that first order gratings have been inscribed using a point-by-point method with any laser source. This result indicates that infrared femtosecond lasers are more suitable than high power UV lasers for point-by-point methods since the highly nonlinear nature of the multiphoton ionisation allows a better control of the dimensions of the modified area and thus, the inscription of smaller structures.

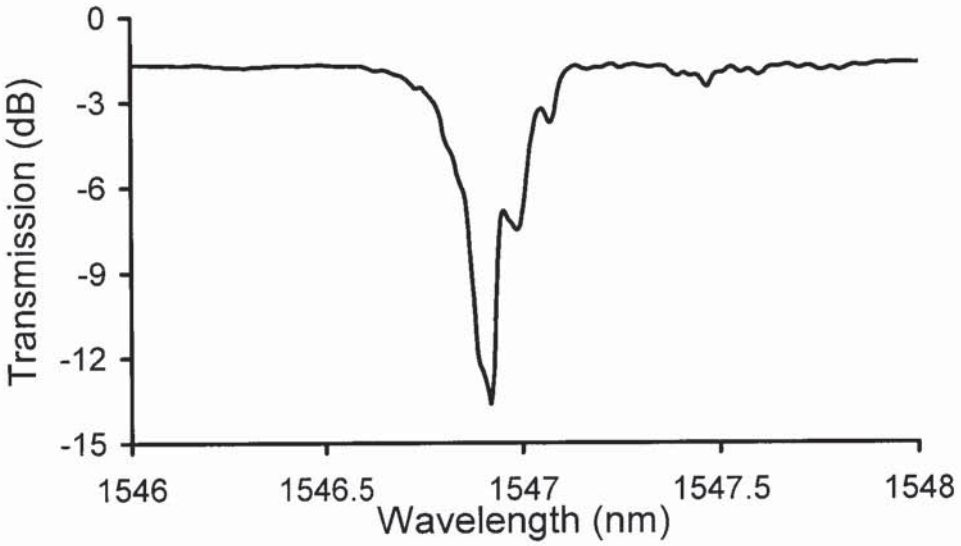

Figure 4.15: Transmission spectra of a fibre Bragg grating inscribed with a 0.535μm period, equivalent to a first order grating for a resonant wavelength of 1550nm. Inscription was made with a X100 objective. Inscription of gratings with a 0.535μm period using the 40X objective was prevented by the large dimensions of the individual structures inscribed by this objective.

Bragg gratings of second order (1.07μm period) with strengths exceeding 50dB for resonant wavelengths in the 1550nm have been inscribed using the 100X objective. A grating with strong reflection is shown in figure 4.16. This grating strength is sufficient for most application. However to fully utilise the flexibility of this technique, for example, to inscribe grating which reflect particularly low wavelengths, or to inscribe multiple gratings in different areas of the core, the inscription of smaller structures may be needed.

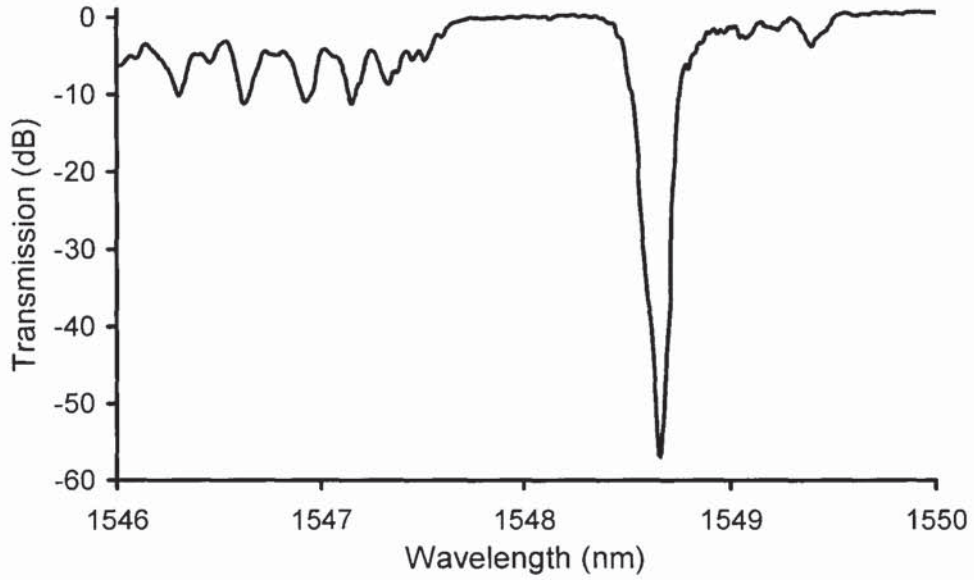

Figure 4.16: Spectral profile of a strong grating with a second order grating pitch.

Tighter focusing is in principle achievable with oil immersion lenses, with dry lenses with higher numerical aperture or by adopting more complex experimental configurations in order to eliminate the cylindrical lens effect of focusing through the fibre surface. Adopting such geometries will give rise to additional experimental complications, particularly in terms of alignment and due to the proximity of the surface of the lens to the fibre, which may increase the vulnerability of the lens. Focusing to dimensions of 0.3μm with similar methods has been reported in planar configurations [114].

The spot size can be further reduced by changing the operating wavelength from fundamental harmonics of the laser (λ=800nm) to the second harmonics (λ=400nm). The second harmonic can be generated in a nonlinear crystal, such as $LiNbO_3$. An alternative method is to control the laser power in such way that the intensity in the central part of the beam reaches the value above the inscription threshold, whilst the intensity at the edges of the beam remains below the threshold value. As a result, spatial resolution below the diffraction limit of the lens could be achieved in principle. However, the feasibility of such technique for this configuration and to inscribe fibre Bragg gratings is questionable.

4.4.2 Dependence on the order of the grating

Using both microscopic objectives, we inscribed period structures with 0.535μm, 1.07μm, 1.605μm. This corresponds to grating pitches of first to third order for a resonant wavelength of 1550nm. Figure 4.17 presents the transmission spectra of second and third order gratings inscribed by focusing the beam into the core with the 40X microscopic objective. All gratings were inscribed in segments of a standard single-mode fibre with 3 mol% concentration of germanium.

Except for first order gratings were the refractive index modulation depth is reduced due to the overlapping of the features inscribed, higher order gratings generally present lower reflection than lower order gratings. When the 40X microscopic is used, the overlapping of the features inscribed is large enough to totally prevent the inscription of the periodic structure. In the case of the 100X objective although the first order gratings were not as strong as the second order grating, the measured strength was over 10dB, which conveys to 90% reflectivity at resonance. This is particularly interesting considering that this is the first demonstration of point-by-point inscription of first order gratings. And alternative point by point methods did not exceed a reflectivity over 70%

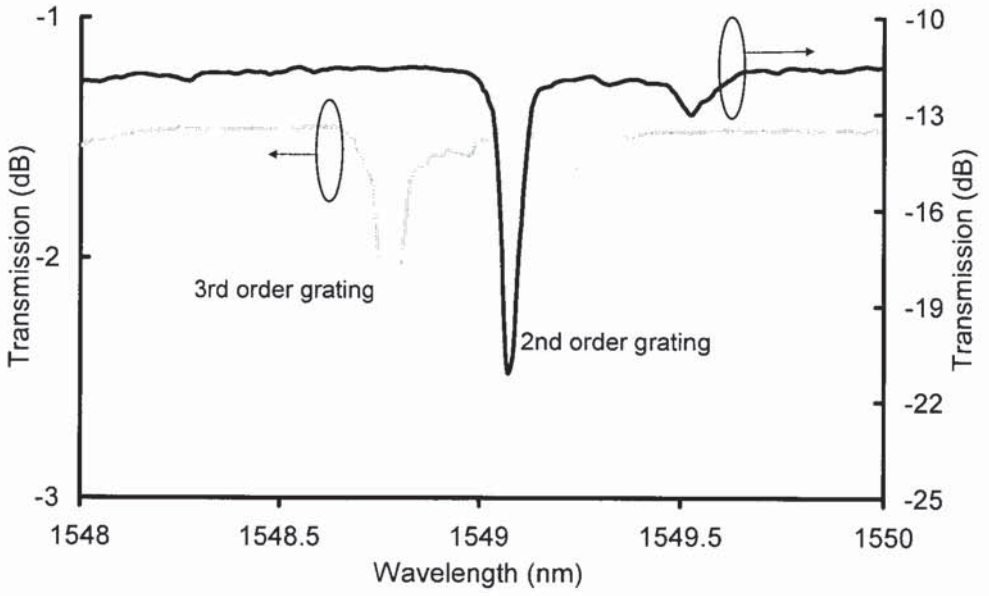

Figure 4.17: Transmission spectra of a 2nd order (1.07μm grating pitch) and 3rd order (1.605μm pitch) gratings inscribed using a 40X microscopic objective for focusing. Inscription of first order gratings was unsuccessful, indicating sufficient overlapping of modified regions to prevent the inscription of gratings.

Figure 4.18 presents the transmission spectra for gratings of first, second and third orders, in this case first order gratings (gratings with 0.535μm pitch, corresponding to first order Bragg reflection) were successfully fabricated.

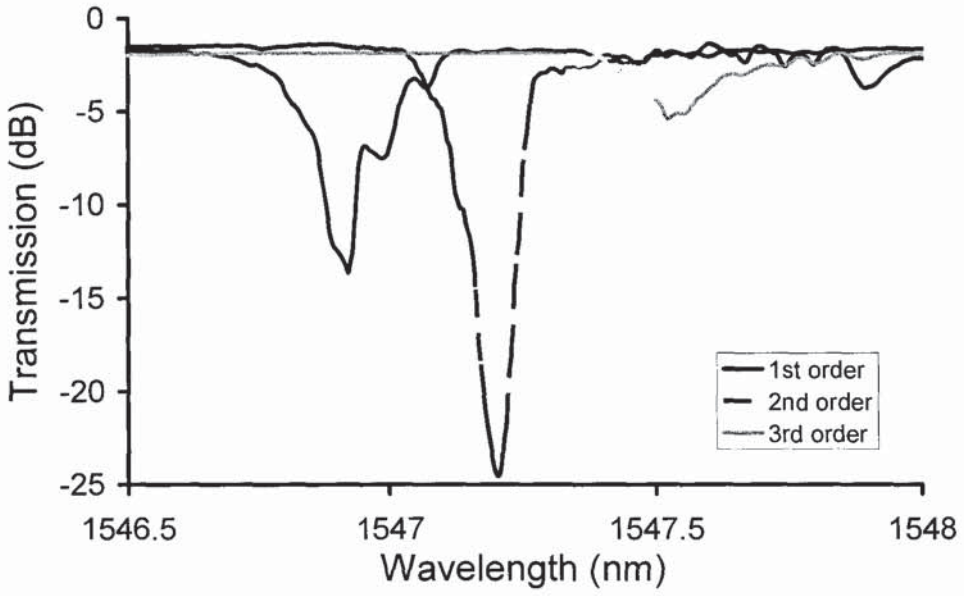

Figure 4.18: Transmission spectra of 1st, 2nd and 3rd order gratings inscribed with a 100X objective.

One can see that the second order grating shows the strongest response. This is in line with an earlier study of gratings produced by femtosecond writing with a phase mask [15]. Unless otherwise stated all gratings mention onwards are second order gratings inscribed using a long working distance 100X objective. The FWHM linewidth of the grating resonance typically ranged between 0.1nm and 0.3nm and did not show a distinct dependence on the grating order. Various gratings present a low quality spectral profile, presenting undesired chirp and double peaks. This comes from the fluctuations in the grating periodicity due to changes in the strain within the fibre, and it is particularly important for longer gratings. The quality of the gratings can be improved by introducing a strain gauge which can keep the strain in the fibre constant.

4.4.3 Out of Band Losses

Fibre Bragg gratings inscribed using standard UV gratings present ultra-low out-of-band losses. Studies in Boron-Germanium codoped fibre show losses to be in the range between $5x10^{-5}$dB/cm and $3x10^{-4}$dB/cm for gratings inscribed with CW light and $5x10^{-3}$dB/cm and $5x10^{-2}$dB/cm for hydrogenated fibre. These losses are therefore negligible for most applications [115].

Inscription of gratings by a phase mask and an infrared femtosecond laser present out of band losses lower than 0.6dB/cm, at least one order of magnitude higher than standard UV inscribed gratings [15]. Gratings inscribed using point-by-point inscription present out of band losses in the range from less than 0.1dB/cm to 0.3dB/cm. Insertion losses values are expected to decrease once power optimisation studies for grating inscription are carried out. Insertion losses are one of the main drawbacks for femtosecond inscription of fibre Bragg gratings and must be reduced if this technology is going to become an alternative to UV inscribed gratings in standard applications.

4.4.4 Cladding and radiation-mode coupling

Gratings inscribed by conventional UV techniques present a structure towards the short wavelength of the Bragg resonance in the transmission spectra. An equivalent effect is not observed in the reflection spectra, indicating that this light is been coupled out of the core through the core-cladding boundary [116]. This is a well known effect, seen more significantly in surface relief gratings, where the grating is physically etched in the surface of the core. This effect is generally more pronounced in highly photosensitive fibres, which therefore present higher refractive index modulation [15].

By submerging the fibre in index matched fluid, the air-cladding boundary is eliminated, this eliminates the periodic peaks observed in transmission, however residual losses remain present. These losses may, despite the use of index match fluid, significantly affect the performance for some grating-based devices, such as chirped or superimposed gratings were at lower wavelengths the reflectivity is lower due to excess losses induced by this coupling.

Cladding-radiation mode coupling is very significant in fibre Bragg gratings inscribed using an infrared femtosecond lasers, a clear example of the coupling to cladding modes is present in figure 4.19. This has been observed both for gratings inscribed using a phase mask and for

gratings inscribed point-by-point. We believe this effect comes as a result of the higher refractive index modulation achieved in femtosecond inscription, and may be enhanced in the point-by-point case by the tight confinement of the grating structure in the cross-section of the core.

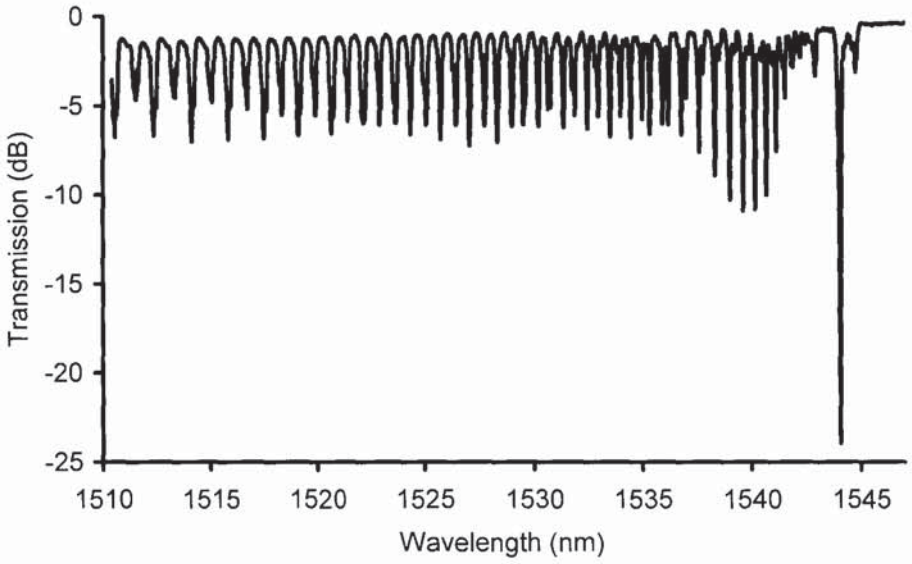

Figure 4.19: Coupling to cladding modes of a grating inscribed Point-by-point by a femtosecond laser.

Strong coupling to the cladding modes may be explained by the asymmetry introduced during inscription and the elliptical morphology of the features that may enhance the scattering of the propagating mode into the cladding. Structural modifications of the core-cladding interface would also modify the propagating properties of the fibre and therefore may also be a factor that increases the coupling to the cladding modes. Significant coupling to the cladding modes was observed in a broad spectral window spreading towards short wavelengths in all the gratings, as shown in figure 4.19. Cladding mode coupling is noticeable as far as 50nm away from the resonant frequency.

A number of methods have been proposed in order to eliminate or reduce the cladding-radiation mode coupling in UV inscription; including using special fibres, such as high NA fibres [117] or depressed cladding fibres [118]. An alternative method proposed having a uniform photosensitive region across the cross-section of the optical fibre in order to eliminate the normalised refractive index modulation [119]. A similar concept has been applied in femtosecond inscription by phase mask that effectively reduced the effect without the need of a

special fibre. In this case, the grating inscription was extended to the cladding [63], allowing almost complete suppression of cladding modes.

Due to the geometrical characteristics of point-by-point inscription, the latter method is not feasible for the configuration adopted in this work. Nevertheless solutions with special fibres such as the ones above proposed should be equally efficient in point-by-point inscription. A through investigation on the parameters that influence the cladding modes and ways in which to minimise their presence has not yet been performed. Indications lead to belief that pulse energy, and relative position with respect to the core cladding interface are the main parameters to consider.

4.4.5 Spectral estimation of the refractive index modulation depth

We can estimate the refractive index modulation that is experienced by the wave propagating through the core using equation 4.7 [69];

$$\Delta n = 2 n_o \sqrt{\left(\frac{\Delta\lambda}{\alpha \lambda_B}\right)^2 - \left(\frac{1}{N}\right)^2} \tag{4.7}$$

where n_o represents the refractive index of the core, $\Delta\lambda$ represents the full width at half maximum, α is ~1 for strong gratings and N is the number of grating planes in the grating. Alternatively, it is possible to look at the reflectivity, R, instead of the full-width at half maximum from equation 4.8;

$$\Delta n = \frac{\lambda}{\pi \eta(V) l} \tanh^{-1}\left(R^{1/2}\right) \tag{4.8}$$

where $\eta(V)$ is a function of the fibre parameter, V, that represents the fraction of the fundamental mode intensity that is contained in the core.

Ideally in order to estimate the effective refractive index modification, long fibre Bragg gratings should be inscribed. This way, the influence of the number of grating planes on the broadening of the linewidth would be negligible. However, the inscription of long gratings leads to non-uniformity leading to chirping, with the consequent broad spectral features. The grating shown in figure 4.20, was used for this estimation, since despite a length of 16 mm, its uniformity is sufficiently high to not compromise the result significantly.

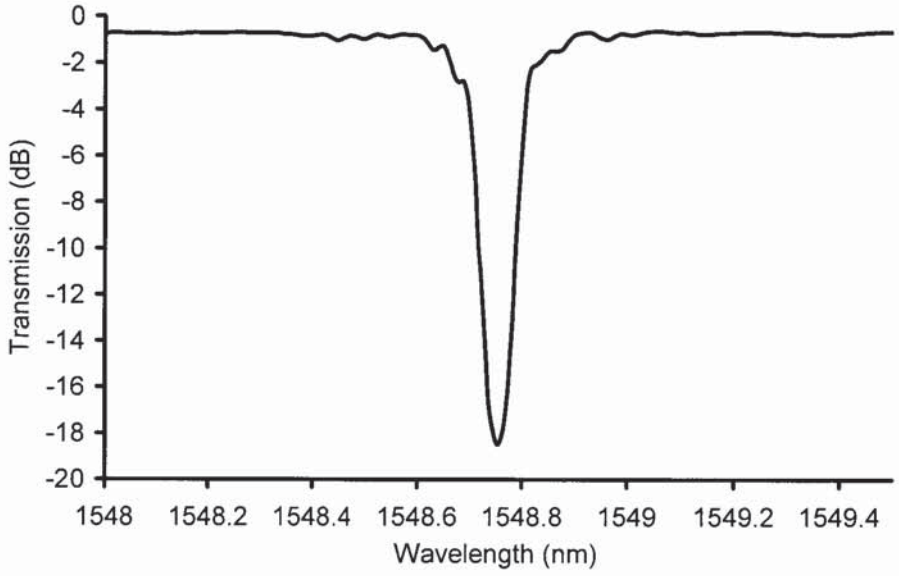

Figure 4.20: Uniform grating with high level of symmetry used for the estimation of refractive index modification.

Considering a length of ~16mm, a reflectivity of ~0.984, and a full width at half maximum of ~0.11nm, both equation 4.7 and equation 4.8 yield a refractive index modulation of ~10^{-4}. A second estimation was done in a grating inscribed through the coating. Its spectral transmission is illustrated in figure 4.21.

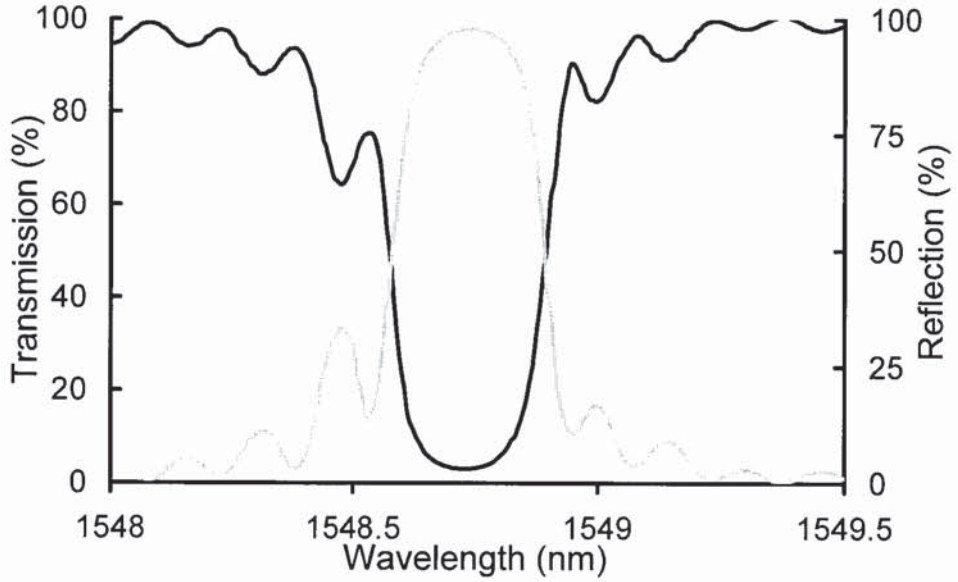

Figure 4.21: Spectral profile at transmission used to determine the index modulation of the grating.

This grating has an approximate length of 5mm, a FWHM of ~0.31nm and a reflectivity of ~0.97. In this case, using equation 4.8, it yields a refractive index modulation of ~2.4×10^{-4}. The accuracy of this estimation is affected by chirping of the gratings due to period variations rising from changes in the tension of the fibre. For this reason, these measurements were done in relatively short gratings. Nevertheless it is evident that these values are at least one order of magnitude lower than the refractive index changes measured directly using phase microscopy (see section 4.3). This is the case, since the modified area in which the refractive index change is confined is localised in a small section of the core. The refractive index modulation is also affected by the overlapping of the pitches which leads to a reduction of the effective index modulation.

4.5 Polarisation properties of femtosecond inscribed gratings

Light propagating through a standard fibre experiences very low birefringence. This is due to the highly symmetrical geometry of the fibre. The inscription of fibre Bragg gratings generally creates an anisotropic refractive index modulation across the core, therefore light couple into the fibre experiences a birefringence proportional to the induced asymmetry of the refractive index.

$$\frac{\Delta\lambda_{pol}}{\lambda_B} = \frac{\Delta n}{n_{eff}} \tag{4.9}$$

where $\Delta\lambda_{pol}$ is the difference in resonant wavelength between the orthogonal polarisations, λ_B, resonant wavelength, Δn is the birefringence induced during inscription, and n_{eff} is the effective refractive index in the core.

Polarisation dependence in the grating response can be used to create devices such as polarisation mode converters [120], rocking filters [121], calibrated wave retarders [122] or single polarisation fibre lasers [123]. Birefringence is, however, undesirable for a number of applications. There are two different theories regarding the process of photoinduced birefringence. One attributes the anisotropy to the direction of polarisation of the UV beam used for inscription [124]. The other is based on the geometrical considerations of the symmetry of the inscription process [125].

We used the set-up illustrated in figure 4.22 to study the birefringence of the gratings. The light from a tuneable laser source with 1pm resolution is initially linearly polarised then a polarisation controller is used to vary the direction of polarisation. Optical power at transmission and wavelength are then measured using a power meter and a wavelength meter.

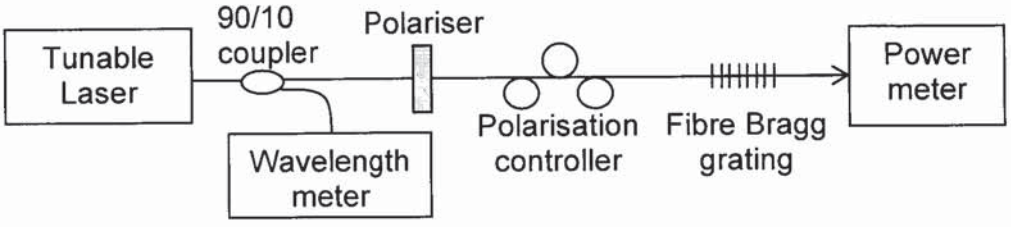

Figure 4.22: Experimental set-up used to measure the birefringence of gratings inscribed point by point by a femtosecond laser.

Gratings inscribed point-by-point present significant polarisation dependence when compared to conventionally inscribed gratings. We believe that the main factors that may affect the polarisation properties are the relative position of the grating structure with respect to the geometrical centre of the fibre, the dimensions of the structure inscribed, and the stresses induced in the surrounding area.

We identified the asymmetry of the modified area with respect to the fibre as the primary contributor to the overall birefringence. Figures 4.23 and 4.24 show the significant difference in birefringence between two gratings, a grating inscribed in the centre of the core (figure 4.23) and one axially offset 3 microns from the centre of the core (figure 4.24).

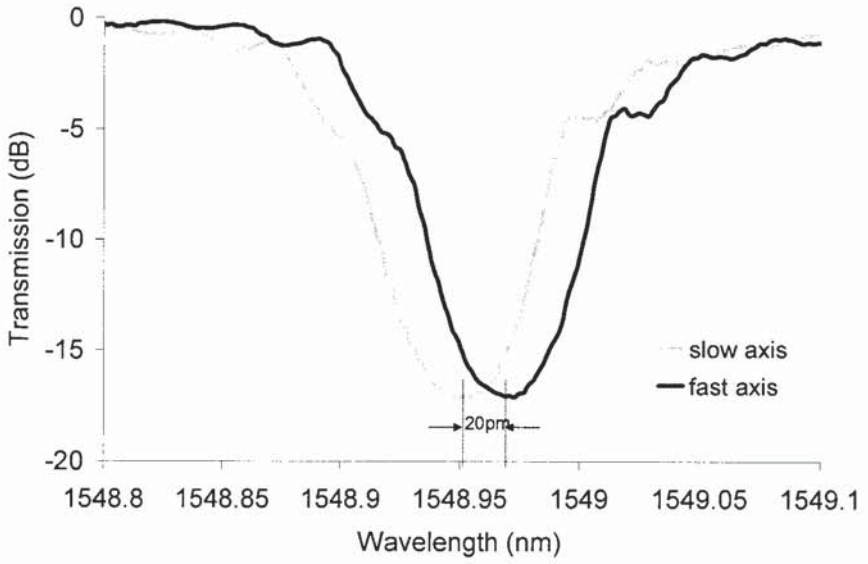

Figure 4.23: Transmission spectra of orthogonal polarisation in a grating inscribed in the centre of the core.

In figures 4.23 and 4.24, we can compare the birefringence of two gratings, one inscribed in the centre of the core, and one which was displaced 3 microns away. As expected results show evidence of the relationship between the birefringence and the asymmetry of the grating. This result indicates that polarisation effects come mainly from the geometrical asymmetry induced in the fibre during the inscription process. It is therefore possible to control the birefringence by adjusting the grating to the centre of the core, for lower birefringence, or near to the core-cladding boundary, for higher birefringence. Nevertheless gratings inscribed point by point will present generally larger birefringence than gratings inscribed by phase mask. Figure 4.24 indicates that different polarisations experience also different grating strengths, as expected

from equation 4.8. Polarisation dependent losses may be as high as 1.5dB for orthogonal polarisations in axially offset gratings.

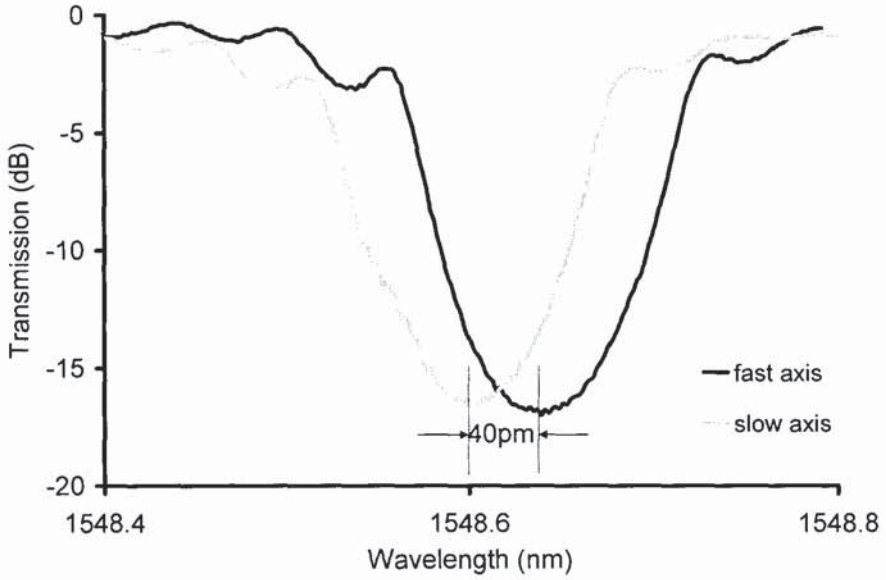

Figure 4.24: Transmission spectra of two orthogonal polarisation of a grating inscribed axially offset 3 microns from the centre of the core.

Another aspect that must be considered is that the modified regions that form the grating are non-symmetrical. Their elliptical cross-section leads to an asymmetry in the refractive index of the core. This may contribute to some level to the overall birefringence of the grating.

A third possible cause for birefringence is the presence of an anisotropic and inhomogeneous distribution of stresses around the inscribed area. This effect has been extensively documented in the femtosecond inscription of waveguides [126]. Stress related birefringence may be erased by annealing the grating at high temperatures, relieving the induced stresses. After annealing for 24 hours at 500°C, not significant changes were observed in the birefringence of the grating. This can be considered as an indication that stress related birefringence is significantly lower than that induced by strictly geometrical considerations. Further studies must be done in order to understand fully the relative contribution of each of these effects to the final birefringence of this type of gratings.

The spectral separation between orthogonal polarisations ranged from 10pm to 46pm, depending on where the grating was inscribed. This corresponds to birefringence ranging from 9×10^{-6} to 43×10^{-6}, which is much larger than that observed in the UV inscribed gratings.

There is a scope of potential applications for such birefringent and asymmetric devices that will be commented on in following chapters, including directional sensing, single-mode, single polarised fibre laser or microwave signal generation by fibre lasers. It is, nevertheless, also a drawback for many standard applications for fibre Bragg gratings. In order to broaden the applicability of these devices, the flexibility to inscribe both polarisation sensitive and insensitive devices will be necessary. A way in which birefringence may be suppressed is by inscribing a grating in a spiral, this can be done simply by twisting the fibre before the inscription.

4.6 Long Period Gratings

Long period gratings (LPG) have periods typically in the range of 100μm to 1mm, these devices promote coupling between propagating core modes and co-propagating cladding modes. The high attenuation of the cladding modes results in attenuation bands centred at discrete wavelengths, each attenuation band corresponds to coupling to a different cladding mode [96]. Long period gratings are particularly interesting devices in sensing applications. As it is the case for Bragg gratings, long period gratings are sensitive to temperature and strain. However their sensitivity to the external environment is much higher than that of a fibre Bragg grating. This is because the cladding modes are intimately related to the cladding-air boundary. The cladding modes are therefore affected by the external conditions more intensely than the core modes. Thus, long period gratings are not only optimum temperature and strain sensors, but also can be used to measure the refractive index of the surrounding environment (useful for example to control gas concentration or leak) and they are also sensitive to bending. A more detailed discussion on the characteristics of long period gratings was presented in section 3.6.

The attenuation bands are centred at wavelengths, λ_i, given by the relation in equation 4.10;

$$\lambda_i = \left[n_{eff}(\lambda) - n^i_{clad}(\lambda)\right]\Lambda \tag{4.10}$$

where n_{eff} is the effective refractive index in the core, n_{cladd} is the refractive index of the cladding modes and Λ is the pitch of the long period grating.

4.6.1 Inscription and spectral characteristics of the femtosecond inscribed long period gratings

Long period gratings were inscribed using the set-up described in section 4.2, the pulse energy ranged between 0.28μJ and 0.6μJ and the beam was focused by the 100X objective and using identical alignment techniques. The translation stage had a constant speed of 70μm/s, combined with the 1kHz repetition rate of the laser approximately 14 pulses will be focused in the sample during the time it travels one micron granting the inscription of a continuous track rather than a periodic perturbation. An electrical pulse generator was used to trigger a shutter in synchrony with the stage in order to create a period of 360μm with a 50% duty cycle. The length of the gratings was approximately 45mm for all the gratings inscribed.

Figure 4.25 illustrates the spectral profile at transmission of one of this long period grating inscribed using this point by point technique. It presents the transmission spectra for two orthogonal polarisations demonstrating strong birefringence in long period grating.

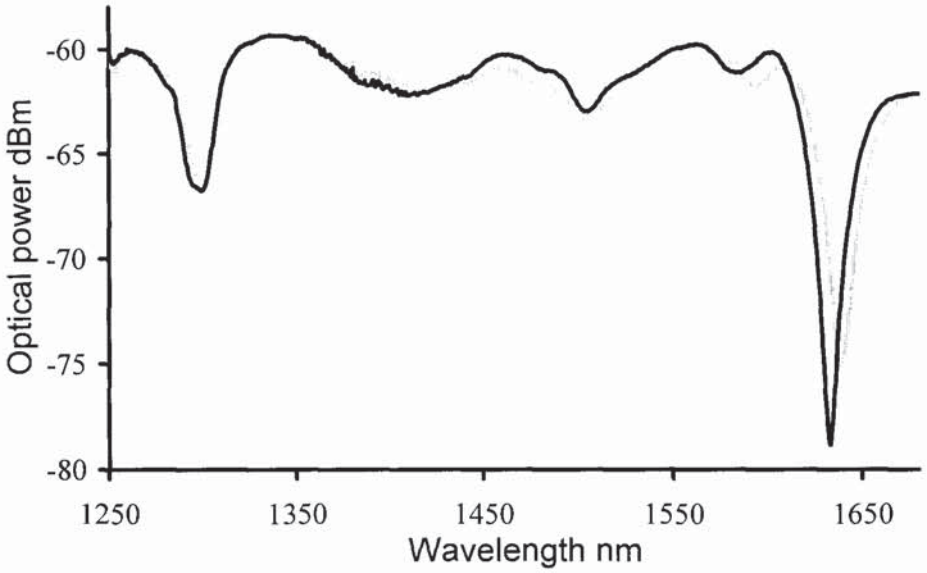

Figure 4.25: Transmission of two orthogonal polarisations in a long period grating inscribed by an infrared femtosecond laser with a 360μm with a 0.5 cycle.

The very strong polarisation dependence, compared to gratings inscribed by standard UV methods, is the most differentiating characteristic of these devices. We can observe that the wavelength separation between orthogonal polarisation modes is as large as 14nm, this spectral separation is significantly larger to what was observed for the Bragg gratings inscribed by the same method, between 10pm and 50pm. However, they indicate similar birefringence, as it yields from equations 4.11 and 4.12;

$$\Delta n_{FBG} = \frac{\Delta\lambda}{2\Lambda_{FBG}} \tag{4.11}$$

$$\Delta n_{LPG} = \frac{\Delta\lambda}{\Lambda_{LPG}} \tag{4.12}$$

Both cases indicate an equivalent birefringence in the order of ~$4x10^{-5}$; these similar results were expected since the method of inscription is in both cases similar and the dimension of the modified regions in the long period and Bragg gratings are comparable, in figure 4.26 a microscopic image of a section of a long period grating is given.

Figure 4.26: Microscopic image of a section of a long period grating inscribed by a infrared femtosecond laser in a single-mode fibre. The beam is focused with a 100X microscopic objective.

Polarisation dependent loss, PDL, was measured to range between 3 to 4dB. The thermal stability and birefringence of long period gratings inscribed by this method are further studied in section 5.2. A investigation on the dependence of the long period grating performance in parameters such as NA of the microscopic objective, writing speed and pulse energy and a detail comparison between these gratings and gratings inscribed by other techniques are yet to be conducted.

4.6 Conclusions

A novel method for direct, point-by-point inscription of fibre Bragg gratings using an infrared femtosecond laser was described in this chapter. The characteristic flexibility of point by point methods is in this case supported by the simplicity of the alignment technique, the overall speed of the inscription process and the high quality of the gratings inscribed.

In these gratings, each grating pitch was produced by a single pulse and the grating period was set by changing the ratio of the translation speed to the pulse repetition rate, writing speeds were therefore approximately 1mm/s. The fast processing times is a major advantage with respect to other point by point methods that use the 'stop and shoot' technique. Furthermore, by translating the stage at a constant speed, the requirements for stability and repeatability are reduced. Two microscopic objectives were used to focus the laser pulses into the fibre. Results indicate that the microscopic objectives that provide tighter focusing conditions produce gratings with stronger reflectivity.

Infrared femtosecond inscription starts after a dielectric breakdown is induced in the material due to multiphoton absorption, this leads to localised melting and a material density change. As a result, for femtosecond inscription doped or hydrogenated fibres are not required. This facilitates the inscription method and more importantly allows inscription in fibres where UV inscription was not possible.

In this chapter we investigated the dimensions and characteristics of the photo-induced structural changes. This was done using a microscope and a quantitative phase microscopy technique. Results indicated that during femtosecond inscription, only a confined portion of the cross-section of the core was modified, with an approximate area of $2\mu m^2$. The structures consisted of central region of less than 1μm in diameter that exhibited a negative refractive index change, surrounded by a ring-like region with a positive index change; index modulation was estimate to be in the order of 10^{-3}. From this result, we cannot conclude the presence of voids in the gratings inscribed, however it is likely that voids of dimensions of hundreds of nanometers, which cannot be resolved by the method of quantitative phase microscopy (QPM).

The inscription of the first order Bragg gratings by an infrared laser for a resonant wavelength of 1550nm was demonstrated for the first time. First and higher order gratings were fabricated and the highest reflectivity was observed in the second order Bragg gratings that experienced reflectivity in excess of 99.9%. The strength of first order Bragg gratings was compromised by the reduced visibility of the refractive index modulation in the grating. The dimensions and physical characteristics of these gratings have a profound effect on their spectral behaviour. Particularly important was the observation of strong birefringence and polarisation dependent

loss which are a result of the asymmetric modification in the core. The gratings inscribed by this method present numerous interesting and unique properties. However, two major shortcomings must be eliminated or reduce before this method of inscription can compete with more established technologies. The out of band losses are significantly higher than the losses induced by UV inscription and a strong coupling between the radiation and the cladding modes leads to losses towards the short wavelength of the Bragg resonance.

Finally, the inscription of long period gratings using the same set-up configuration that was used for the inscription of fibre Bragg gratings was demonstrated. The only addition was a shutter synchronised with the laser which allowed an extra flexibility of the exposure regime. The duty cycle of the long period grating was 0.5 and as it was the case with the Bragg gratings, they presented strong polarisation dependence.

Only uniform fibre Bragg gratings and uniform long period gratings have been studied in this chapter. However, the great potential of this method is based on the great flexibility to inscribe highly complex structures without introducing any additional components in the system but just by adjusting basic parameters such as speed and acceleration in the translation stage or laser intensity.

CHAPTER 5: Characteristics of gratings inscribed by an infrared femtosecond laser and their applications

5.1 Introduction

In this chapter, the main potential applications of femtosecond inscribed gratings are explored. The thermal properties of gratings inscribed by a femtosecond laser are investigated. Gratings inscribed by infrared femtosecond lasers offer improved thermal stability and comparable sensitivity to thermal variations than UV inscribed gratings. Thus, it is possible to produce sensors for hostile environments where standard UV inscribed gratings cannot operate. The conclusions reach in this study are applicable to fibre Bragg gratings based on infrared femtosecond inscription either by phase mask or point-by-point.

Properties particular to point-by-point inscription are also exploited and novel designs for specific applications are highlighted. In particular, using the method proposed in this work, we demonstrate for the first time the feasibility to inscribe highly reflective grating through the coating, with the consequent advantages in mechanical strength, and simplicity of the inscription process.

Two different configurations for curvature sensing based on the unique dimensions and flexibility of femtosecond inscription are presented. Both method offer directional discrimination in standard fibre, which simplifies the requirements for interrogation and inscription of other alternative methods proposed based on asymmetric fibres. The first method utilises the possibility of axially offsetting the FBG in a small region of the core to produce the asymmetries necessary for directional discrimination. The second method inscribes a continuous structure in the cladding of a standard fibre where a long period grating has been previously inscribed. This structure in effect introduces an asymmetry that allows the device to be sensitive to the orientation of the bending. The merits of both techniques are examined, and possible methods towards more sensitive devices discussed.

Finally, we utilise the confine dimensions of these grating structures to fabricate superimposed, non-overlapping fibre Bragg gratings. The relative merits of such multiple-grating devices and their potential for applications in sensing or communications are examined in the latter part of this chapter.

5.2. Thermal properties of gratings inscribed by a femtosecond laser

There are vast amounts of studies on the dynamics of fibre Bragg gratings at different thermal conditions. The thermal expansion of the fibre and thermally related changes in the refractive index of the fibre leads to variations in the spectral behaviour of the device. For this reason, fibre gratings have been widely implemented as temperature sensors, the range of temperatures at which they may be applied is nevertheless greatly limited by the decay of conventional UV-inscribed structures under modestly high temperatures. This thermal decay, not only significantly reduces the working range of the sensing device but also its lifetime and reliability [20,127]. Although there are a number of reports of gratings with improved thermal stability using UV inscription [79], gratings decay rapidly at temperatures that range between the 300°C and 500°C, depending on the grating type.

Thermal robustness is drawing much attention towards femtosecond inscribed gratings, since structures written by infrared femtosecond lasers offer improved thermal stability due to the different mechanisms that lead to the refractive index modification [7, 15, 19]. The robustness has been demonstrated to be superior to that of the standard silica fibre, and for this reason reports have demonstrated the stability of gratings at temperatures as high as 1500°C inscribed in sapphire fibre [62]. The optimal properties of this method of inscription may lead to the fabrication of thermal sensors or other grating devices capable of operation at extreme temperatures.

5.2.1 Thermally induced wavelength shift

A fibre Bragg grating will experience under varying thermal conditions a wavelength shift due to changes in the fibre in volume (thermal expansion) and in its refractive index (thermo-optic effect). These variations have been thoroughly studied, particularly in the context of fibre sensing. The thermally-induced wavelength shift may be approximated to a linear function when the thermal changes are modest, and not exceeding temperature variations of the order of approximately 200°C [128]. Under these conditions the resonant wavelength of the grating will shift according to equation 5.1. This shift comes as a result of the thermal expansion or contraction of the material that leads to a change in the pitch of the grating and from the thermo-optical effect that leads to a thermally induced refractive index change in the material.

$$\frac{\Delta\lambda}{\lambda} = (\alpha + \xi)\Delta T \tag{5.1}$$

where α is the linear thermal expansion coefficient, approximately $0.55x10^{-6}C^{-1}$ for silica, and ξ is the thermo-optic coefficient, approximately $6.1x10^{-6}C^{-1}$ [69, 128]. Equation 5.1 indicates that the thermo-optic effect is the primary contributor to the wavelength shift. This leads to an approximation related to the resonant wavelength as shown in equation 5.2;

$$\frac{1}{\lambda_B}\frac{\delta\lambda_B}{\delta T} = 6.67x10^{-6} \quad {}^{o}C^{-1} \tag{5.2}$$

where λ_B is the resonant wavelength of the grating. Considering the preferred wavelength for optical transmissions at 1.55μm the wavelength shift is approximately 10.3 pm/°C.

The wavelength shift for a femtosecond inscribed grating should shift at approximately the same rate since the materials used are essentially the same. This was studied using an environmental chamber. Measurements were taken using a tuneable laser and a high performance analyser with a resolution of 5pm. The environmental chamber has an accuracy of 0.1°C and measures were taken after each temperature had stabilised. The results are shown in figure 5.1.

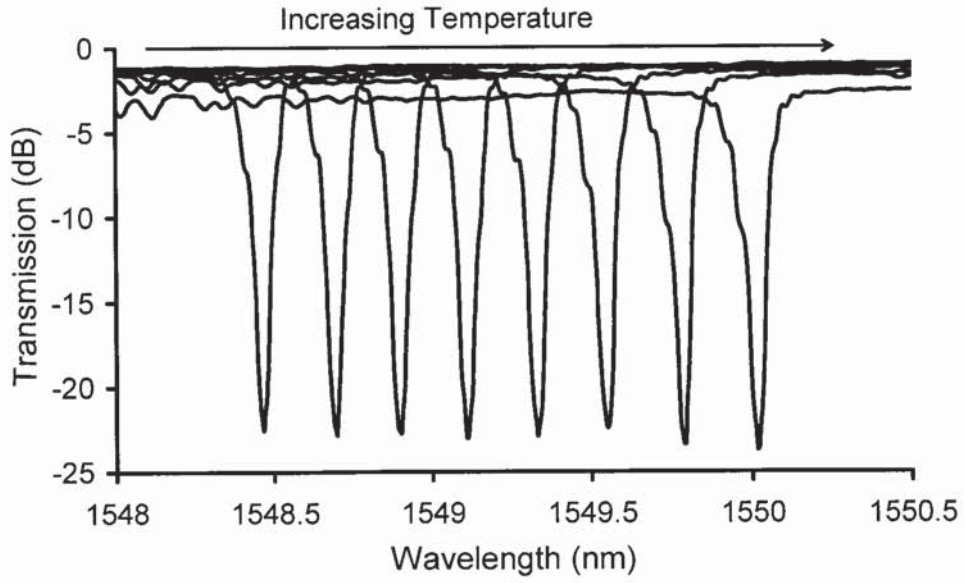

Figure 5.1: Wavelength shift of a fibre Bragg grating after successive increases in temperature in 20°C steps from 30°C to 170°C.

The result shown in figure 5.1 yields a temperature dependent shift of 11pm/°C, in line with the shift predicted by equation 5.2. The wavelength shift as a function of the temperature change and its linear approximation are shown in figure 5.2

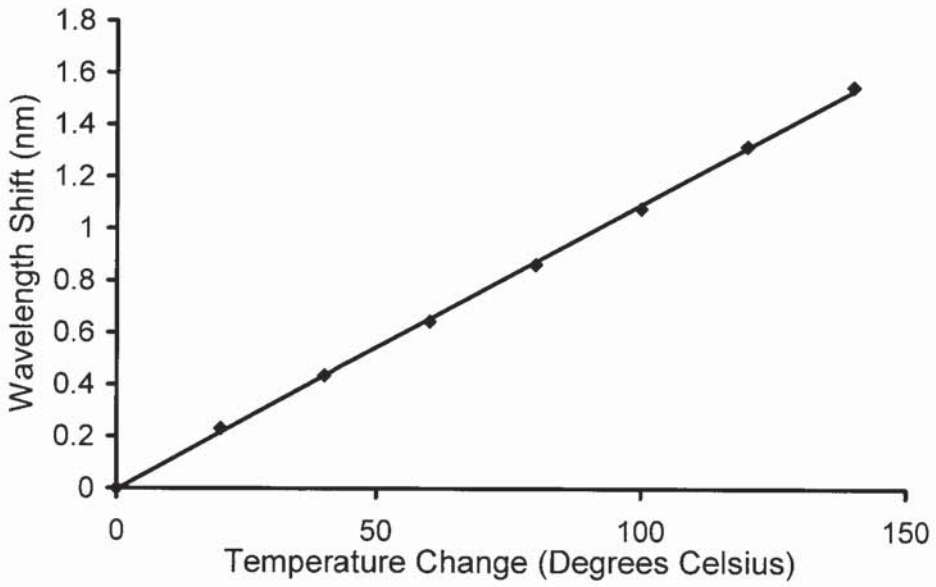

Figure 5.2: Wavelength shift as a function of the temperature change from the data of figure 5.1.

Three different gratings were studied simultaneously one of which had been annealed previously at high temperatures (600°C), identical wavelength shifts were observed for the three samples, no changes were observed in the spectral characteristics of the gratings.

The commonly adopted linear approximation is suitable for standard gratings since they do not operate at high temperatures and, as seen in figure 5.2; it is also applicable to femtosecond inscribed gratings. It is however necessary to take into account second order thermal effects when studying the thermal evolution at higher temperatures [129-130]. The thermally-induced wavelength shift is in this case given by a Taylor expansion such as described in equation 5.3;

$$\frac{\Delta\lambda}{\lambda_B} = (\alpha + \xi)\Delta T + \alpha^{*}(\Delta T)^2 + Higher\ order\ terms \qquad (5.3)$$

At low thermal changes the second order component can be neglected, it must however be considered at high temperatures. In figure 5.3 the wavelength shift at temperatures up to 600°C is studied. For this study a tube furnace oven was used and a thermostat was used to measure the temperature in the centre of the oven. The accuracy of these measurements is significantly

lower than that of the environmental chamber previously used. This is because the temperature gradient was significant across the length of the oven and measuring the temperature at the exact position where the grating is located is complicated. Furthermore the temperature gradient led to chirping in the spectral profile of the grating.

Despite these inaccuracies, the furnace tube oven was used since it could reach temperatures up to 1200°C. The temperature was measured using a thermo-coupler and there was evidence of a temperature gradient of tens of degrees across the ~50cm furnace oven, The gratings of approximately 15mm to 40mm were placed in the centre of the oven to reduce the effect of this thermal gradient to the minimum. The dynamics of the grating shift are illustrated in figure 5.3.

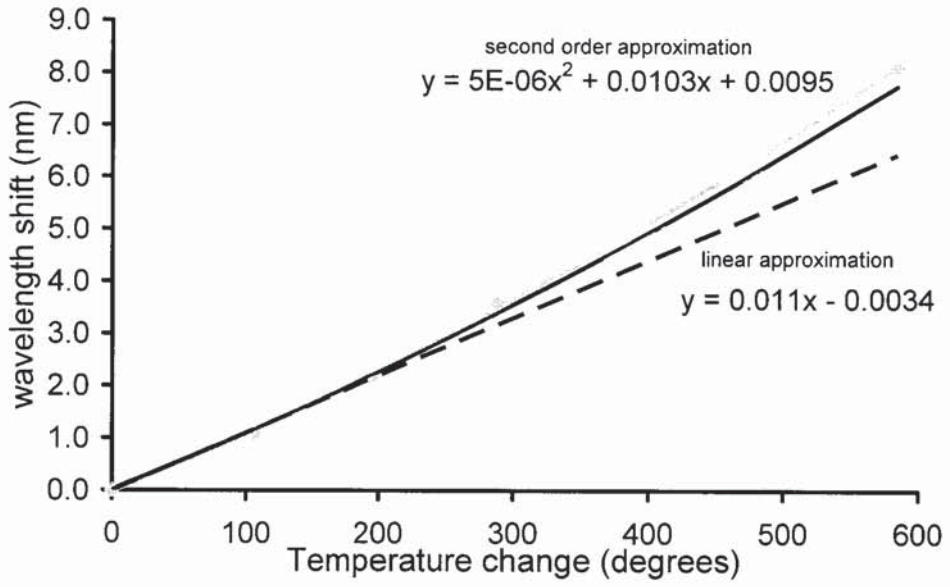

Figure 5.3: Wavelength shift of a grating at high temperatures. This figure shows the nonlinear relationship at high temperatures of the resonant wavelength and temperature.

From figure 5.3, it is clear that the linear approximation yields a large error for high temperatures and it is necessary to use a second order approximation. This approximation can be extract from our experimental results and is given by equation 5.4;

$$\Delta\lambda(pm) = 10.3\Delta T + 0.005(\Delta T)^2 \tag{5.4}$$

It is worth noting that the first order coefficient from equation 5.4 is in close agreement with the expected value considering thermal expansion and the thermo-optic effect.

The nonlinear behaviour of the thermally-induced wavelength shift is evident from figure 5.3. At low temperatures (up to 200°C), the wavelength shift is ~11pm/°C while at 600°C the response was in the order of 16pm/°C. A second order approximation to the results obtain in the furnace oven yield a linear coefficient of 10.4pm/°C, which is in very good agreement to the linear coefficient reported in literature of 10.3pm/°C, the second order coefficient was measured to be $6x10^{-3}$pm/°C^2. The small discrepancy between the coefficients estimated from the environmental chamber results and the furnace oven results are a consequence of the errors inherent to measurements in the oven.

Up to approximately 500°C, thermal expansion is linear; the glass acts in this range as a true solid. At temperature above 500°C thermal expansion is expected to slow down and show anomalous behaviour as a result from structural changes in the glass, different mechanical relaxation process take place rearranging the glass structure towards equilibrium. At higher temperatures in the order of 1100°C the silica starts to dissociate deteriorating the wave-guiding properties of the fibre [131]. There is not available literature on the thermo-optic coefficient at elevated temperatures. Thus, further analysis will be required in order to fully characterise the spectral behaviour of gratings inscribed by femtosecond lasers. The following sections concentrate in evaluating the thermal stability at high temperatures regardless of the wavelength shift induced.

5.2.2 Thermal decay of fibre Bragg gratings

A main concern in fibre grating fabrication is the low tolerance to high temperatures. The thermal decay of fibre Bragg gratings has been studied in depth in UV inscribed fibres [20, 127], significant decay of the grating strength takes place at modestly high temperatures, and is even evident at room temperature. This decay is observed both in hydrogenated and non-hydrogenated fibre. The dynamics of this decay have been thoroughly studied and it has been demonstrated that its effect can be controlled and reduced by post-annealing [20]. This is possible since the rate of the decay is a function of temperature and time. By annealing the grating, the initial period in which the grating significantly deteriorates is accelerated, this way the device only suffers minor bleaching during its working lifetime. Pre-annealing offers an accurate and useful solution for gratings that are design to work at room temperature allowing a stable performance throughout the lifetime of the device. At higher temperatures however, UV inscribed gratings are destroyed. This limits significantly their functionality. It is been reported that inscription in special fibres such as codoped Sb-Ge fibre significantly improve the stability over standard fibres, but even for this fibre the decay implies that only 18% reflectivity would remain after 24 hours at 900°C.

Fibre Bragg gratings written by an infrared femtosecond laser offer an improved thermal stability. Thermal studies both in gratings inscribed by a phase-mask [15] and point-by-point [132] have proved to be stable up to temperature where the actual molecules of silica start to dissociate at temperature over 1000°C. Furthermore inscription have been demonstrated using a phase-mask in sapphire fibre, this way temperature sensors stable to temperatures up to 1500°C have been implemented [62].

The extremely high thermal stability is a result of the mechanisms that take place in the material in order to produce a refractive index change. Both mechanisms for UV inscription (chapter 3) and femtosecond inscription (chapter 2) have been discussed. In femtosecond inscription, at the energy levels used in this work, the modification appears after localised melting in the bulk of the material follow by densification. On the other hand UV inscription relies strongly in defect formation and compaction, and those defects are prone to recombination at high temperatures.

In order to demonstrate the expected thermal stability of fibre Bragg gratings inscribed point by point by an infrared femtosecond laser a number of experiments were carried out in which gratings were subjected to temperatures as high as 1050°C. In the initial experiment, three similar samples of fibre Bragg gratings inscribed by a femtosecond laser with reflectivity ranging from 80% to 90% were placed in an oven and annealed at constant temperatures of 500°C, 700°C and 1000°C, respectively, for a period of 24 hours. The grating spectra were monitored every 30 minutes by an analyser with a resolution of 5pm. After the annealing period, the oven was switched off and the gratings were allowed to cool down to room temperature. Monitoring of the grating spectra with 30 minutes intervals was continued during the first 10 hours of the cooling process. The oven consisted of a tube furnace such as described in the previous section. A temperature gradient in the oven leads to chirping of the grating due to the different thermal conditions across the grating. Gratings were place at the centre of the tube in order to minimise the chirp.

Two fibre Bragg gratings inscribed by UV light[2] were used as control samples. These were inscribed in hydrogenated fibre by using a 90mW beam from a CW laser operating at a wavelength of 244nm. After inscription, these gratings were post-processed by annealing at 80°C for 24 hours. The resultant reflectivity of control samples before the tests was in excess of 98%. The three control samples were subjected to the procedures of annealing and measurement identical to the ones applied to the samples inscribed by the femtosecond laser. The evolution of gratings at the temperatures above stated is presented in figure 5.4.

[2] UV- inscribed fibre Bragg gratings were fabricated by Rachel Won at the Photonics Research Group, Aston University.

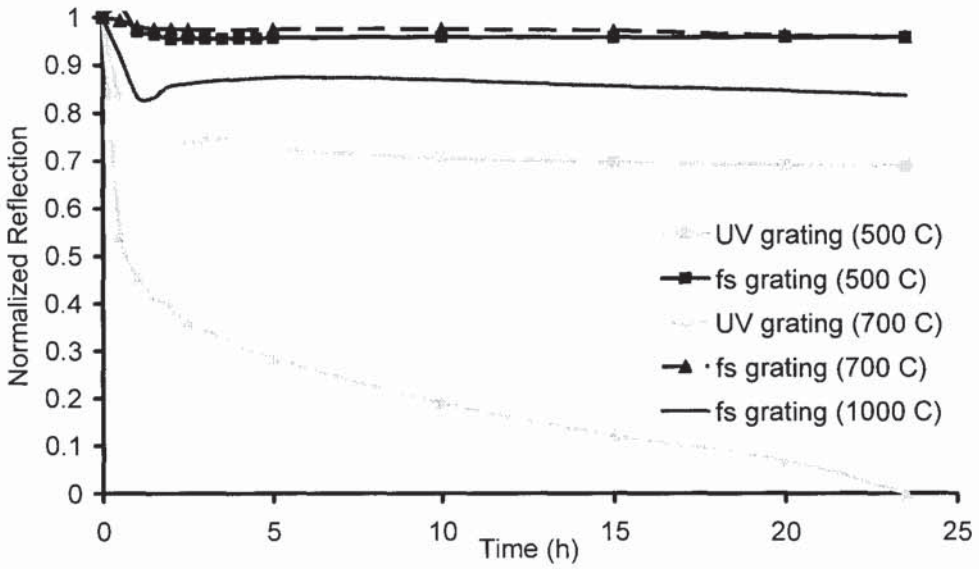

Figure 5.4: Evolution of reflection of fibre Bragg gratings inscribed point by point by a femtosecond laser and inscribed by standard UV techniques during 24-hour annealing.

It is evident from figure 5.4 that fibre Bragg gratings inscribed by an infrared femtosecond laser presented significantly improved thermal stability compared to those inscribed by UV light. The gratings inscribed by UV light suffered significant degradation at 500°C and were rapidly erased at 700°C. The gratings inscribed by the femtosecond laser only presented significant decay at temperatures of 1000°C. Comparison with similar studies from literature shows that thermal stability of the gratings inscribed with the femtosecond technique is significantly better than that of UV inscribed Type I and Type IIA gratings and is at least as stable as Type II damage gratings, based on optical damage [72]. Furthermore the degradation observed in the grating at 1000°C is likely to be an effect of degradation in the fibre rather than degradation of the grating itself.

The dynamics of the grating reflectivity when it is cooling down to room temperature are shown in figure 5.5. The gratings that endured 24 hours at 500°C and 700°C not only recovered to the initial reflection level but showed increased reflectivity.

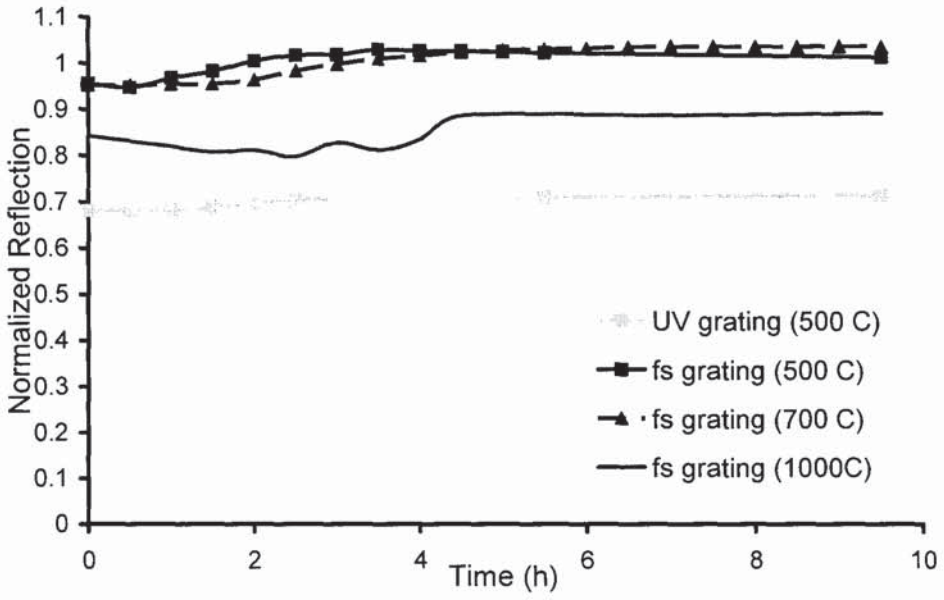

Figure 5.5: Evolution of reflection of gratings inscribed by a femtosecond laser and by UV-light during 10 hours of cooling down after 24 hours of thermal annealing at the temperatures stated.

In all cases, we observed that the grating reflectivity after cooling down to room temperature was greater than that at high temperature. This could be explained to be a result of the relaxation of mechanical stresses created in the outer regions of the modified area. Similar type of annealing at high temperatures has been previously reported in the femtosecond inscription of photonic crystals [13]. As a result, the resulting reflectivity actually increased after the annealing-cooling cycle in the gratings that endured 500°C and 700°C. Subsequent cycles at temperatures up to 600°C did not affect the grating reflectivity further. Cycles at temperatures below 200°C did not affect in any way the reflectivity of the gratings indicating that a threshold temperature at which the mechanical stresses are relaxed should be between 200°C and 500°.

The spectral evolution of the grating as it is cooling down to room temperature after 24 hours at a temperature of 700°C is shown in figure 5.6. The initial transmission spectrum in the pre-annealed grating is also presented.

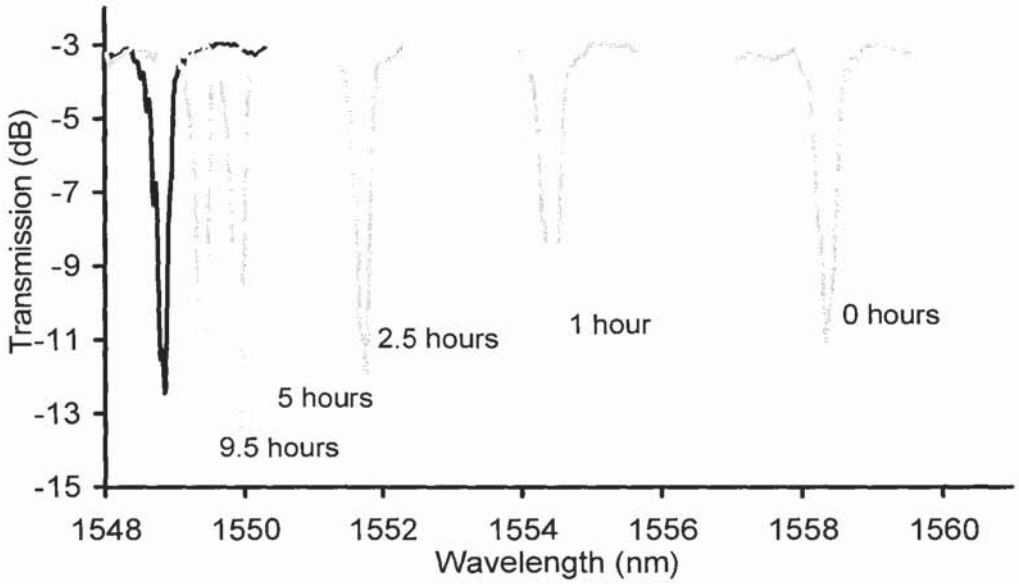

Figure 5.6: Spectral evolution of a fibre Bragg grating during the cooling down process after 24 hours at 700°C. Trace in black correspond to the pre-annealed FBG, it was shifted -1nm for clarity.

In the next experiment, the same femto-inscribed grating was annealed successively at increasing temperatures of 500°C, 700°C, 900°C, 1000°C and 1050°C. Annealing at each temperature lasted for 20 hours, after which the grating was allowed to cool down for 5 hours to room temperature before the next annealing cycle. The dynamics of the grating reflection during this experiment is shown in Figure 5.7.

The reflectivity of the grating dropped during each heating period and subsequently increased during the cooling period, this was similar to the behaviour observed in the experiment described above. Summarising, a certain increase in the reflectivity was observed after heating-cooling cycles at temperatures of 500°C and 700°C. The 900°C cycle produced a small overall reduction of reflectivity and, the 1000°C cycle caused a significant permanent degradation of the grating performance. Finally, annealing at a temperature of 1050°C practically erased the grating, rapidly and irreversibly reducing the reflection coefficient to a level below 20%.

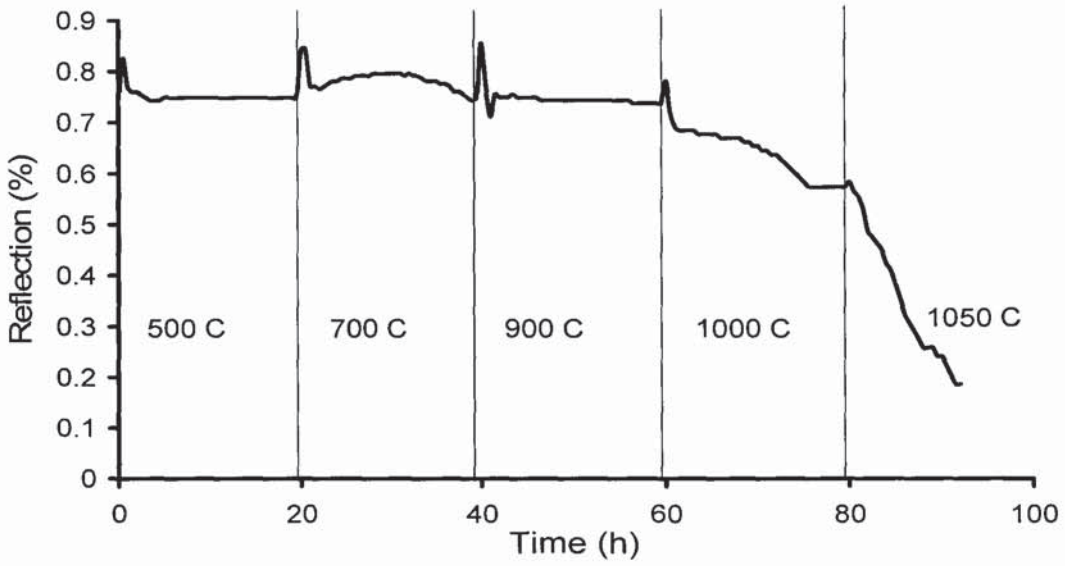

Figure 5.7: Dynamics of the reflection of the fibre Bragg grating at the resonant wavelength during annealing at the set temperatures of 500°C, 700°C, 900°C 1000°C and 1050°C.

Overall, the results in this work are complementary to those reported in previous studies of the thermal behaviour of the structures inscribed in glass by ultrafast lasers [15, 62, 132]. Thermal stability of gratings inscribed by a femtosecond laser is comparable to that of type II, UV-inscribed gratings formed by optical damage. Reports in literature indicate that gratings inscribed using a phase-mask and an infrared femtosecond laser have different thermal stability depending on the fluence used for inscription. The gratings inscribed by phase-mask with the highest thermal stability were the ones with the higher fluence, and those present a thermal stability equivalent to that reported in this work.

Summarising, gratings inscribed by a femtosecond laser were thermally stable up to temperatures of the order of 1000°C. This represents a significant improvement compared to the conventional, UV inscribed gratings. Dynamics of reflectivity during the annealing-cooling cycles indicates, in particular, that the strain in the material volume adjacent to the modified region is a significant factor affecting the performance of the grating.

5.2.3 Thermal annealing of long period gratings inscribed by a femtosecond laser

In order to study the thermal stability of long period gratings inscribed by femtosecond lasers, we subjected a sample to temperatures increasing in steps from 200ºC and 825ºC. In figure 5.8, we can see the dynamics of the thermal annealing of the grating inscribed by the method of femtosecond point-by-point inscription. The results obtained are not equivalent to those previously observed for the Bragg gratings. Bragg gratings inscribed by femtosecond lasers presented thermal stability at temperatures as high as 900°C. In long period gratings, significant decay was observed even at modest temperatures between 100°C and 200°C.

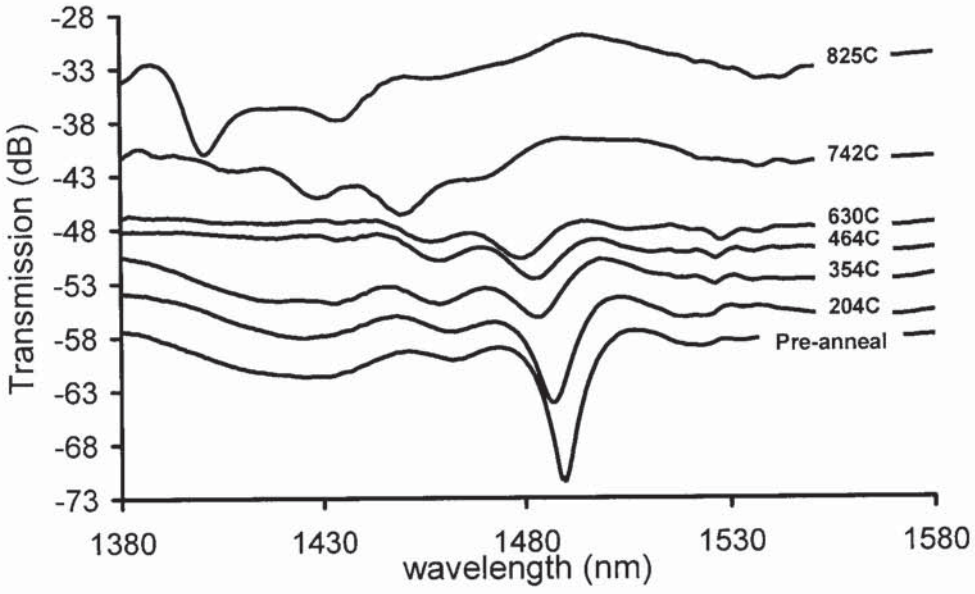

Figure 5.8: Dynamics of a long period grating inscribed point-by-point by a femtosecond laser under increasing temperatures.

The complexity on the behaviour at high temperatures of the long period grating, and the fact the long period gratings are generally longer than Bragg gratings suggests that the gradient in temperature of the furnace oven where the studies were conducted, may affect more drastically the measurements presented in figure 5.8. Further studies are been conducted to investigate the dynamics of long period gratings inscribed with various pulse energies, and scanning

speeds. Nevertheless from the preliminary data presented in figure 5.8, relevant information can be extracted.

Figure 5.9(a) indicates the decay of the attenuation band as a function of temperature. This was measured at room temperature after a period at the given temperatures. Figure 5.9(b) indicates the permanent shift in the central wavelength of the attenuation band after annealing.

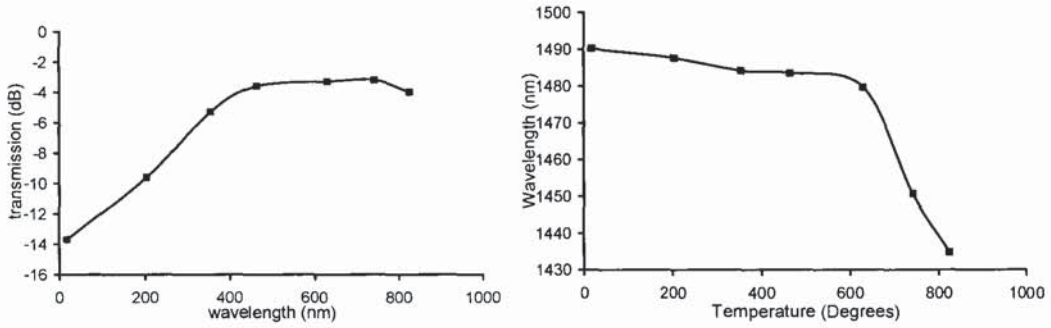

Figure 5.9: (a) Decay in the strength of the attenuation band after annealing, (b) permanent shift endure by the attenuation band after annealing.

In figure 5.9(a), we can see a rapid decay at the initial temperature which tends to stabilise after temperatures between 400°C to 500°C, when the attenuation band is approximately 4dB dip. On the other hand, in figure 5.9(b) we observed a slow blue-shift in the central wavelength, followed by a drastic blue-shift after temperatures in the order of 600°C.

5.2.4 Discussion on the discrepancy between the thermal stability of fibre Bragg gratings and long period gratings

The dynamics of annealing of fibre Bragg gratings and long period gratings present significant differences, Bragg gratings present strong thermal stability, withstanding temperatures as high as 1000°C (figure 5.4 and 5.7), while the strength of long period gratings starts to decay at temperatures below 200°C (figure 5.8). The reason for this can be found in the method of inscription and the nature of the devices inscribed. If we consider the structure produced by a single pulse in the fibre, it can be described as a central region with a negative refractive index surrounded by an area with a positive change. In addition, the laser light is believed to affect a larger region in which stress changes lead to a higher refractive index. When this feature is

inscribed periodically in the fibre in order to create a fibre Bragg grating, the stress induced by the laser due to its large dimensions compared to the period of the grating reduces the visibility of the index modulation. In the case of the long period gratings, a continuous structure is inscribed. This means that the laser is focused in an area which has already been modified, therefore affecting the focusing conditions of subsequent pulses. This should lead to a more dominant presence of photo-induced stresses. In the case of long period gratings the stress and positive index changes can contribute positively to the period of the structure since the dimensions of the period are orders of magnitude larger than in the case of a Bragg grating and therefore in that case the periodicity is not affected by overlapping of neighbouring pitches.

5.3. Inscription of fibre Bragg gratings through the coating

Development of fibre Bragg grating inscription has rapidly evolved since the first demonstration of inscription by side exposure to UV light in the late 80s. Methods of inscription have been greatly refined to the point that gratings are nowadays widely used in areas such as communications and sensing. Nevertheless, conventional inscription methods still require the removal of the protective polymer coating of the fibre prior to inscribing the grating. This is mandatory since the standard polymer used for coatings is opaque to the UV light used in inscription. The removal of the coating leads to a longer fabrication process and a reduction in the fibre strength.

Inscription through the coating has been demonstrated by a number of methods. Using near UV light [23] permits inscription through the conventional coating since the polymer is less absorbent to the wavelengths used (between 300nm and 364nm), but this technique requires a special phase mask suitable for the source wavelengths and high doping concentrations (up to 30mol% of Germanium) or the used of additional dopants such as Tin [24] or Boron [23] to compensate the reduced photosensitivity to near UV light. Other methods use special coatings which are transparent to UV light [25, 26]. These methods permit the inscription of highly reflective gratings with the added advantage of using the conventional wavelengths for inscription (244nm and 248nm). This means that gratings are inscribed using standard phase-masks and a standard concentration of dopants. They do require however special coatings making this solution less cost effective. More complex methods have been proposed such as inscribing the grating directly as the fibre is been pulled [133], with the resulting reduced flexibility for inscription.

Inscription of fibre Bragg gratings through the coating using infrared femtosecond lasers is feasible. In particular, the proposed method to inscribe highly reflective Bragg gratings using a point-by-point technique poses significant advantages for this task. In this section, we demonstrated for the first time the inscription of highly reflective gratings through a standard acrylic coating in non-photosensitised fibre.

5.3.1 Inscription and characteristics of gratings inscribed through the coating

Infrared femtosecond pulses are particularly suitable for inscription through the coating. This is the case because neither core, cladding nor polymer coating present linear absorption at the

wavelength of the laser emission. Structural changes rise from highly nonlinear processes such as multiphoton absorption. As a result structural changes are strongly dependent on intensity. It is therefore, in principle, possible by tightly focusing the beam in the core to create the grating without affecting the coating.

Inscription of long period gratings had been attempted previously with infrared femtosecond pulses [36], only to ablate the polymer coating before any change in the core was observed. This can be explained since surface threshold ablation for the polymer is significantly lower than the threshold in bulk silica, and in that experiment a 20X microscopic objective was used, therefore the gradient of the intensity was not sufficient to make up for the discrepancy between the core and coating thresholds. This result indicates that, the inscription of gratings through coating in standard fibre may not be possible by using a phase mask and an infrared femtosecond laser since tight focusing is not achieved.

Inscription of fibre Bragg gratings through the coating by an infrared femtosecond laser is achievable using the point by point technique described in this work. The method maintains the properties and advantages which were previously detailed for bare fibre gratings, such as; not requiring special coatings, a photosensitive fibre or a special phase mask, thermal stability and polarisation sensitivity. Additionally, the mechanical strength of these gratings is significantly greater than that of gratings inscribed in bare fibre by the same method.

The inscription process is as detailed in section 4.2, the pulse energy was approximately 1μJ, roughly double the required energy for inscription of an equivalent grating in bare fibre. Gratings were inscribed in standard telecommunication fibre (SMF) and grating length ranged between 4mm and 26mm.

Infrared femtosecond inscription relies on multiphoton ionisation, since this is a highly nonlinear process the thresholds for inscription and ablation are strongly dependent on the intensity of the beam at a given plane [7]. This strong dependence on intensity permits the inscription of buried structures in transparent dielectric materials; it also allows the inscription through a material with a lower threshold than the inner inscription, given the appropriate focusing conditions. Inscription in the core takes place at lower pulse energies than ablation at the surface of the coating due to the significantly lower intensity endured by the coating compared to the intensity levels present at the focal point in the core, after focusing with a microscopic objective with a numerical aperture, NA~0.55.

The difference in intensity endured by the core and the coating may be estimated considering the focusing conditions. Based on Gaussian optics and the Rayleigh criterion, $\omega_o = 1.22\lambda/NA$, where ω_o is the radius of the spot size at focal position, and λ is the laser wavelength, it is possible to estimate the beam radius at any given point along the propagation axis, equation 5.5;

$$\omega(z) = \frac{z\lambda}{\pi\omega_o n} \tag{5.5}$$

Where ω_o is the beam radius, z_r is the Rayleigh range and $\omega(z)$ is the beam radius at a given distance, z, along the propagation axis. If we assume diffraction limited focusing, and ignore the effect of self-focusing, since the intensity of the beam is inversely proportional to the square of the beam radius, we can write equation 5.6;

$$I_{Surface}\omega^2 = I_{Focus}\omega_o^2 \tag{5.6}$$

We can rewrite equation 5.6, using equation 5.5 as equation 5.7;

$$I_{Surface} = \left(\frac{\pi n}{z\lambda}\right)^2 \omega_o^4 I_{Focus} \tag{5.7}$$

Now, by introducing equation 4.1 and 4.2 in equation 5.7, we can estimate the difference in intensity between the surface of the coating, $I_{Surface}$ and the focal point, I_{focus} as a function of the numerical aperture in equation 5.8;

$$I_{Surface} = \frac{I_{Focus}}{\sqrt{1+\kappa^2 NA^4}} \tag{5.8}$$

where κ is a constant given by equation 5.9;

$$\kappa = \frac{0.61^2 \pi n\lambda}{z} \tag{5.9}$$

From equation 5.8 it is possible to write an equation to estimate the minimum numerical aperture, NA_{min}, for a fibre with given dimensions of coating radius, z, and threshold for material change of both coating, $I_{th,\,coating}$ and core, $I_{th,\,core}$, as shown in equation 5.10;

$$NA_{\min} \geq \sqrt{k\frac{I_{th,\,core}}{I_{th,\,coating}}} \tag{5.10}$$

This estimation only takes into account Gaussian optics, and does not consider deviations in the focusing and hence intensity that may rise from effects such as self-focusing or aberrations due to the focusing through the cylindrical surface and not at the optimum focusing depth.

An illustration in the way in which the beam is focused through the coating of a fibre is shown in figure 5.10, including the relevant parameters in the process such as the beam radius and the Rayleigh length.

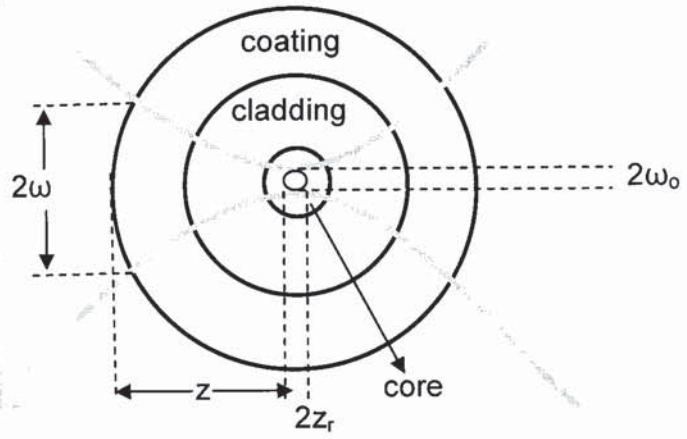

Figure 5.10: Illustration of the focusing conditions through the cladding, with the key parameters for inscription through the coating.

Considering the focusing conditions, the beam radius at the coating surface (z~125μm) is larger than the beam waist (ω_o~1μm, z_r~1.5μm) by an approximate factor of 80. The intensity at the region where the grating is inscribed is therefore three orders of magnitude higher that the intensity at the surface of the coating. Much information on the irradiance threshold for structural changes in silica can be found in literature, which typical ranges between 3-4x10^{13}W/cm^2, less work has been carried out in plastics, such as the acrylic of the coating of the fibre. Only for estimation we will consider the irradiance used for the inscription of a bulk grating in a PMMA polymer of approximately 10^{12}W/cm^2. Using this values and equation 5.10 to estimate the minimum numerical aperture, it yields a value in the region of NA~0.5. In order to consider equation 5.10 as a quantitative equation rather than a qualitative explanation of the need for tight focusing, it is necessary to carry out a study on the threshold for the coating material, and to introduce deviations from the Gaussian focusing conditions.

In figure 5.11, we can see the transmission and reflection spectral characteristics of a 5 mm long fibre Bragg grating inscribed through the coating of a standard single-mode fibre. A grating

strength of -16dB was observed at the resonant wavelength for this grating, the bandwidth of the grating was ~0.3nm. The inscription of this grating induced 0.3dB non-resonant losses. Gratings of lengths between 5mm and 15mm, typically induced losses of less than 1dB. Bandwidth ranged from 0.1nm to 0.3nm depending on grating length and uniformity.

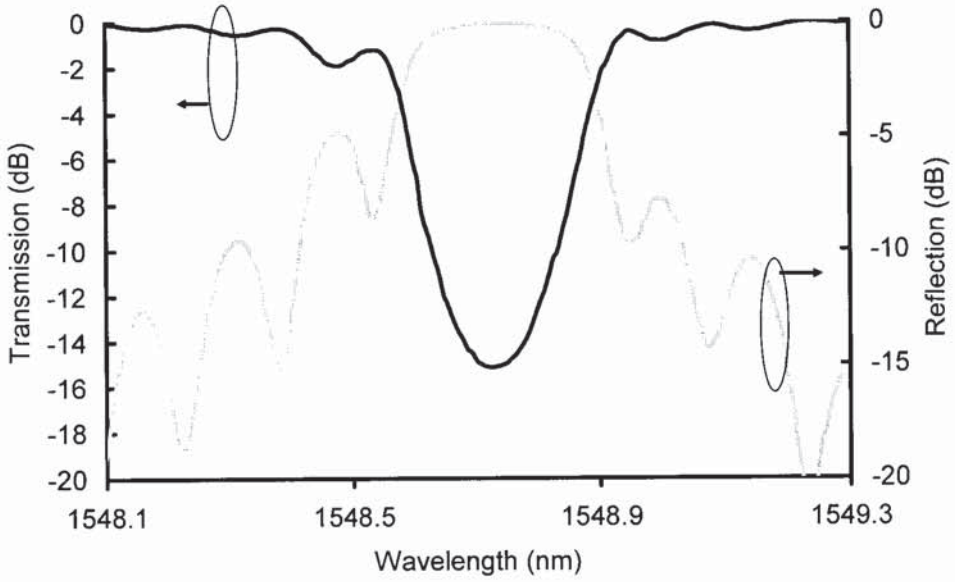

Figure 5.11: Reflection and transmission spectra of a uniform 5mm-long second order grating inscribed through the coating in a standard single-mode fibre.

Since the cladding is not directly exposed to air, coupling to forward propagating cladding modes is significantly reduced compared to fibre Bragg gratings in bare fibre. However, as it can be observed in figure 5.12, at lower wavelengths losses can still be observed from this interaction. Losses due to coupling to the cladding modes rise from the high refractive index changes induced in the fabrication of the grating and due to the geometry of the structures inscribed enhancing the scattering of the propagating light to the cladding.

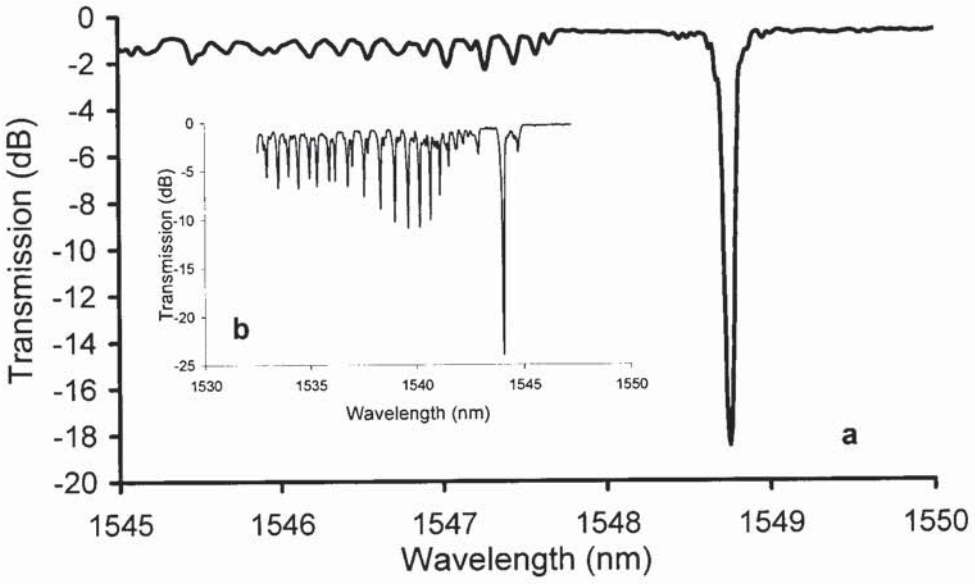

Figure 5.12: (a) Transmission spectra of an 8mm long grating, presence of coupling to cladding modes is reduced but still significant despite inscription through coating. (b) Typical transmission spectra of grating inscribed in bare fibre, strong presence of coupling to cladding modes.

Such as in bare fibre, gratings with a stronger reflection can be inscribed by inscribing longer gratings and using higher pulse energies. Figure 5.13 shows the transmission profile of a 26mm grating, a certain level of deterioration in the uniformity of this grating is evident in the transmission spectra of this grating, product of the tension changes within the fibre during the inscription process of long fibre Bragg gratings, and external vibrations.

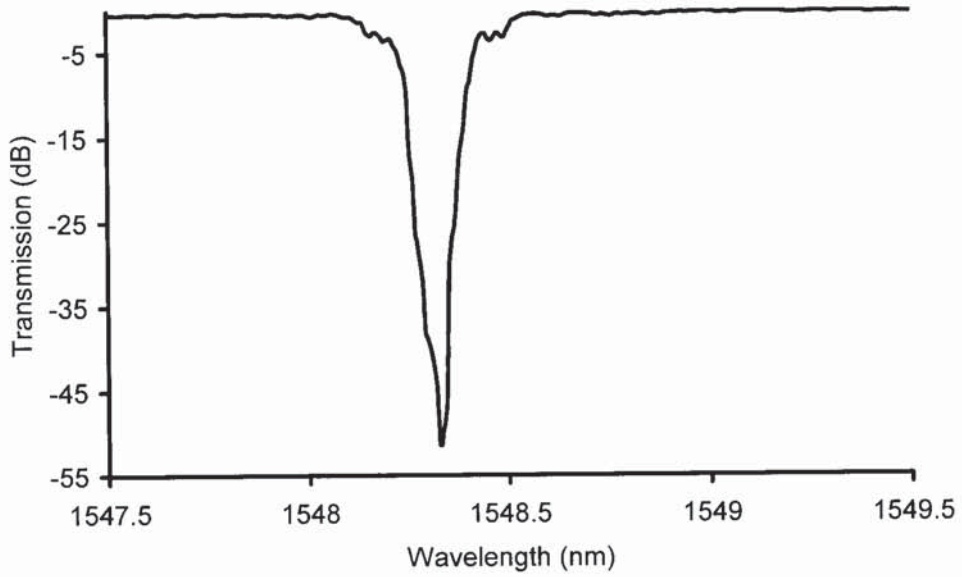

Figure 5.13: Transmission spectra of a 26mm long grating inscribed through the coating of a standard fibre. Out of band losses in this grating were 2.0dB, Transmission at resonant wavelength is -50dB. Chirp in the grating indicates lack of uniformity during inscription for long gratings.

5.3.2 Strain induced wavelength shift

The resonant wavelength of a fibre Bragg grating will vary as a function of strain in the fibre following equation 5.11 [18];

$$\lambda_B = 2n\Lambda\left(\left[1-\left(\frac{n^2}{2}\right)\left[P_{12}-\nu(P_{11}+P_{12}\right]\right]\varepsilon\right) \tag{5.11}$$

where P_{ij} are the Pockell's coefficients of the electro-optic tensor, v is Poisson's ratio, ε is the applied strain.

The properties of UV-inscribed fibre Bragg gratings under strain have been thoroughly studied and are relevant for a number of the main applications of fibre Bragg gratings, such as fibre laser tunability or strain sensing. The sensitivity of fibre Bragg gratings to strain rises from the inherent properties of the material and should therefore not depend significantly on the

inscription method. Equation 5.12 determines the wavelength shift of the resonant frequency as a function of longitudinal strain.

$$\frac{\Delta\lambda_B}{\lambda_B} = (1 - p_e)\varepsilon_Z \tag{5.12}$$

Where λ_B, is the resonant wavelength of the grating, p_e is the photo-elastic coefficient which represents the effect of strain in the refractive index of the fibre and is roughly 0.22 for silica glass and ε_z, is the longitudinal strain along the fibre. Leading to equation 5.13;

$$\frac{1}{\lambda_B}\frac{\delta\lambda_B}{\delta\varepsilon} = 0.78x10^{-6}\,\mu\varepsilon^{-1} \tag{5.13}$$

This means that for a resonant wavelength of 1550nm the expected wavelength shift is approximately 1.2nm.mε^{-1}. Figure 5.14 shows the response of a fibre Bragg gratings inscribed by an infrared femtosecond laser to strain. The grating was inscribed in bare fibre, which was mechanically stripped. The wavelength shift in the femtosecond inscribed grating was ~1nm.mε^{-1}.

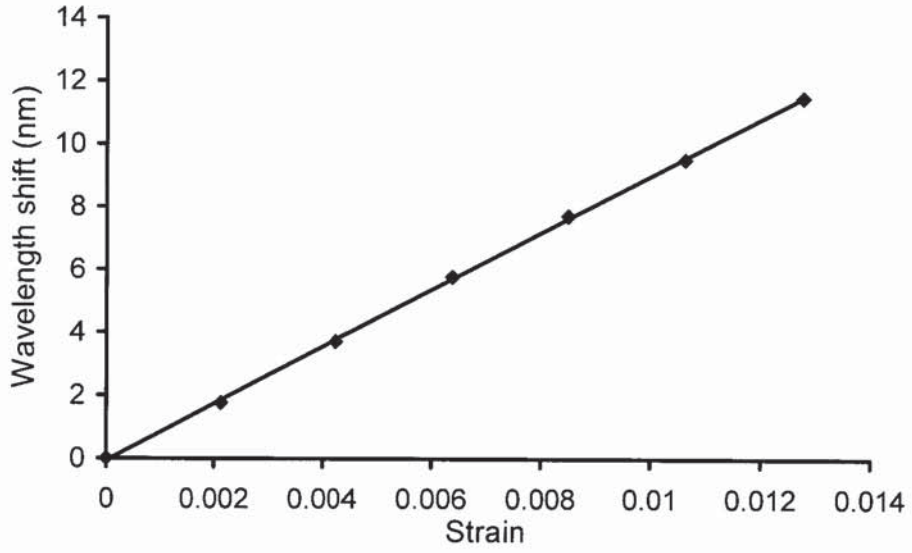

Figure 5.14: Strain sensitivity of a grating inscribed point-by-point by an infrared femtosecond laser in bare fibre. Strain is measured as the elongation, Δl, over the length of fibre, l, placed under the strain.

5.3.3. Mechanical strength after femtosecond inscription

Inscription of fibre Bragg gratings reduces the strength of the bare fibre. There are also reports in literature that indicate that hydrogenated and germanium doped fibres are less resistant to strain [134]. Thus, the mechanical strength is reduced in all three steps during fibre Bragg grating fabrication; photosensitising, removing the coating and inscribing in the fibre. The tensile limit prior to breaking the fibre is approximately 1% for the standard gratings inscribed by UV-light. This means that the resonant wavelength can be tuned roughly 10nm prior to fracture [135, 136]. The failure of a bare single-mode fibre unexposed to either UV or infrared femtosecond light fails at around 0.92GPa. This would represent a wavelength shift of ~16nm prior to failure if a grating was inscribed without affecting the strength of the bare fibre. Inscription at the preferred wavelength of 248nm reduces significantly the strength of the grating to failure at 0.69GPa which leads to a maximum wavelength shift of approximately 11.8nm.

A number of factors must be considered regarding the mechanical strength degradation present during inscription by femtosecond lasers. During femtosecond inscription the fibre suffers the effect of high intensities. Thus, we would expect a more considerable reduction on the fibre strength after inscription than it is observed by UV methods. On the other hand, Inscription by infrared femtosecond lasers is possible in non-photosensitive fibre. This means that the initial strength of the fibre prior to inscription is higher for methods based on femtosecond inscription than for methods based on UV inscription.

An experiment was carried out in order to estimate the strength of fibre Bragg gratings inscribed point by point by a femtosecond laser. The objective of this experiment was first to compare the mechanical strength with gratings inscribed by other methods, and second to compare it with gratings inscribed through the coating. Ideally, this experiment must be carried out in tens of gratings due to the statistical nature of the breakage of the fibre, particularly in bare fibres. In this case, we only measure the tensile limits for four gratings inscribed in bare fibre and four inscribed in coated fibre. Therefore these results may be used for guidance on the behaviour of these fibres but not as a complete result. A systematic investigation will be carried out in the near future to investigate fully and comprehensibly the mechanical limits of these gratings.

The maximum strain before failure varied significantly. Maximum wavelength shifts ranged from approximately 9nm to 13nm. This represents maximum strains between 1% and 1.5%. In figure 5.15, the evolution of a grating under strain is presented. The large variations in this result can be partly credited to the mechanical stripping of the fibre which is known to lead to uneven reductions of the strength by introducing micro-cracks. Studies in chemically stripped fibre must be carried out in order to eliminate this source of error. In any case, these results indicate that

gratings inscribed point by point by a femtosecond laser present a mechanical strength similar to that of gratings inscribed in identical fibres with conventional UV methods.

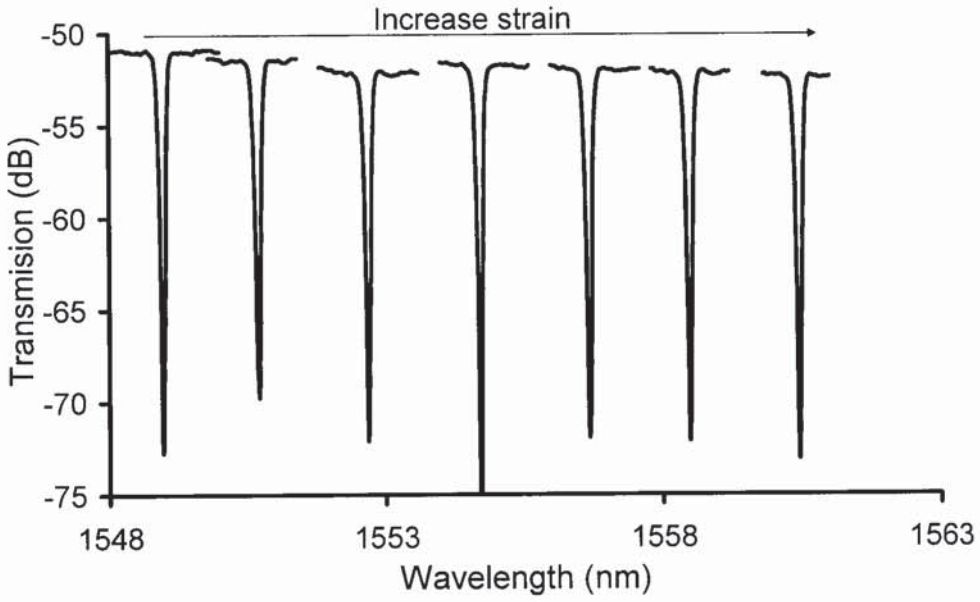

Figure 5.15: Dynamics of the transmission spectra of a fibre Bragg grating inscribed by an infrared femtosecond laser under increasing strain until strain-induced fibre failure.

The mechanical strength of the grating is affected by the inscription process but it remains mainly constrained by the strength of the material itself. The flexibility of femtosecond inscription to fabricate structures in a wide variety of materials offers the possibility to inscribe gratings in fibres more robust to strain should it be required for specific applications such as fabricating widely tuneable fibre lasers or robust strain sensors. This flexibility is not available in UV inscription where the number of materials in which inscription is feasible is very limited.

5.3.4 Mechanical strength of gratings inscribed through the coating

After inscribing fibre Bragg gratings through the coating of a standard fibre, we examined under the microscope the surface of the fibre in search for any evidence of photoinduced damage. Microscopic examination of the fibres did not reveal any modification on the coating. A significant level of damage in the coating is unlikely since it would affect the focusing conditions

of the beam and would have ultimately prevented from successfully inscribing the grating. However, a detailed study on induced strains in the coating would be required to rule out any inscription-related deterioration of the fibre.

As it was mention in the previous section, the stripping and handling of bare fibre contributes to reduce the overall mechanical strength of the fibre [134]. Furthermore the inscription of fibre Bragg gratings by conventional UV methods contributes to the mechanical degradation of the device. This leads to a maximum strain tuning of the Bragg grating limited to approximately 10nm [135, 136]. In order to compare the mechanical strength of coated and bare fibre, a total of four gratings inscribed in bare fibre and four gratings in coated fibre were strained until failure. In figure 5.16, the wavelength shift under strain of gratings inscribed through coating is presented.

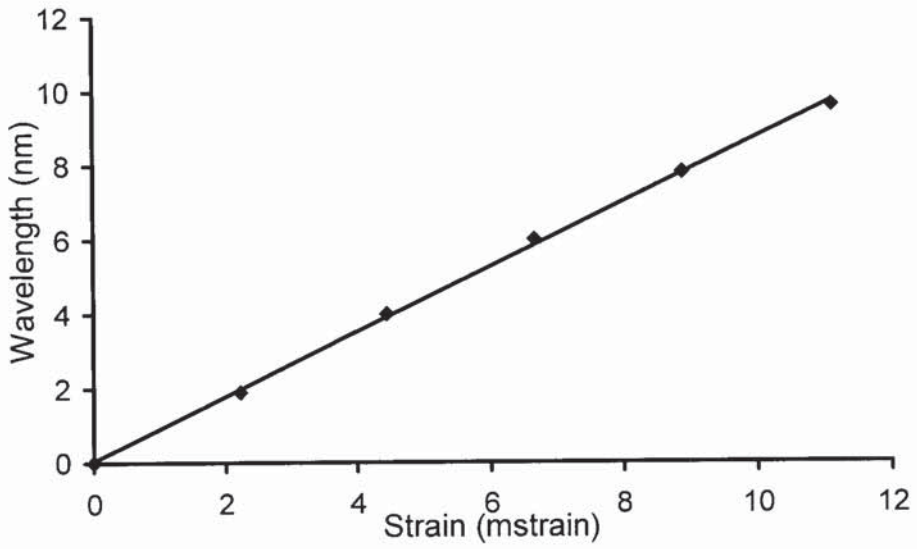

Figure 5.16: Strain-dependent wavelength shift of a grating inscribed through the coating in a single mode fibre. Strain is measured as $\Delta l/l$ where Δl is the elongation and l is the length of the fibre elongated.

The resulting sensitivity to strain of the grating is unaffected by whether the grating was inscribed in bare or coated fibre, evidently this was expected since the sensitivity is only related to the mechanical properties of the core.

Figure 5.17 presents the dynamics under increasing strain of the transmission spectra of a grating inscribed through the coating. The apparent different grating strengths in the grating profile observed in figure 5.17 rises from the transmission dip been close to the noise level of the spectrum analyser and its low resolution, 50pm.

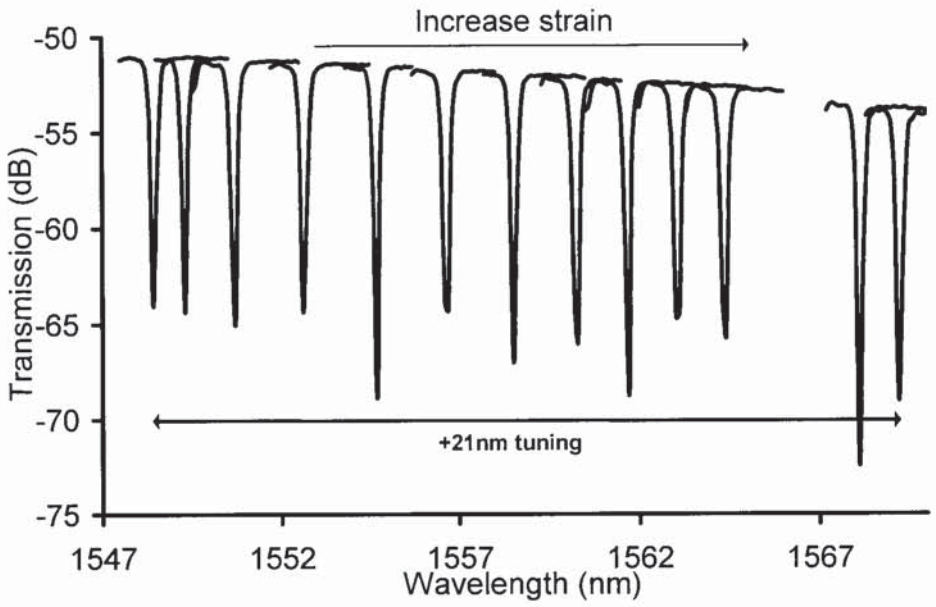

Figure 5.17: Wavelength shift induced by increasing strain for a grating inscribed by a femtosecond point by point in (a) bare fibre and (b) coated fibre.

The maximum wavelength shift induced by strain in bare fibre varied significantly from 9nm to 13nm, which considering the strain response of silica [18] is equivalent to strains of 0.75mε to 1.1mε [134]. This fluctuation rises from the inconsistent introduction of micro-cracks during the stripping process and the handling of the bare fibre. Nevertheless, result indicates that gratings inscribed by femtosecond lasers point-by-point in bare fibre have mechanical strengths comparable to those inscribed by UV methods.

The maximum wavelength shift in the coated fibre ranged between 21nm and 22nm, which indicates strains of the order of 1.8mε, a significant increase in strength compared to gratings inscribed in bare fibre by the same method.. The coated gratings not only present a higher mechanical strength but also a better determined breakage threshold.

5.4 Fibre Bragg grating-based directional bending sensors

Direction-sensitive, or vectorial, fibre grating sensors have been the subject of intense research for many years. The development of bending sensors has gather attention due to its numerous applications in smart structures in engineering and biomedical applications [18]. The fabrication of such devices requires more complex solutions due to the characteristics of the measurand. For instance, fibre Bragg gratings are generally not sensitive to this measurand, as a result long period gratings are conventionally used for this purpose. Nevertheless while long period gratings in standard fibre are bend-sensitive, they do not offer directional-sensitivity. Thus, more complex and expensive solutions are needed. In this section, a novel fibre Bragg grating with directional sensitivity to bending is presented.

5.4.1 Bending sensitivity of an asymmetric fibre Bragg grating

In general, vector sensors based on fibre gratings can only be realised in specially designed fibres, such as multicore fibres, D-shaped fibres, Flat-clad fibres, etched fibres and eccentric core fibre [137-140]. Figure 5.18 illustrates the cross-section of various fibre designs that have been used for the inscription of bending sensors.

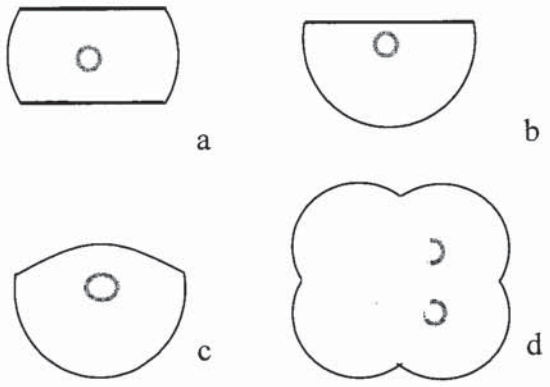

Figure 5.18: Scheme of the cross section of various fibre designs for the fabrication of vectorial sensors; (a) flat-clad fibre, (b) D-shape fibre and flat-clad fibre, (c) single-mode fibre after plasma etching and (d) multi-core fibre.

In all these devices, the direction-selective sensitivity is based on the broken cylindrical symmetry of the fibre. These devices offer the desired vectorial sensitivity, but the drawbacks of using these fibres are evident, both during fabrication and interrogation. Not only these fibres are more expensive but the alignment and inscription in these fibres is more complex due to the asymmetric shape. Interrogation techniques must also be adapted to the fibre and splicing to a standard fibre incurs in higher losses. These difficulties result in the higher manufacturing cost of these special fibres and the need for dedicated coupling and complex interrogation techniques which considerably reduce the practicality of this type of sensors [137-140].

Fabrication of vector sensors in fibres of conventional, circular, geometry would be a very attractive proposition as this would alleviate the need for special fibres and reduce the complexity and cost of the interrogation systems. A straightforward way to achieve directional sensitivity would be to introduce the required asymmetry by the inscription process itself. However, this is difficult to realise by using conventional UV inscription techniques, since these techniques usually affect a large fraction of the cross-section of the core and generally do not allow precise control of the transverse structure of the inscribed features. As it has been extensively documented in the previous chapter, precise positioning and high-contrast of introduced modifications in the fibre material can be achieved by employing femtosecond laser inscription. This permits the fabrication of a novel, direction-sensitive bending sensor based on an asymmetric fibre Bragg grating inscribed by an infrared femtosecond laser.

The technique is based on tight transverse confinement of the femto-inscribed structures. This confinement of the induced modification of material within a fraction of the fibre cross-section is characteristic of the point-by-point method, other femtosecond techniques use phase-mask based technology which leads to grating cross-sections as large as the cross section of the core. Point by point, it is possible for Bragg grating structures to be precisely placed in any desired location within or in the vicinity of the core. The transverse size and shape of the structure can be controlled by the focusing conditions and the exposure regime. By inscribing an axially-offset fibre Bragg grating, an intrinsically asymmetric sensing device can be produced. When acting as a bending sensor, the device shows a shift of the Bragg resonance which depends on the orientation of the grating structure with respect to the bending direction.

5.4.2 Inscription of asymmetric fibre Bragg gratings

The inscription process was identical to that described in section 4.2 of the previous chapter. Standard single-mode fibre was used and the pulse energy after the objective was approximately 0.5μJ. The asymmetry of the device was induced by focusing the beam away from the centre of the core in a plane located 3μm before the fibre axis. The length of the fabricated grating was 40mm. The overall characteristics of the grating did not differ from those reported in chapter 4. Figure 5.19 shows the proposed structure of the device, with the grating structure away from the geometrical centre of the core.

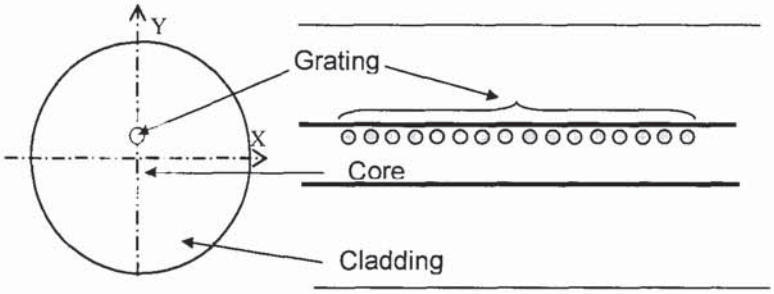

Figure 5.19: Schematic of the cross-section profile of the fibre grating

Figure 5.20 shows a microscopic image of the cross-section of a grating structure equivalent to that used in this experiment. The grating was inscribed with a displacement of 3μm from the centre of the core. The grating cross section was slightly elongated along the direction of the laser beam with the transverse dimensions of 1μm by 1.5μm, approximately. As it has been discussed previously in this section, this inscription method directly induces the asymmetry required for the fibre Bragg grating to be direction sensitive. The device was inscribed in a single-mode fibre permitting a simple interrogation scheme.

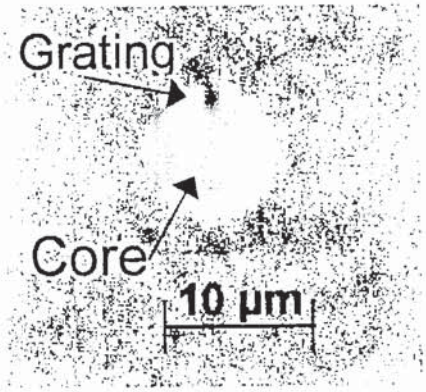

Figure 5.20: Microscope photograph of the cross-section of the grating proposed as a directional sensor.

The key difficulty for the proposed method raises from the low sensitivity of fibre Bragg gratings to bending. Fibre Bragg gratings are not sensitive to bending since the strain and compression induced into a cylindrical body such as a fibre by bending is dependent on the distance from the radius of the cylinder, with the geometrical centre been effectively free of either elongation or compression.

Long period gratings depend on propagation through the cladding. Cladding modes spread through the cladding area and are thus affected in a stronger manner by bending than the radiation modes that propagate confined in the core and are the ones that are affected by Bragg gratings. Despite this obvious disadvantage, a fibre Bragg grating sensitive to bending is an interesting proposition since there is more flexibility to implement Bragg gratings into sensing devices which may lead to higher resolution, and more complex devices.

The following geometrical considerations were taken in order to estimate the sensitivity of the fibre Bragg grating. This estimation considers a single-mode perfectly symmetric fibre and a grating which have been inscribed with a 3µm displacement from the centre of the core. This estimation is only aiming to judge the feasibility of the device and therefore parameters such as the actual dimensions of the inscribed structures are not considered.

The length of the arc, Ω, formed by a curve fibre in its geometrical centre (illustrated in figure 5.21) is given by equation 5.14;

$$\Omega = R \times \theta \tag{5.14}$$

Where R is the radius of the circumference and θ the angle that covers the arc (figure 5.21). The centre of the symmetrical fibre does not experience neither compression nor strain but a grating which has been displaced a distance, d, from the centre would experience a strain or

compression. If we consider the grating pitch, Λ, in the geometrical centre of the fibre and one displaced from the centre of the fibre, Λ_d under the same bending conditions the pitches are given by equation 5.15 and 5.16;

$$\Lambda = R \times \theta \tag{5.15}$$

$$\Lambda_d = (R+d) \times \theta \tag{5.16}$$

Equations 5.15 and 5.16 lead to equation 5.17;

$$\Lambda/R = \Lambda_d/(R+d) \tag{5.17}$$

since the resonant wavelength, λ_B, is directly proportional to the pitch, Λ (equation 3.5), we can rewrite 5.17 as equation 5.18;

$$\lambda_{Bd} - \lambda_B = \Delta\lambda_B = \lambda_B \times d/R \tag{5.18}$$

Considering that the effective displacement is dependent on the on the angle between the grating and the plane of bending, as shown in figure 5.21b, and the strain-optic effect, we can estimate that the Bragg wavelength shift caused by bending as is given by equation 5.19;

$$\Delta\lambda = \left[\gamma \cdot \lambda \cdot d\cos(\alpha)\right] \cdot \left(\frac{1}{R}\right) \tag{5.19}$$

where λ is the Bragg wavelength, γ is the strain-optic coefficient (0.78 for SMF fibre), R is the radius of the bending curvature, d is the displacement of the grating and α is the angle of displacement defined as the angle between the plane of the displacement and the plane of curvature, as shown in figure 5.21b.

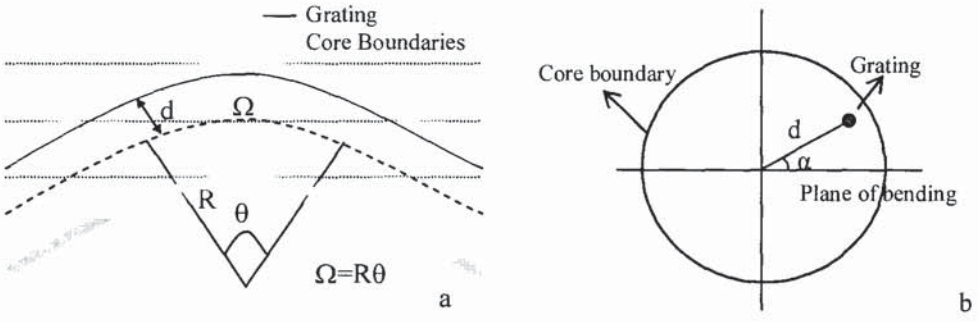

Figure 5.21: (a) Bending geometry of fibre with axially-offset grating (b) illustration of the cross-section of the core.

Equation 5.19 predicts a blue or red spectral shifts depending on the direction of the bending, indicating the directional sensitivity of the device. Using values d = 3μm and α = 0°, the sensitivity of the device $\Delta\lambda R$, is expected to be of the order of $3.6 \times 10^{-12} m^2$. This sensitivity is significantly lower than that of other reported bending devices [137-140]. However the flexibility of possible designs that will be later discussed and the advantages of creating a bending sensor in standard fibre compensate for the lower sensitivity.

5.4.3 Characterisation of the directional sensitivity of an asymmetric fibre Bragg grating.

The grating was then tested in a bending rig installation, illustrated in figure 5.22. The grating transmission spectrum was measured by using a tuneable laser in conjunction with an optical spectrum analyser (OSA). The system resolution was 1 pm.

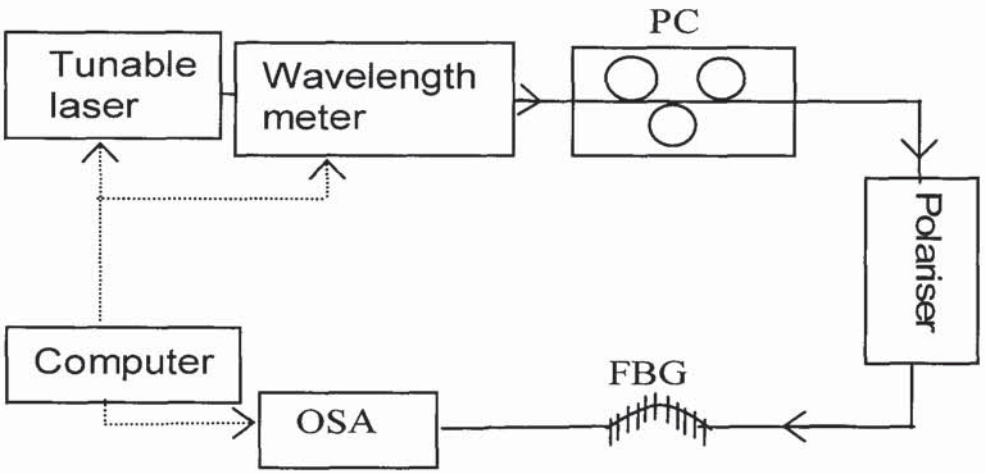

Figure 5.22: Experimental setup for the bending measurements. PC stands for polarisation controller and OSA for optical spectrum analyser.

Point-by-point femtosecond-inscribed gratings typically exhibit strong polarisation dependence. Therefore it was essential to ensure that all measurements be carried out along the same polarisation axis. This was achieved by introducing a polarisation controller and a polariser in

the system. Care was taken to place the fibre Bragg grating in the position in which the induced bending is in the same plane of the displacement of grating with respect to the geometrical centre of the core. Any departure from this alignment leads to a reduction in the sensitivity of the device.

The shift in the transmission spectra that results from increasing bending in either direction is illustrated in figure 5.23. Evidence of blue and red shift indicates the directional sensitivity of the device.

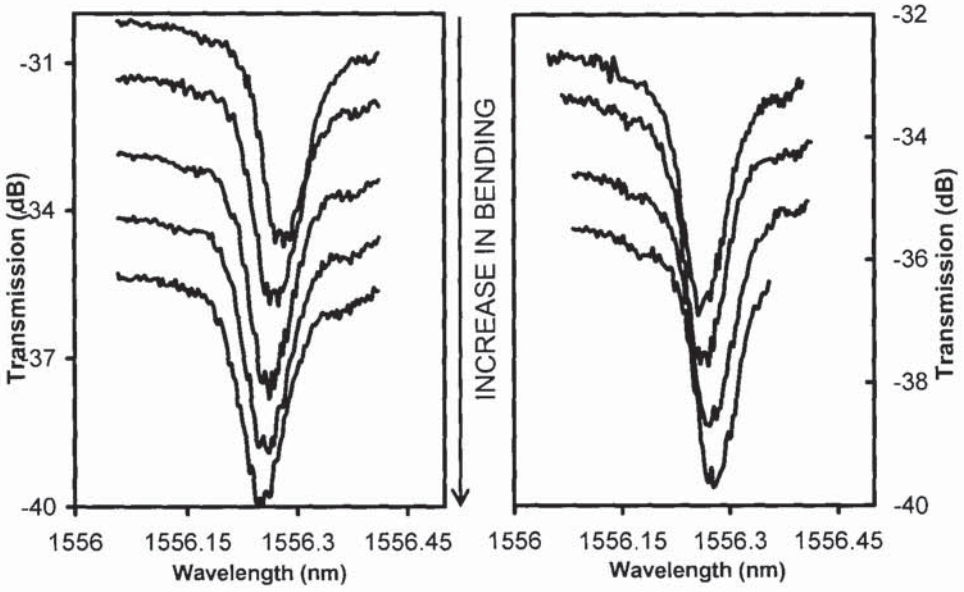

Figure 5.23: Transmission spectra during (a) concave and (b) convex bending, blue and red shift is observed respectively.

Equation 5.14 predicts the variations of the Bragg wavelength caused by concave and convex bending to induce a red or blue shift in the resonant wavelength and it is in fact observed in figure 5.23. Nevertheless the experimentally observed sensitivity of the device is of the order of $0.77 \times 10^{-12} m^2$; this is considerably lower than the estimated value of $3.6 \times 10^{-12} m^2$ yielded from equation 5.14. This discrepancy is most likely to arise from the fact that equation 5.14 does not take into account the relatively complex spatial distribution of the induced refractive index change across the fibre core. Although the size of the grating cross-section (~1μm) is smaller than that of the core, it is comparable with the displacement distance of 3μm. In order to model the device more precisely, the exact distribution of the refractive index would need to be taken into account as well as the Gaussian profile of the fibre mode.

In figure 5.24, the estimated and experimentally observed spectral shift are compared, the experimental results present a very low sensitivity. The applicability of this device as a directional sensor would require a significant improvement in the sensitivity, in order to alleviate the requirements of the interrogation system. This may be done by producing a grating structure more tightly confined within the desired area of the core. Other methods to optimise the design of these sensors are proposed in section 5.4.4.

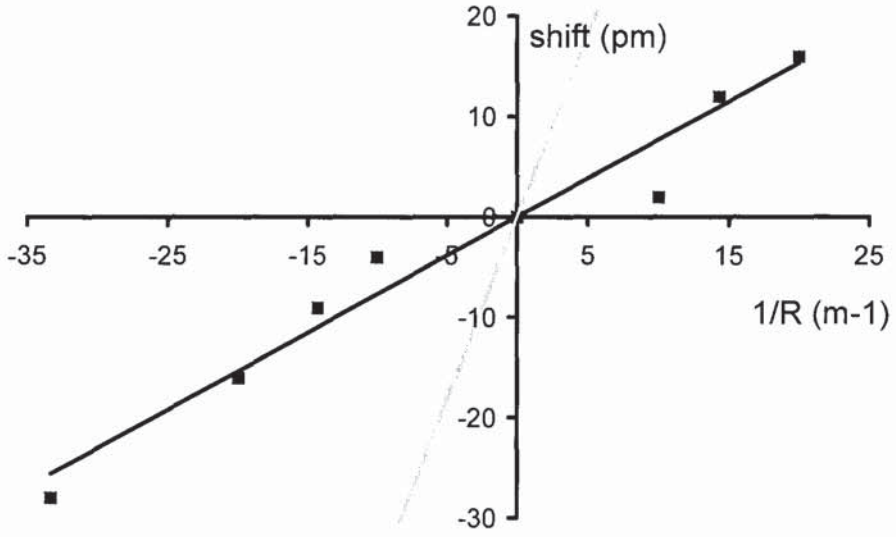

Figure 5.24: Wavelength shift plotted as a function of bending strength and direction, (gray line) estimation, (black squares) experimental result and (black line) linear approximation to experimental results.

5.4.4 Omni-directional sensor based on truly vectorial sensing

As we mentioned above, the major disadvantage of this technique is the very low sensitivity of this device compared to other methods. One can suggest that the sensitivity of the device can potentially be improved by inscribing smaller spatial features and perhaps by implementing more complex grating designs aimed at maximising the effect of strain.

It is also important that the demonstrated device is designed for detection of bending in only one plane. A major advantage of the proposed technique arises from the possibility to inscribe more than one grating in different segments of the cross-section of the fibre. By inscribing two

orthogonally displaced gratings the bending of the fibre in the corresponding orthogonal planes can be analysed simultaneously. This feature is a unique characteristic of the proposed device inscribed for gratings inscribed in a standard single-mode fibre.

Furthermore, the sensitivity of the vectorial bending device can be increased by combining two pairs of gratings in each plane with spectral separation of the order of 0.2nm. Depending on the direction of the bending, the spectral separation of the gratings would increase or decrease, the direction and strength of the grating can be accurately monitored by measuring the electrical beat signals of the reflected peaks of the two gratings. In figure 5.25, we present a diagram of the proposed sensor, with four gratings combined in pairs allowing omni-directional measurement of strength and direction of bending in the fibre. The sensitivity in such conditions would be improved since the two gratings in the same plane will undergo opposite spectral shift and the beat signal of the two gratings will change according to the variation of this wavelength change.

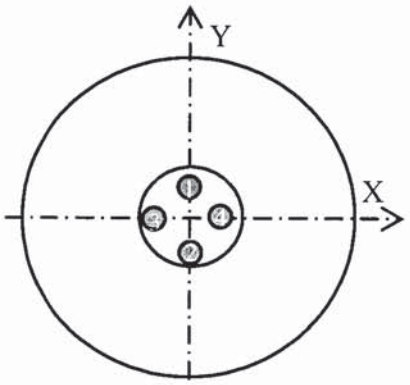

Figure 5.25: Design of the final proposed sensor for omni-directional bending sensing, based on the feasibility of inscribing non-overlapping gratings in the core.

Ideally, the sensor proposed in figure 5.25 would consist of four fibre lasers such as the ones that will be described in chapter 6. Using a scheme based on fibre lasers to measure bending offers numerous advantages other than the possibility to measure the dynamics of the beat frequency between gratings. The resolution of a fibre laser sensor is much higher than a uniform grating since the linewidth of the former is significantly narrower. A second major advantage is that, as it will be demonstrated in chapter 6, using point-by-point inscription it is possible to ensure emission in single polarisation, eliminating the inaccuracies that rise form the use of the polariser and polarisation controller and simplifying the interrogation system. However, we must

deal with numerous engineering challenges before we can implement such complex structures. The major challenges to consider are; reducing the insertion losses and improving the accuracy of alignment.

5.5 Directional sensors by femtosecond-induced asymmetrisation

Long period gratings offer a number of significant advantages compared to fibre Bragg grating due to their higher sensitivity to external environment. As a result, they have been suggested for a number of potential applications in the field of sensing [97].

A promising application is as a curvature sensor, sensitivity to curvature is not however direction sensitive, limiting significantly the applicability of such devices. As we mentioned earlier, a number of designs have been proposed to produce direction-sensitive curvature sensors. They are based on asymmetric fibres, including D-shaped fibres, multiple core fibre and eccentric core fibres [137-140]. All these solutions offer directional sensitivity but they present a number of practical difficulties such as more complex inscription processes, and interrogation systems.

Direction-sensitive bending sensors inscribed in standard fibre are therefore and interesting proposal as they simplify the interrogation requirements and reduced the overall cost of the system. The previous section offered a solution based on an axially-displaced fibre Bragg grating, however the sensitivity of this device was very low compared to other methods [137-140]. In this section, we propose a method by which, using infrared femtosecond inscription an asymmetric structure is created in standard fibre in order to introduce directional discrimination. Instead of directly inscribing a grating with directional sensitivity [64], the sensitivity is induced by femtosecond post-processing of the cladding in a determined region. This modified region affects the propagation of the cladding modes and therefore the coupling from the radiation modes into the cladding modes.

5.5.1 Fabrication procedure

The device was fabricated in two stages; a long period grating was first inscribed using standard UV inscription[3], afterwards a structure was inscribed in the cladding using femtosecond inscription in order to change the symmetry of the fibre. The long period grating was inscribed into a standard communications step-index optical fibre with a core radius of 3.5μm and a cladding radius of 62.5μm. The fibre was not specifically designed to be photosensitive and so its photosensitivity was increased by hydrogenation at a pressure of 120Bar for a period of two

[3] Long period gratings inscribed by a UV source by T. Allsop and F. Floreani at the Photonics Research Group, Aston University.

weeks at room temperature. The long period grating was fabricated using a frequency-doubled argon-ion laser with a point-by-point writing technique. The grating period was 400μm and the length 5cm.

The asymetrisation of the fibre by modifying a region of the cladding with a femtosecond laser was done after the long period grating was inscribed, thus, it was possible to characterise the grating before and after femtosecond inscription was carried out. The set up used for the process only differed from that detailed in section 4.2 in the addition of a cylindrical lens, f=100mm, that was placed in the proximity of the 100X (NA=0.55) microscopic objective. An scheme of the focusing arrangement is shown in figure 5.26 . The purpose of adding this lens is to modify the focusing conditions and therefore the size and shape of the structure inscribed.

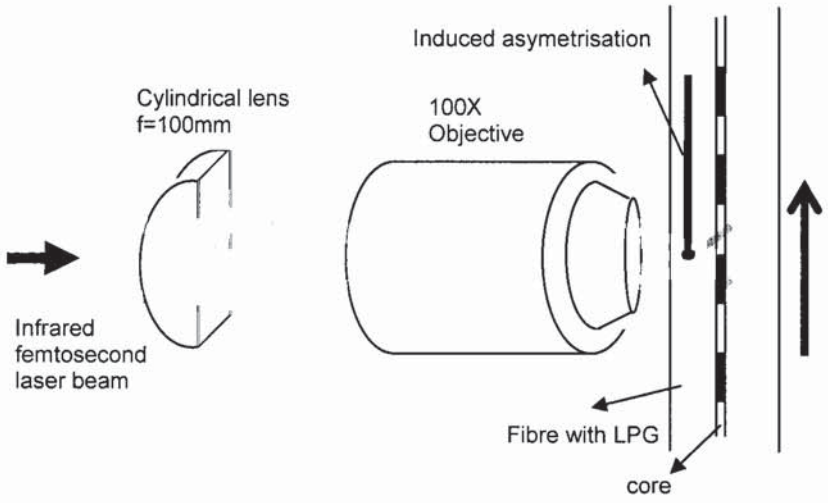

Figure 5.26: Scheme of the focusing optics used for the inscription of structures in the cladding of the optical fibre. The Cylindrical lens was place at approximately 10mm from the microscopic objective aperture.

Two separate experiments were carried out. In the first case; three structures were inscribed in the cladding. The structures were quasi-cylindrical waveguides parallel to the core with a cross section approximately 5μm^2. Pulse energy used was similar to those used for grating inscription, approximately 0.5μJ, and we estimated a refractive index change in the order of 1.5×10^{-3}. The repetition rate of the laser was 1kHz and the inscription speed was set at 50μm/s, allowing therefore sufficient overlapping of the laser pulses to allow the inscription of continuous structures. Two of such structures were inscribed 2μm away from the core at opposite sides. The third structure was inscribed 20μm away from the core, in the same plane as the other two structures.

A second device was inscribed in which a single structure was inscribed 5μm away from the core. In this case, the cylindrical lens was removed from the system, and writing speed remained 50μm/s. The results from both experiments are described below. Figure 5.27 shows a microscopic image of a single-mode fibre with femtosecond-induced asymmetrisation, the structure is parallel to the core and has relatively large dimensions with a visual diameter of 5μm.

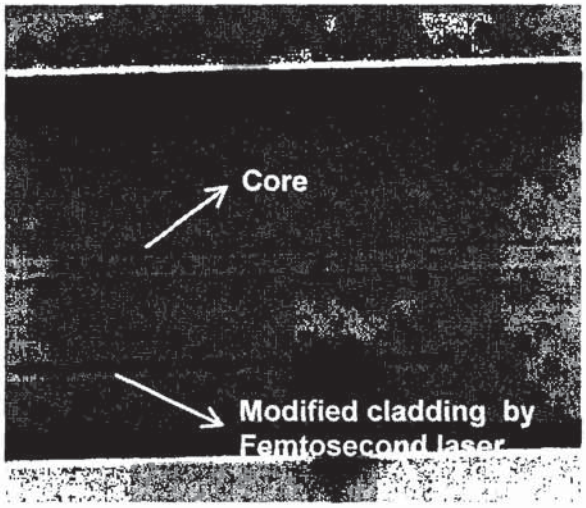

Figure 5.27: Asymmetrisation in a single mode fibre; A structure is inscribed in the cladding by means of a tightly focused infrared femtosecond laser. The diameter of the written structure is approximately 5μm.

5.5.2 Characterisation and results

In order to study the directional sensitivity of the device, the long period grating was inserted into a 4 mm diameter flexible rubber tube, and both the fibre and the tube were clamped between two towers with one of the clamps mounted on a translation stage, such as illustrated in figure 5.28. When the stage is moved inwards, a bend is induced in the tube and thus the optical fibre. The convention that will be used from here onwards defines convex bending as that when the structure inscribed away from the core is on the outermost side of the bend. Likewise, we will refer to concave bending when this structure is in the inside of the bend. The fibre was inserted in a tube in order to ensure that the fibre will not change orientation during bending.

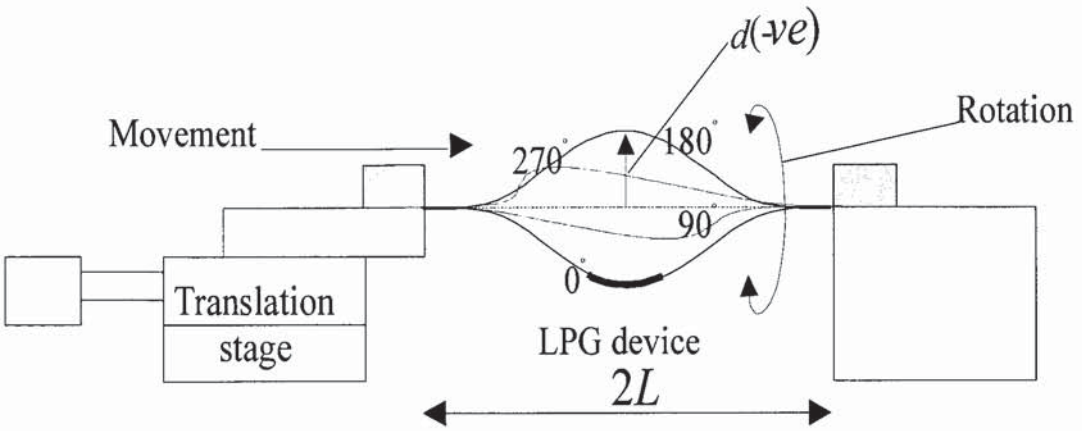

Figure 5.28: Scheme of the test rig used for the bending sensitivity investigation of the long-period gratings.

Using such arrangement with the long period grating centred between the clamps, the curvature of the sensor, R, is given by [141];

$$R = \frac{2d}{\left(d^2 + L^2\right)} \tag{5.20}$$

where L is the half distance between the edges of the two towers and d is the bending displacements at the centre of the long period grating. To characterise the attenuation bands of the device, light from a broadband light source was coupled into the fibre and the transmission spectrum was monitored using an optical spectrum analyser with a resolution of 50 pm.

As it was mention above the first device investigated consisted of a long period grating inscribed by UV light in the core of the fibre and three regions modified using infrared femtosecond radiation inscribed in the cladding along the fibre, two of them separated 2μm from the core cladding interface at opposite directions in the same plane and a third structure inscribed with 20μm separation, in the same plane. Figure 5.29, illustrates the dynamics of the transmission spectra of this device during convex and concave bending. The bend-induced wavelength-shift in the normal and bend induced attenuation bands can be obtained from the figure 5.29 and are presented in figure 5.30.

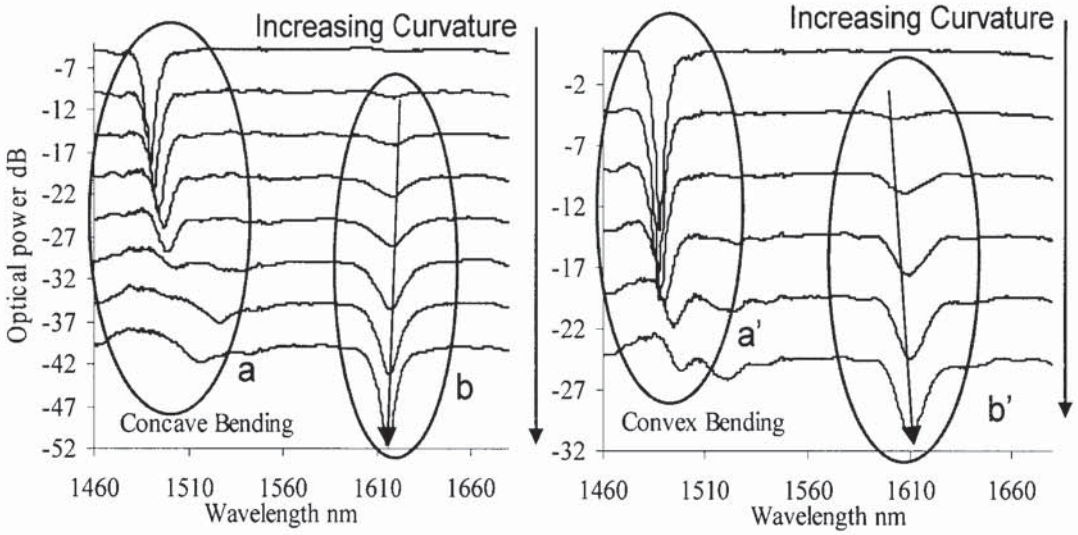

Figure 5.29: Dynamics of the transmission spectrum of and LPG fibre device with varying direction and radius of curvature. (a) and (a') correspond to the normal attenuation band under concave and convex bending respectively. (b) and (b') correspond to the bend-induced attenuation band.

The spectral sensitivity for the normal attenuation band (i.e. those present in the absence of bending, attenuation bands (a) and (a') in figure 5.29) was $d\lambda/dR$ +5.6±0.1nm.m for concave bending and $d\lambda/dR$ +4.6±0.2nm.m for convex bending (figure 5.30). This indicates a lack of directional-sensitivity in this attenuation band. On the other hand, the bend-induced attenuation band ((b) and (b') in figure 5.29) present a spectral sensitivity of $d\lambda/dR$ -1.6±0.1nm.m for concave bending and $d\lambda/dR$ +3.8±0.5nm.m for convex bending (figure 5.30). The bend induced attenuation bands do therefore experience red or blue shift depending on the direction of the bending. These wavelength shifts are expressed in figure 5.30 as a function of the curvature.

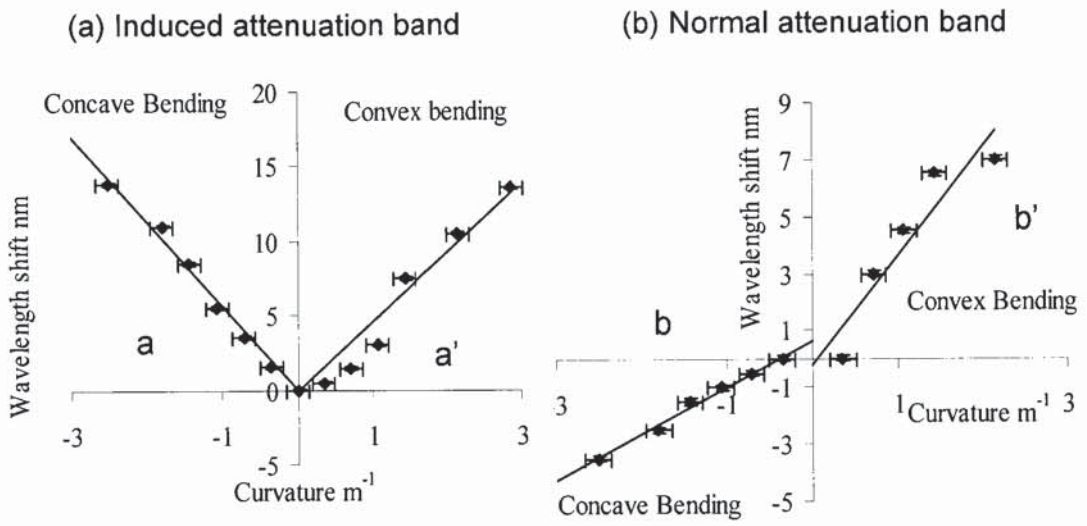

Figure 5.30: Spectral sensitivity of the (a) normal attenuation bands and (b) bend-induced attenuation bands to bending in the concave (a, b) and convex (a', b') directions.

The results from figure 5.29 and 5.30 indicate that the asymmetry introduced in the cladding during femtosecond inscription has been sufficient to introduce directional discrimination in the plane where the structures were inscribed.

A second device was inscribed in which a single structure was inscribed 5μm away from the core. The characterisation of the device was done in the same way as for the previous device. In this case, the bending sensitivity of the long period grating was studied before the asymmetric modification was introduced and then compared to the sensitivity after inscription. The results are shown in figure 5.31 and demonstrate that the structure inscribed by the femtosecond laser introduces directional discrimination in the plane where the structure was inscribed.

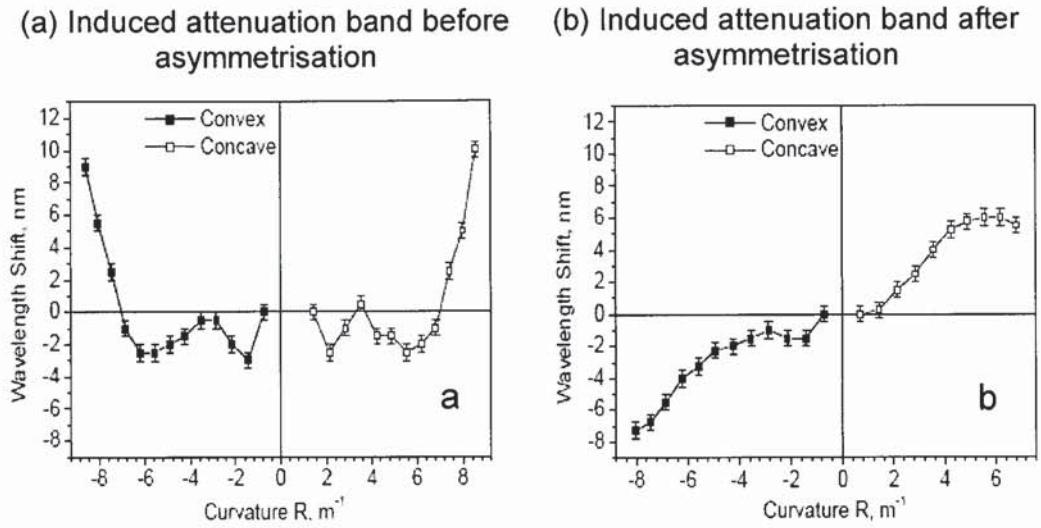

Figure 5.31: Spectral sensitivity of the bending induced attenuation band of a long period grating before (a) and after (b) inscription of the structure was introduced 5μm away from the core of a long period grating.

As it was the case for the first device investigated, directional sensitivity has not been observed in the normal attenuation bands but only in the bend induced bands. In figure 5.32, the wavelength shift induced by convex and concave bending is compared for the normal attenuation band and the bend induced band, it is evident that the wavelength shift is under any direction of bending positive. This has been observed for all the devices inscribed. Evidently, directional sensitivity in the normal attenuation band would be more beneficial, and current efforts are been directed in this direction.

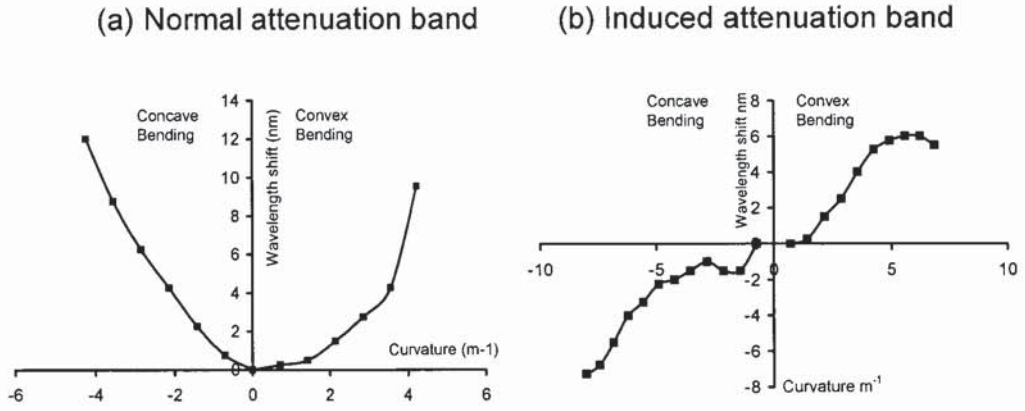

Figure 5.32: Spectral sensitivity of the normal attenuation band (left) and the bend induced attenuation band.

In both devices, we observed directional sensitivity, characterised by red and blue shift depending on the direction of the bending that the device experienced. The main advantage over other methods that offer orientation sensitivity is that it is inscribed in standard single-mode fibre, allowing simple integration into an interrogation system. Compared to the method we described in section 5.4, it presents improved sensitivity.

We have demonstrated directional sensitivity in the bend-induced attenuation band. It would be advantageous to observe directional sensitivity in the normal attenuation bands. In chapter 4, we demonstrated the inscription of long period gratings by femtosecond inscription. By inscribing those long period gratings out of the core, or in the core-cladding interface the normal attenuation band should discern between bending directions. Furthermore, by inscribing a second grating with a 90^{o} angle with respect to the first long period grating, omni-directional sensitivity could be achieved.

5.6 Superimposed non-overlapping gratings

Point by point inscription has the characteristic of creating structures smaller than the core. A number of applications have been proposed regarding this geometrical characteristic of the device. Those included the possibility of inscribing gratings with strong polarisation dependence in standard fibre and the inscription of bend sensitive gratings. A further potential application, mentioned in relation to previous studies, is the possibility to inscribe superimposed gratings in the same length of the fibre but not overlapping in the cross-section of the core. In this section, we look at the method, applications and limitations of superimposed non-overlapping gratings. Tight focusing by high aperture optics, combined with the nonlinear nature of the process, allows reaching feature sizes as small as 0.3μm [114]. Superimposed gratings represent an interesting type of passive optical device with a number of important applications such as Wavelength Division Multiplexing (WDM) components in optical communications [142] and as wavelength-selective mirrors in multi-wavelength fibre lasers [143]. Available technologies of inscribing superimposed gratings inevitably involve repeating modification of the same volume of material during the process of writing. As a result, the number and the accuracy of the overlapping structures in a single fibre are to some extent limited by the physical interaction between the structures [144].

By adjusting the inscription geometry and the regime of exposure, one can control the size and position of the modified volumes of material inside the sample. In particular, it is possible to confine a Bragg grating in a fraction of the cross-section of the core. This way, the interactions mention above can be minimised or eliminated. It is possible, in principle, by inscribing in different segments of the fibre core, the inscription of several gratings in the same length of fibre without effects of blurring of the grating pitch caused by overwriting. Inscription of multiple gratings was done using the set-up presented in chapter 4; parameters used for inscription were equivalent. The focal point of the laser within the core was axially displaced 3 μm from the centre of the core. The writing speed varied between 1.07mm/s and 1.075mm/s to spectrally separate the different gratings.

Location of the grating structure inside the core was determined by focusing the highly-attenuated laser beam in the appropriate volume. The position of the focal spot was monitored from the top and from the side of the fibre by two CCD cameras, as described in section 4.2. A typical cross-section size of an inscribed grating structure was approximately 1μm by 2μm. Hence, the area of a grating cross section was only $2\mu m^2$. This means that, in principle, it is possible to inscribe several tens of non-overlapping gratings in the core of a typical telecommunication fibre with the mode area of the order of $70\mu m^2$.

Non-overlapping gratings were produced by writing one grating at a time and then displacing the fibre to inscribe the next grating. Spatial separation in the transverse plane was achieved either

by a parallel translation of the fibre in lateral direction, or by rotating the fibre with respect to the axis. In each case, the grating structures in the pair were distinctly separate.

Figure 5.33 presents the transmission spectra of two gratings inscribed in different parts of the cross-section of the core. Both gratings in the structure show strong resonances with line-widths of approximately 0.25nm. Importantly, the spectral features of the grating that was inscribed first remained unchanged during and after inscription of the second grating in the same length of fibre.

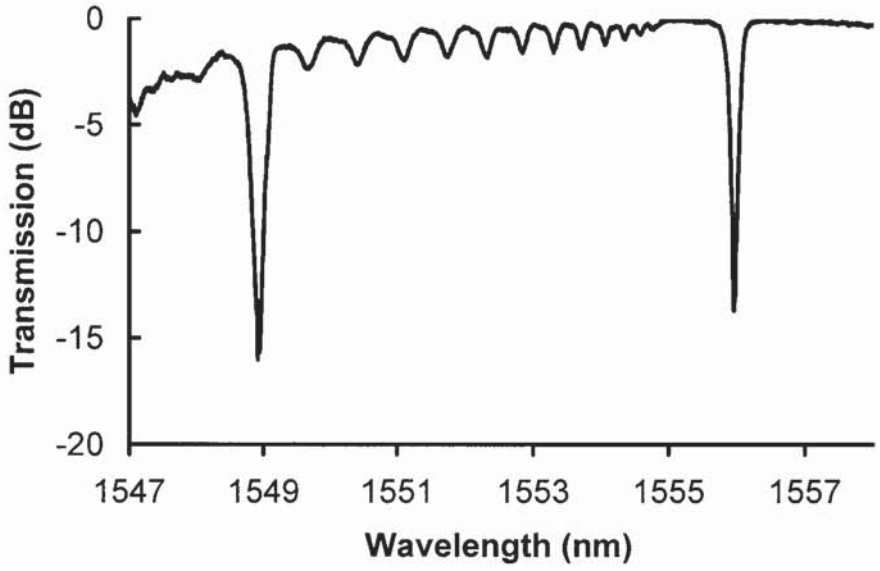

Figure 5.33: Reflection and transmission spectra of a two superimposed, but non-overlapping gratings. Grating periods are 1.07μm and 1.075μm.

Three factors limit the number and quality of gratings that can be inscribed in the same length of the fibre; the dimensions of the grating, the insertion losses and the coupling to the cladding modes. The dimensions of the modified structure may be reduced by optimising the optics and compensating for the effect of a strong cylindrical lens formed by the side surface of the fibre. Focusing the laser beam into a smaller spot will reduce the lateral size of the grating, thus allowing the inscription of a larger number of non-overlapping, superimposed gratings in a single fibre core. Assuming the spatial resolution of 0.3 μm approximately, already achieved in bulk glass samples, estimated number in excess of a hundred of non-overlapping gratings can be in principle superimposed in a single length of fibre. Gratings of this type would be of course important for a number of applications in wavelength division multiplexing (WDM) data transmission, sensors and microwave photonics.

The quality of the gratings inscribed by this technique presents a number of drawbacks for the inscription of superimposed gratings for telecommunications. Although the losses induced for the inscription of each grating generally range between 0.1dB/cm and 0.3dB/cm, the inscription of various gratings will attenuate the signal significantly. Another problem rises from the strong coupling to cladding modes that is observed in gratings inscribed point-by-point that would become an important source of losses for gratings with lower resonant wavelengths. These problems make this method undesirable for multiplexing applications until this problem is fully address.

Considering their deficiencies as multiplexers, a more realistic potential application for superimposed non-overlapping gratings is likely to be in sensing, particularly bending sensing, such as proposed in section 5.4. The requirements in terms of attenuation and losses are less stringent for sensing applications and the number of gratings needed in the cross section of the fibre is limited to four. It is therefore possible to produce directional sensors with the present inscription procedure and set-up.

5.6.1 Moiré structures in overlapping gratings

Gratings have been inscribed by rotating the fibre in order to write a second grating with a different angle and section of the core. Results showed a strong Moiré grating that comes from the modulation of the refractive index profile produce by the combination of the two superimposed gratings [145]. This effect was not present for gratings neither inscribed by translating the fibre in the direction of the beam, see figure 5.33, nor for gratings inscribed translating the fibre perpendicular to the beam.

In order to understand the principle of Moiré gratings, we may assume that the grating inscribed present a refractive index with a sinusoidal profile. In this case we may write the index modulation as equation 5.21;

$$\Delta n(x) = \Delta n \cos(\frac{2\pi x}{\Lambda}) \tag{5.21}$$

Where n is the refractive index and Λ is the grating pitch. When two gratings overlap in the same area the refractive index change will be the sum of both gratings. This leads to a refractive index modulation with pitches given by equations 5.22 and 5.23;

$$\Lambda_{1+2} = \frac{2\Lambda_1\Lambda_2}{\Lambda_1 + \Lambda_2} \tag{5.22}$$

$$\Lambda_{1-2} = \frac{2\Lambda_1\Lambda_2}{|\Lambda_1 - \Lambda_2|} \tag{5.23}$$

The grating pitch Λ_{1-2}, from equation 5.23, is not relevant in this study due to its very large period. However the grating with pitch Λ_{1+2}, from equation 5.22, lies between the two inscribed gratings as seen in figure 5.34.

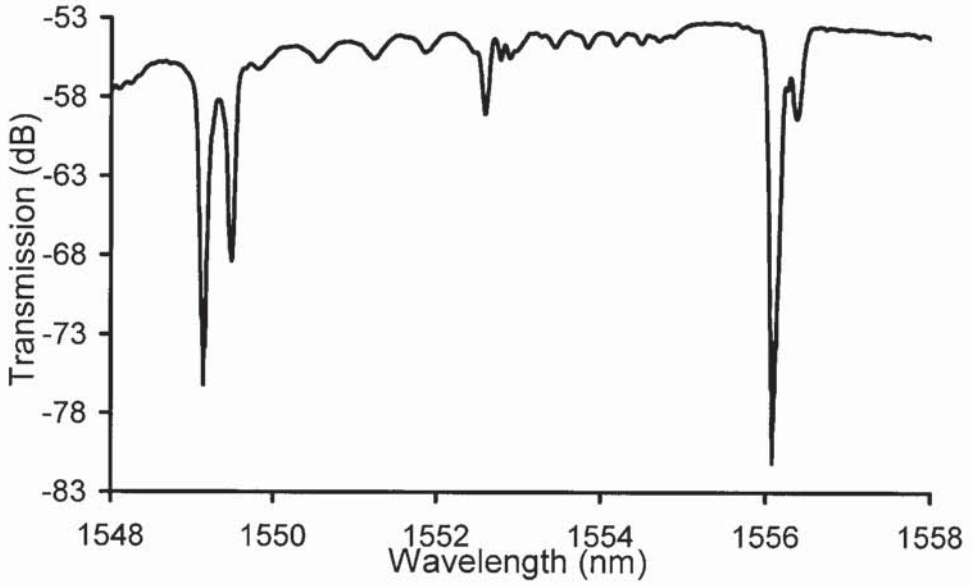

Figure 5.34: Shows two superimposed gratings written with pitches 1.07μm and 1.075μm and a resulting Moiré grating.

Means of exploitation of Moiré gratings have not been investigated in this work. Once higher levels of control in the inscription process are achieved such Moiré structures may be used to produce phase shifted gratings, and they may be considered for the fabrication of distributed feedback (DFB) lasers.

5.7 Conclusions

In this chapter, various properties of gratings inscribed point by point by a femtosecond laser were investigated and ways in which to apply these characteristics were proposed.

The thermal stability of gratings inscribed using an infrared femtosecond laser was studied, showing stability at temperatures as high as 1000°C. This significant improvement compared to the conventional, UV inscribed gratings arises from the different processes that lead to the refractive index change in the material. Thermally-induced wavelength shift was observed to follow an equivalent pattern than those observed in UV inscribed gratings. This is the case since it is a function of the thermal expansion coefficient and thermo-optic coefficient, which are intrinsic characteristics of the material rather than the method of inscription.

The inscription of highly reflective fibre Bragg gratings in standard, non-photosensitised single-mode fibres, through the coating was demonstrated for the first time. Infrared sources are especially suitable for inscription through the coating, since the polymer coating is transparent to the infrared source used for inscription. The removal of the coating prior to inscribing the grating is not only time consuming but it significantly reduces the mechanical strength of the fibre and complicates its handling. Therefore, avoiding this step is a significant advantage in the inscription of fibre Bragg gratings.

Two configurations for directional bending sensors were proposed. Both methods utilise the inscription of an asymmetric structure in the fibre by an infrared femtosecond laser to allow discerning between orientations. The primary merit of both configurations is that directionality may be achieved in standard fibre and this is of particular interest since it significantly reduces the requirements for the interrogation system. Alternative methods have proved to be efficient for the proposed task, but they require complicated interrogation techniques to adapt to the unconventional geometries of the fibres used in the system.

The first proposed method introduces an axially-offset fibre Bragg grating, which experience a red or blue shift depending on whether the bending is concave or convex in the plane where the asymmetry was induced. The main drawback of this method is the low sensitivity of the device. The second method proposes a hybrid device in which an asymmetry is introduced in the cladding of a long period grating by post-processing with an infrared femtosecond laser. This method has lower requirements than the Bragg grating configuration since long period gratings are more sensitive to bending than fibre Bragg gratings and therefore the sensitivity was higher. A number of more complex arrangements were proposed to upgrade these direction-sensitive devices to an omni-directional configuration.

CHAPTER 6: Fibre Lasers inscribed point by point by an infrared femtosecond laser

6.1 Introduction

Fibre grating technology has had a particularly strong impact on the design of active devices, such as fibre lasers or fibre amplifiers. By directly inscribing the fibre Bragg gratings into the core of an active fibre, a resonator with extremely low loss and a highly selective spectral feedback can be fabricated with unrivalled compactness. The design requirements and number of components needed to fabricate a single-longitudinal mode fibre laser are therefore greatly reduced compared to alternative propositions, such as diode lasers. As this technology develops, numerous applications alternative to telecommunications are been proposed including material processing and sensing. Despite the lower, but ever increasing peak powers, fibre lasers offer significant advantages, such as superior energy efficiency, beam quality and stability as well as reduced cost [19].

Fibre laser work has been carried out primarily in two types of fibre, erbium-doped fibre and erbium-ytterbium co-doped fibre. The use of either gain material depends on the requirements of the laser configuration, the merits of both types of fibre and their applications will be considered in this chapter, as well as the merits of the different laser configurations. Another aspect on fibre laser fabrication is the low sensitivity of the gain fibre. The use of conventional Er:Yb-codoped gain fibre is limited by the difficulty to create UV-inscribed gratings into its non-photosensitive phosphosilicate glass host [146]. Consequently, the fabrication of short-length, linear cavity Er:Yb fibre lasers continues to rely on the use of special double-clad Er:Yb-codoped fibre [146]. With femtosecond inscription, the low photosensitivity of the fibre does not affect the inscription process, and thus, fibre lasers can be inscribed directly in the gain fibre allowing precise control on the characteristics of the resonator.

The fabrication of fibre lasers by femtosecond inscribed gratings poses numerous challenges, such as minimising the insertion losses in the resonator, or the uniformity of the structures inscribed. However, as it will be shown in this chapter, once these issues are overcome, the advantages of this method of inscription, allow for the fabrication of fibre lasers in non-photosensitive fibre with controlled polarisation properties and very high thermal stability.

6.2 Rare-earth doped fibres and laser configurations

The development of fibre Bragg grating lasers has been accompanied by the developments in the fabrication of single-mode fibres with an active media core. Particularly relevant to fibre lasers has been the development of fibres with an Erbium (Er^{3+}) doped and Ytterbium codoped Erbium (Yb/Er) fibre. The relevance of these fibres is that their operating regime lies in the optical communications window of 1.5μm. Initial developments were made in erbium doped fibre when fibre amplifiers [147] and fibre lasers [148] were implemented.

6.2.1 Erbium-doped fibre

Erbium-doped fibres have attracted the most interest among rare-earth doped fibres. The reason for this interest rises from the fact that they are suitable for amplification at the preferred telecommunication window of 1.55μm. Thus erbium-doped fibre amplifiers (EDFA) are, to this date, the preferred technology in fibre amplification, and together with Er:Yb fibres are also preferred for fibre laser configurations.

Erbium doped glass can be understood as a three energy level system such as shown in figure 6.1. The wavelengths used to pump erbium fibre lasers are predominantly 980nm and 1480nm [149-153], being the former the preferred wavelength since in this region the gain efficiency is higher, and the noise characteristics lower, as well as been a region free of pump excited state absorption.

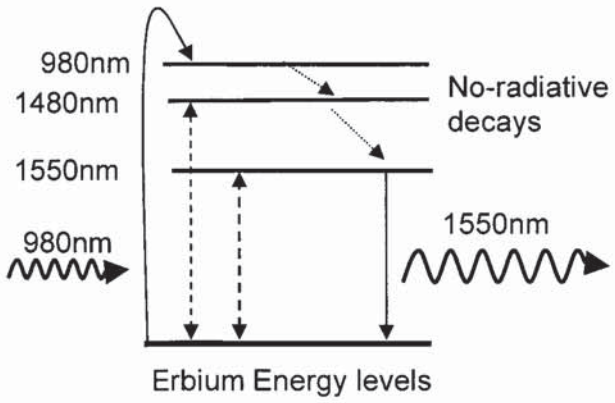

Figure 6.1: Relevant energy levels in erbium and transitions.

Erbium fibre lasers however present a number of difficulties for the fabrication of efficient single-mode fibre lasers. Erbium has low pump absorption per unit length. It also has a low absorption cross-section compared to other rare-earth materials. Increasing the concentration levels is not a suitable solution since it leads to clustering and ion pair interactions. It is therefore necessary in order to achieve sufficient gain to create a longer laser cavity.

Despite the drawbacks mentioned above, fibre lasers based on erbium fibres have been achieved using configurations with a long gain fibre, such as the ring cavity laser proposed in section 6.4. In this case the laser operated in a multimode regime, a filtering component within the cavity would be required to achieve single mode operation.

6.2.2 Erbium-Ytterbium codoped fibre

The low pump absorption of erbium doped fibres impedes the implementation of short cavity fibre laser configuration such as distributed Bragg reflector (DBR) lasers and distributed Feedback (DFB) lasers, which are described in section 6.4. Such laser configurations can offer improved compactness, narrower bandwidth, single-mode operation and wavelength stability.

The use of ytterbium (Yb^{3+}) as a co-dopant with erbium offers a number of advantages over solely erbium doped fibre [154-158]. The amount of erbium concentration in a fibre is restricted by concentration quenching. This problem is not encountered when loading the fibre with ytterbium, thus, higher concentration levels are available. Furthermore the absorption cross-section for ytterbium is larger than that of erbium. These characteristics lead to a highly efficient absorption of the pump, which can be as much as two orders of magnitude higher than that of erbium fibre.

With ytterbium sensitisation, the optical pump is primarily absorbed by the Yb^{3+} ions. This energy is then transferred to the Er^{3+} ions where the irradiative transition takes place. Unlike Er^{3+} ions, Yb^{3+} ions have a broad absorption band from 800nm to 1100nm, with a particularly high peak-absorption cross-section. Ytterbium doped fibre presents absorption level of 980nm pump light two orders of magnitude higher than those of a non-sensitised Er^{3+} doped fibre. These very high levels of absorption permit, in principle, the fabrication of short cavity fibre lasers without the need for highly doped fibre [159].

The energy levels of ytterbium and erbium, as well as the energy transitions that take place from pump absorption to emission at 1550nm are illustrated in figure 6.2

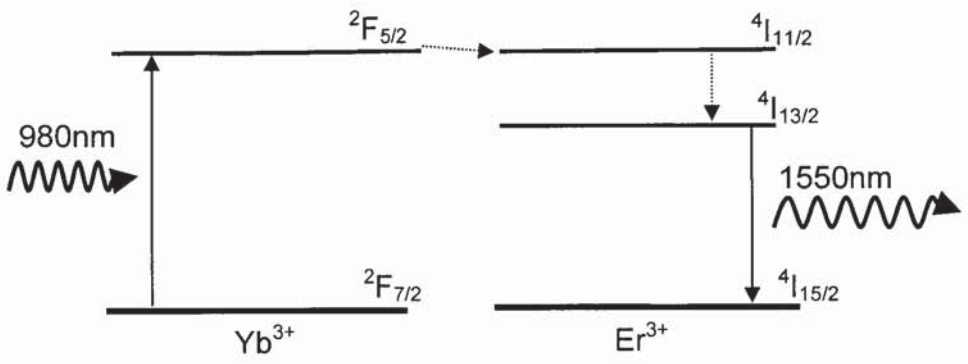

Figure 6.2: Energy levels of Erbium and Er:Yb co-doped materials and the absorption and emission in a fibre laser configuration.

The energy transfers between Yb^{3+} and Er^{3+} ions are efficient provided that the electrons relax to the Er^{3+} upper state $^4I_{13/2}$ rather than back to the $^2F_{5/2}$ level of the Yb^{3+} ion. In order to ensure this transition the glass that composes the core must be a phosphosilicate glass. The need for a phosphate glass presents a technological challenge since the use of phosphate is known to reduce the photosensitivity of the fibre to UV light, hindering the inscription of highly reflective gratings necessary for the inscription of a laser resonator [19].

Evidently, a resonator cavity can be achieved by splicing the gain media between two photosensitive fibres in which the gratings can be inscribed [159]. This solution although effective and simple is not optimal since it introduces intracavity losses from the splices. Furthermore the flexibility in the laser design is greatly reduced, since the grating structure cannot overlap with active media, and configurations such as the distributed feedback (DFB) lasers are not possible. A number of solutions have been considered to improve the UV inscription efficiency of Er:Yb fibres, those included hydrogenation of the fibre, co-doping with tin and using specially design fibres with a double cladding.

Even though hydrogenation leads to an increase in photosensitivity, it is not a feasible alternative since it induces important losses at the pump wavelength after UV exposure due to the creation of OH formations which are highly absorbent to radiation in the order of 0.95μm. These losses have been measured to be in the order of 0.2dB/cm in the gratings [115], jeopardising the efficiency of the laser. Tin co-doping leads to an increase in the photosensitivity without the need for hydrogenation. Using this type of fibre, lasing has been achieved in a 10cm long DFB laser configuration. The photosensitivity is however not sufficient to allow the inscription of shorter laser devices using Sn/Yb/Er co-doped fibre [160].

The most accomplished solution to date uses a special fibre with a photosensitive ring around a standard Er^{3+}/Yb^{3+} co-doped core [146]. This type of fibre, known as double-clad, consists of a core co-doped with Er^{3+}/Yb^{3+}, which is encircled by a highly photosensitive B/Ge/Si region which allows the inscription of fibre Bragg gratings, see figure 6.3.

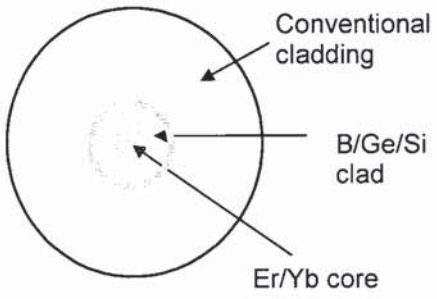

Figure 6.3: Design of double cladding Er:Yb codoped fibre used in reference [141].

The presence of Boron grants increased photosensitivity, as does the germanium. Photo-induced index changes in the sensitive area are in the order of 10^{-3}, however since the guided optical field only undergo a reduced overlap with the grating the effective index changes that may be induced are of the order of 10^{-4}. The development of these fibres partially solves the problem of sensitivity but direct inscription in the core is still desirable since the use of double-clad fibres increases the cost of the devices and also reduces the efficiency of the device because the grating structures are not inscribed directly in the core.

Direct inscription can be achieved by femtosecond inscription permitting the fabrication of efficient fibre laser directly in the Er:Yb core. This is possible since the presence of a certain concentration of phosphate dopant does not affect the highly nonlinear processes of absorption that take place during inscription with infrared femtosecond lasers.

The geometrical configuration adopted in a fibre laser depends on the active fibre that is used for gain. This way, the master oscillator power amplifier [161] and the ring laser [162] are commonly used for erbium based fibre lasers, since the low absorption of the pump characteristic of erbium fibres requires a long cavity in order to achieve enough gain. Erbium/ytterbium codoped fibres provide very high absorption and therefore lasers can be inscribed in very short cavities such as the distributed Bragg reflector (DBR) laser and distributed feedback (DFB) laser. Both DBR and DFB laser configurations offer narrow linewidth, single mode operation. However due to its geometry, the DFB laser is more stable and has stronger side-mode suppression than the DBR lasers.

6.3. Influence of birefringence in the performance of a fibre laser

One of the key parameters in the performance of a fibre laser is the birefringence of the gratings that form the resonator. Numerous studies have given attention to the effect of polarisation in the fibre laser performance and in ways to suppress or enhance their influence in the performance of the device. However, standard methods for UV inscription are not well suited to control the polarisation properties of the gratings, limiting the potential to exploit this area. Point by point femtosecond inscription, on the other hand, offers a level of control that may be used to inscribed single-mode, single polarisation laser and potentially microwave signals.

6.3.1 Dual polarisation beat frequency noise

Birefringence induced by UV inscription in single-mode fibres poses a significant problem for fibre lasers. The grating structure itself usually presents a birefringence of the order of 10^{-6} to 10^{-5}, this leads to the fibre laser operating at both polarisations with an uneven distribution of power between the two modes.

The difference in optical frequency between the two modes, Δv_{pol}, is given by equation 6.1;

$$\Delta \nu_{pol} = \frac{B_\nu \nu}{n} \tag{6.1}$$

where B_v, is the birefringence of the device, v is the optical frequency, and n is the mode index.

This leads to a polarisation mode splitting in a fibre laser inscribed by standard UV techniques in a single-mode standard telecom fibre of the order of a few hundred megahertz [163]. The result of dual polarisation emission is polarisation mixing which creates detrimental beat noise at the receiver.

A number of solutions have been proposed to solve this problem, including operating at low powers where only one of the polarisation reaches threshold, twisting the fibre or using a highly birefringent fibre. Operating just above threshold is a simple and efficient solution for gratings with high birefringence. It does however restrict the use of the laser to low powers [164-165]. It has been demonstrated that by twisting the fibre, circular birefringence is introduced in the laser, and this reduces the beat frequency noise [166]. Finally using a highly birefringent fibre, the polarisation dependent losses are different which leads to a significant difference in the

threshold of the two polarisations [167]. The disadvantages in this case rise from the need of a specially designed fibre. Furthermore, the coupling to a standard fibre for the transmission signal would bring additional losses.

6.3.2 Optical generation of microwave signal by frequency beating of polarisation modes

Although it will not be thoroughly discussed in this work, generation and transmission of high frequency signals by optical means is an interesting proposition for a number of applications and particularly for telecommunications. Microwave photonics consists on the transmission of optically modulated signals at microwave rates. Most applications make use of microwave rates between 1GHz and 30 GHz. Optical techniques to achieve radio frequency (RF) signal are based on heterodyne mixing of two laser signals with frequency separation suited for microwave generation.

The optical field of the two laser signals is expressed by equation 6.2;

$$E = E_1 e^{i(\omega_1 t + \phi_1)} + E_2 e^{i(\omega_2 t + \phi_2)} \tag{6.2}$$

where $\omega_{1,2}$ correspond to the optical frequencies of the frequencies of the laser signals, and $\phi_{1,2}$ is the phase noise of the respective signals. The current, I, generated in a photo-detector by the two sources, E_1 and E_2 is given by equation 6.3;

$$I \propto E_1^2 + E_1^2 + 2E_1E_2 \cos\left[(\omega_1 - \omega_2)t + (\phi_1 - \phi_2)\right] \tag{6.3}$$

In equation 6.3, the beat signal rises from the frequency component ω_1-ω_2, the phase component, ϕ_1-ϕ_2 is a source of high frequency noise which leads to broadening of the linewidth of the beat signal unless there is high correlation between the two sources. Complex laser configurations have been proposed in order to achieve high correlation, and low phase noise, the simplest proposition consisting of a dual-mode semiconductor laser diode.

Fibre lasers are ideal devices for this application due to their very narrow optical linewidth, and good frequency stability. Furthermore, they do not require any of the external devices that alternative solutions require. The optimum solution would consist on using the dual-polarisation characteristic of fibre lasers in order to create the beat signal. The frequency separation between the two polarisations of a fibre Bragg grating inscribed by standard UV methods would

lead, from equation 6.4 to frequency beating in the order of 0.37 to 0.75GHz, since the spectral separation between the two polarisation states is typically between 3pm and 6pm.

$$\Delta f_{pol} = \frac{c}{\lambda_B^2} \Delta \lambda_{pol} \tag{6.4}$$

where Δf_{pol} is the separation between frequencies, λ_B, is the resonant wavelength, $\Delta \lambda_{pol}$ is difference in wavelength between the two polarisations.

Evidently a larger spectral separation between the two polarisation modes would be desirable for this particular application. Attempts to increase the spectral separation have consisted on inscribing gratings using UV sources offset from the centre of the fibre. There is also evidence that gratings inscribed in double clad Er:Yb fibre tend to observe higher birefringence due to their ring-like photosensitive region and its high photosensitivity, leading to higher refractive index changes in the side of the fibre exposed to UV radiation. The used of either of these techniques has lead to signal generation of frequencies as high as 2 GHz, it would be therefore desirable to increase the frequency for this technology to be applied in high frequency signal generation. As it was described in chapter 4, point-by-point femtosecond inscription of fibre Bragg gratings can provide higher birefringence than UV inscription. Therefore this method of inscribing fibre Bragg gratings may be considered for microwave generation.

6.4. Fibre Lasers inscribed directly by femtosecond lasers

The inscription of gratings with a femtosecond laser offers a number of benefits in the inscription of fibre lasers. Unlike UV methods, femtosecond techniques permit direct inscription in Er:Yb codoped fibre, thus, special double-clad fibre designs are not necessary. Furthermore these gratings should exhibit improved thermal stability and polarisation properties that can expand the number of applications of these devices. The main concerns and potential applications related to fibre lasers have been raised in the preceding sections. Those included low pump absorption for the erbium doped fibre, low photosensitivity for the co-doped erbium/ytterbium fibre and polarisation related problems such as the dual polarisation beat-signal noise. Using point-by-point inscription of fibre Bragg gratings by femtosecond irradiation, not only offers unique solutions for these problems, but also improves the thermal stability and lifetime stability of fibre lasers.

Femtosecond inscription in Er:Yb fibre is an interesting proposition because it makes possible the inscription of gratings directly in the core of the non-photosensitised fibre, unattainable by standard UV inscription. In addition, the characteristics of gratings inscribed by femtosecond lasers offer numerous technological advantages which are investigated in this chapter. In particular, we study the birefringence and thermal characteristic of the fibre lasers produced and consider novel applications.

Initially efforts were focused at using highly birefringent gratings in order to use the spectral separation between the two states so the beat signal between the states could be used to generate microwave signals useful in telecommunications. Microwave signal generation has not yet been achieved. However, we have demonstrated single polarisation lasing due to gain competition between the two polarisations allowing only one of the modes to reach threshold. This is simple for gratings inscribed point by point by a femtosecond laser since the polarisation dependent losses can be made very high. As well as attractive unique properties, direct point by point inscription of fibre Bragg gratings comprises a number of challenges for the fabrication of fibre lasers; insertion (out of band) losses induced during inscription must be low and high uniformity along the grating is required. The uniformity along the grating is an important factor since the lengths required for fibre laser configurations are generally between 30mm and 50mm long, and the fluctuations in the uniformity are more significant in long gratings.

This chapter integrates the technology of femtosecond inscription into fibre laser fabrication. Two fibre laser configurations realised by direct femtosecond inscription are reported, a ring cavity laser in an erbium-doped fibre, and a distributed Bragg reflector (DBR) laser in an erbium: ytterbium codoped fibre. Initially a ring laser configuration was adopted since its realisation is the easiest to achieve in terms of the complexity of the femtosecond inscribed structures.

6.4.1. Ring cavity lasers

In erbium doped fibres, high pump absorption cannot be achieved. For this reason a long active fibre is required to achieve laser operation. A ring laser configuration, commonly used with gratings inscribed by conventional UV methods was employed, such as seen in figure 6.4. This configuration was chosen for its simplicity, to study the properties and merits of fibre lasers in which the reflective mirror is a fibre Bragg grating inscribed by a femtosecond laser. The only requirements for lasing are a uniform highly reflective grating with low insertion losses. Those requirements, as demonstrated in chapter 4, are satisfied by the gratings inscribed using the point-by-point inscription.

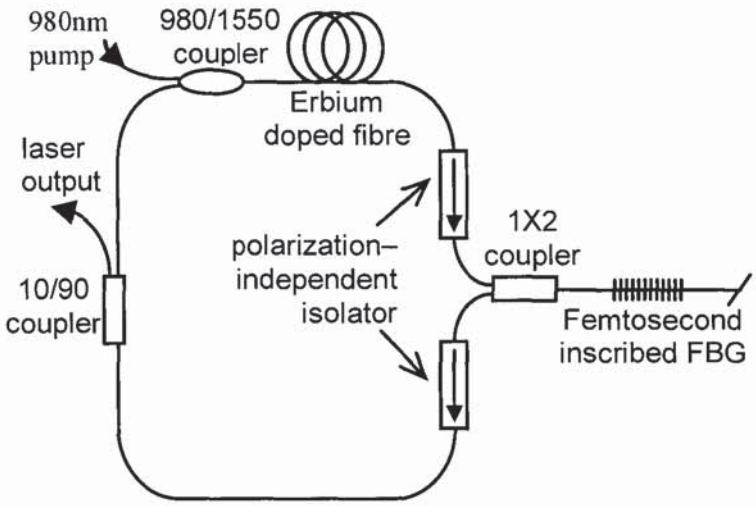

Figure 6.4: Ring cavity fibre laser configuration based on and erbium doped gain fibre and a grating inscribed with a femtosecond laser forming the resonator cavity.

Gratings inscribed using femtosecond lasers can be fabricated with increased birefringence, the objective of this experiment was to use a highly birefringent grating and study its performance as a fibre laser and investigate the potential uses as a microwave signal generator.

Spectral separations as large as 50pm have been observed in gratings inscribed by this point-by-point method. By using such highly birefringent grating it is in principle possible to create

beat frequencies as high as 6GHz. It is worth noting at this point, that the spectral separation of 50pm correspond to an engineering limit rather than a fundamental one. Future work will investigate in detail the parameters that affect birefringence and together with the optimisation of the writing set-up used for alignment, it should allow us to increase significantly the spectral separation and therefore the beat frequencies.

Figure 6.5 shows the laser output of the ring laser configuration illustrated in figure 6.4. This represents the first time that a fibre laser configuration is implemented with a grating inscribed point by point by a femtosecond laser. However, due to the high insertion losses of the grating the output power of the laser did not exceed the -30dBm. Insertion losses with the method of inscription proposed in this work have been significantly reduced through the course of this work and thus output powers can be higher. Despite the low output power observed, these devices may be considered to fabricate high temperature sensors with the probe been the grating inscribed by the femtosecond laser.

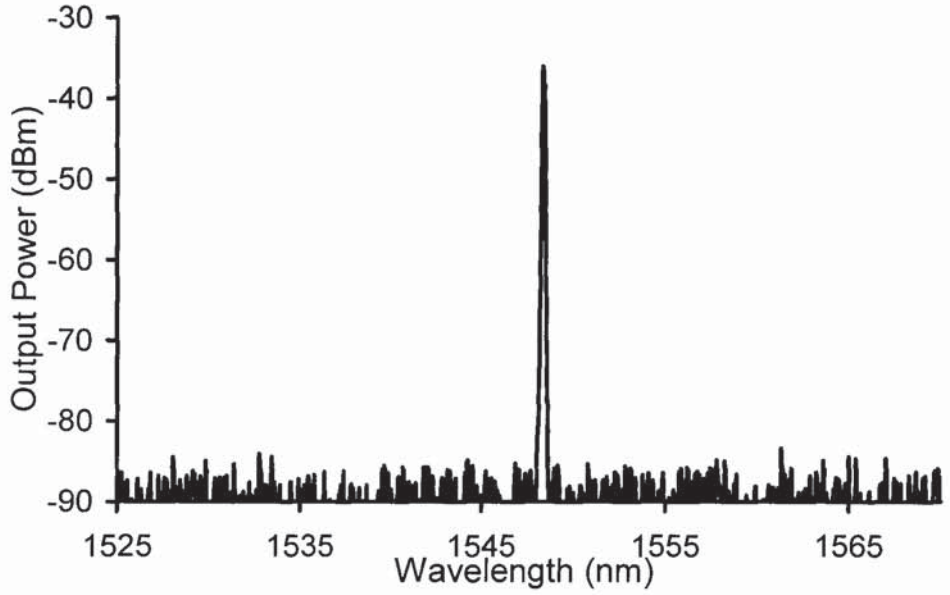

Figure 6.5: Laser output from the ring cavity laser illustrated in figure 6.4.

The bandwidth of the fibre Bragg grating used in this configuration did not permit single mode operation. Therefore, the beat frequency of the laser could not be analysed due to the significant spectral noise. In order to achieve single-mode operation a DBR configuration was adopted and it is described in the next section. Single-mode operation can be also realised in the ring cavity configuration by introducing a narrow-band filter, such as a Fabry-Perot within the cavity.

6.4.2. Distributed Bragg Reflector (DBR) Lasers

Rare earth doped fibre Bragg grating lasers are an attractive alternative to their semiconductor counterparts in a wide range of communication, sensor and spectroscopic applications. To realise useful and robust fibre laser configurations, the gain fibre and the grating characteristics are generally important design considerations. In the previous section a fibre laser was implemented based on a uniform grating inscribed by a femtosecond laser in standard fibre and a ring laser configuration with an erbium doped fibre used as gain media. Although laser operation was demonstrated, low output power and multimode operation made it undesirable for most applications.

In this experiment, a distributed Bragg reflection (DBR) laser configuration is adopted in order to achieve single-mode operation. This is required for telecommunications and desirable for sensing applications. Work on this configuration was chosen over DFB configurations due to the lower requirements for the fabrications of DBR lasers. DFB laser fabrication demand the inscription of highly uniform grating of lengths in the range between 40mm to 50mm, with very low insertion losses. While DBR lasers can be achieved by only inscribing in 10mm to 15mm of the fibre, therefore reducing the insertion losses.

Inscription Method and Laser configuration

The gain media used for this laser configuration was a standard co-doped Er:Yb fibre with a core diameter of 6μm and 730dB/m absorption of 980nm pump wavelength. Such high levels of absorption are possible due to the presence of a high concentration level of ytterbium, and it implies that laser operation is available even with reduce resonator sizes in the order of tens of millimetres.

The fabrication system setup is identical to that described in chapter 4. An amplified Ti:Sapphire laser system producing 150fs pulses at 800nm at a repetition rate of 1kHz was focused into the fibre core by a 100X microscopic objective. It is worth noting that there was no significant difference in the required pulse energy for grating inscription in the Er:Yb-codoped phosphosilicate fibre compared to the standard telecom fibre, and it was in both cases approximately 0.5 μJ. A translation speed of 1.07mm/s was adopted to create a grating pitch of 1.07μm so that the second order Bragg resonance occurs within the 1550nm window. By synchronising the fabrication exposure with a shutter, two 8mm-long uniform fibre Bragg gratings spaced 15mm apart were inscribed in a one-step, 30 second inscription process into

the Er:Yb-codoped fibre to create a DBR fibre laser configuration, such as the one illustrated in figure 6.6.

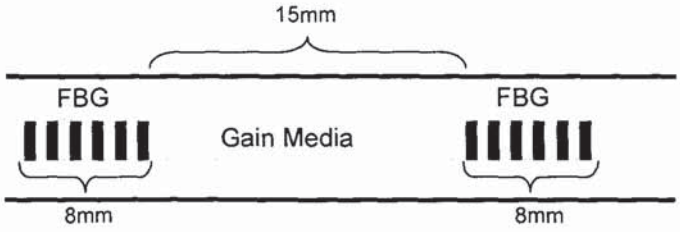

Figure 6.6: Illustration of a standard DBR fibre laser, a Fabry-Perot resonator is produced in a fibre with a gain core fibre.

The laser configuration emulates the classic laser configuration in which a gain media is enclosed by two highly reflective mirrors, with the only difference of all components being integrated in the core of a fibre.

The fibre laser was pump by a 980nm diode laser using a set-up such as illustrated in figure 6.7. The output was measured in reflection using an optical spectrum analyser; a polariser and a polarisation controller were introduced before the output in order to study the polarisation properties of the device.

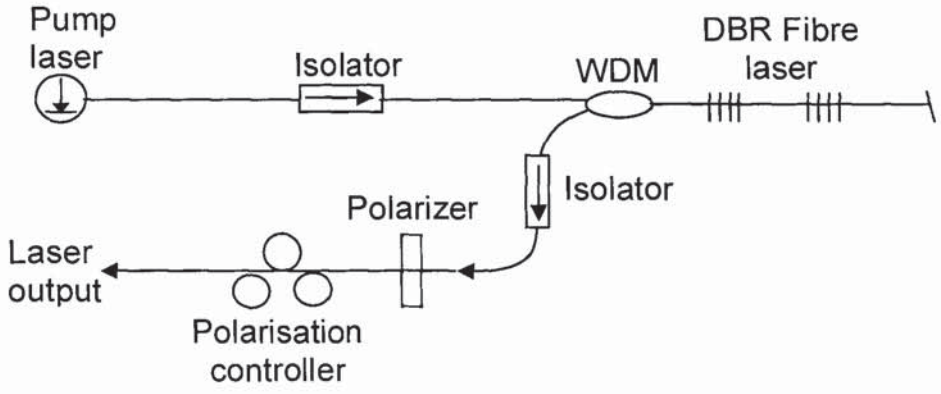

Figure 6.7: Experimental set-up for DBR Er:Yb fibre laser.

The end of the fibre at transmission was immersed in index matching fluid in order to suppress reflections from the fibre end. The fibre laser did not require any stabilising devices and directional isolators were introduced to avoid parasitic reflections.

Spectral Characteristic of DBR Laser

Before pumping the DBR fibre laser, we looked at the spectral characteristics at transmission of the Fabry-Perot cavity using a tuneable laser and a wavelength meter. The inscribed structure showed the characteristic profile of a Fabry-Perot cavity as it is shown in figure 6.8. The out of band losses measured were less than 0.2dB, for the 15mm inscribed length, with a grating strength in excess of 45dB.

Figure 6.8: Transmission profile of the DBR fibre laser cavity showing distinct resonance peaks.

The resonance features in the spectral profile indicate clearly that a FBG resonator has been realised in the Er:Yb codoped fibre. Each resonance peak corresponds to a longitudinal mode with the dominant lasing mode being at the Bragg centre under the homogenous gain medium.

$$\Delta\lambda_{FSR} = \frac{\lambda^2}{2n_{cav}l_{cav}} \tag{6.5}$$

The longitudinal mode spacing measured 43pm, corresponding to an effective cavity length of 19mm.

The 31mm-long DBR fibre laser was then operated using a 980nm laser diode as the pump source. Using a pump power of 55mW, the laser delivered -7.4dBm at approximately 1548.8nm which was expected from figure 6.8. The output optical spectrum is as shown in figure 6.9.

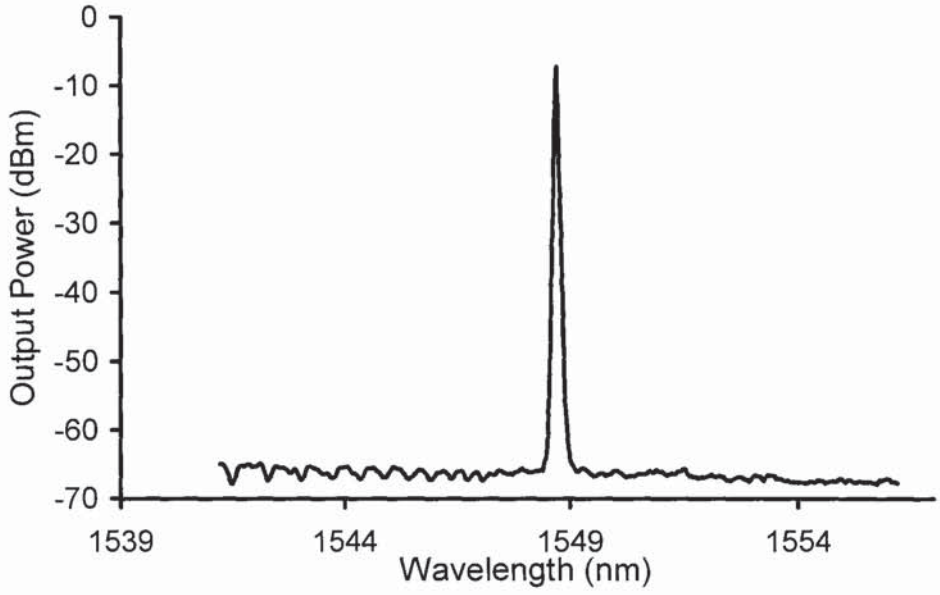

Figure 6.9: Fibre laser output optical spectrum during operation. Maximum laser output was -7.3dBm.

From figure 6.9, we observe that the linewidth of the DBR laser emission is as narrow as 50pm at FWHM. Single-mode operation is demonstrated in this laser, mode-hoping was not observed during operation even after exposure to high temperatures.

Polarisation properties

By performing beat signal analysis on the laser output after a polariser, single-mode, single-polarisation mode operation, with polarisation purity in excess of 40dB, is verified by the absence of any mode beating signals.

This is likely to be a result of the highly localised index modulation, defined by the focusing geometry, which leads to polarisation dependent characteristics in the inscribed fibre grating laser structure. Detailed measurements on several uniform fibre Bragg gratings fabricated under the same conditions show that the birefringence, Δn, and corresponding grating strength difference between orthogonal polarisations axes, ΔR, are on the order of $\Delta n \sim 0.9 \times 10^{-5}$ to 4.3×10^{-5} and $\Delta R \sim 0.4$dB to 1.5dB respectively, depending on the focused beam alignment. The relative difference in coupling coefficients between orthogonal polarisation axes which was inferred from first-order grating model is therefore ~ 0.02 to 0.07. Single-polarisation mode operation is hence achieved based on this distinct dependence on polarisation of the grating strength.

Power fluctuations and Noise levels

The short-term output power stability of the laser, maintained at room temperature, was evaluated over 1 hour, during which time 30000 sample measurements were taken and shows < 0.05dB fluctuation as shown in figure 6.10.

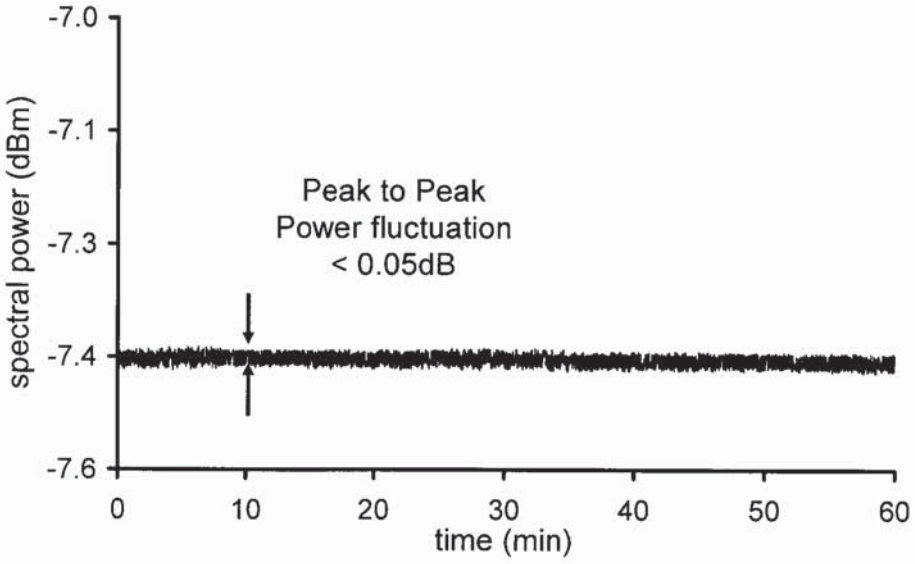

Figure 6.10: Measured fibre laser output power over 1 hour. Inset shows the RIN spectrum of the laser output. The typical relaxation oscillation peak is evident.

The fundamental prerequisite of optical sources suitable for optical communication applications is a low Relative Intensity Noise (RIN). The measurement of RIN describes the laser's maximum available amplitude range for signal modulation. It is defined as the ratio of the mean-square optical intensity noise to the square of the average optical power. Since the ratio of optical power squared is equivalent to the ratio of detected electrical power, RIN can be expressed as

$$RIN = \frac{N_{electrical}}{P_{electrical}} \text{ dB/Hz} \qquad (6.6)$$

where $N_{electrical}$ is spectral power density of the photocurrent at a specific frequency and $P_{electrical}$ is the average power of the photocurrent.

Fibre lasers typically have relaxation oscillation frequencies in the range of a few hundreds kHz to 1.5 MHz. The RIN reaches a peak at that frequency before decreasing rapidly at higher frequencies. Hence RIN at the relaxation oscillation frequency can be used as a comparative quality indicator.

The RIN of the fibre laser was measured using a low-noise receiver (New Focus 1811). The output power of the fibre laser was attenuated to a level within the linear operation range of the receiver. The electrical spectrum analyser (ESA) spectrum around the relaxation frequency of a fibre laser is as shown in figure 6.11. The output power of the fibre laser after attenuation was measured prior to the noise level measurement. The noise level obtained from the ESA spectrum at a specific frequency represented the total noise at that frequency. The laser intensity noise was thus obtained by subtracting the thermal noise and the shot noise from the total measured noise level at the same frequency. The thermal noise level for the system was simply read off from the ESA spectrum with the fibre laser removed from the receiver. The average electrical power of the laser was then used to divide the laser intensity noise to derive the relative intensity noise RIN_{laser} of the fibre laser. By similarly carrying out the measurement and computation at various frequencies, the general RIN profile of a fibre laser over a frequency range can be plotted. In general, RIN values <-130dB/Hz at high frequencies (>50MHz) are required for optical communication transmission purposes.

The relative intensity noise (RIN) of the fibre laser output was measured and exhibits a typical relaxation oscillation peak at 261kHz with intensity -94dB/Hz. The noise level decreases rapidly to < -120dB/Hz beyond 500kHz as shown in figure 6.11. It is worth noting that higher output power is achievable by increasing the cavity length and consequently the accessible gain of the laser and feedback mechanism can be installed to remove the intensity noise peak.

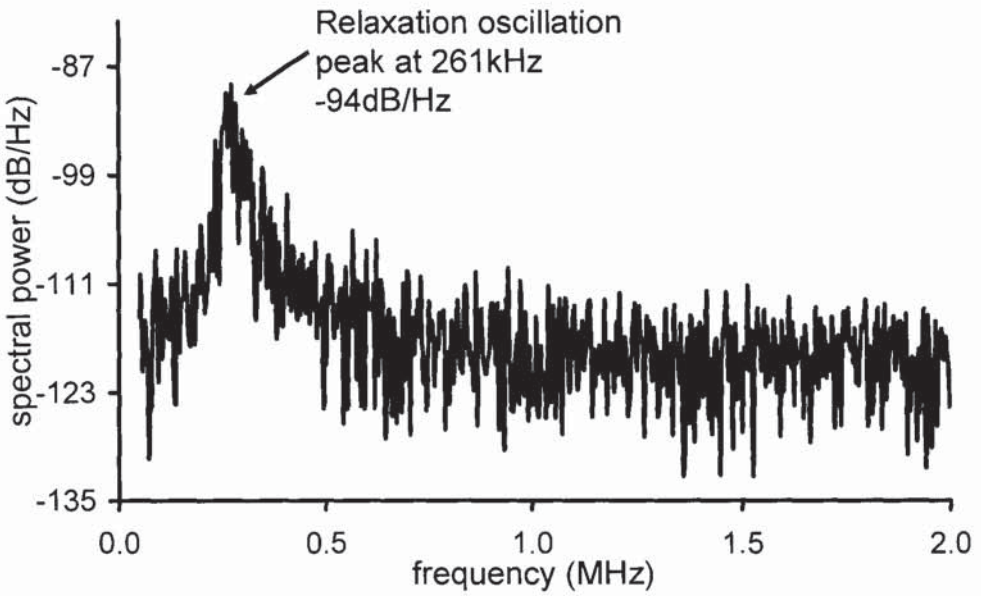

Figure 6.11: Noise level spectrum of the fibre laser in the proximity of the relaxation oscillation frequency. The measured noise level at one frequency represented the total system noise at that frequency.

The DBR fibre laser inscribed by femtosecond laser inscription does therefore compare well with similar DBR laser configurations inscribed using conventional UV inscription. While the output power and RIN figures are similar, single-mode operation is demonstrated throughout the operation regime of the laser.

Thermal dynamics of a DBR laser inscribed by a femtosecond laser

To verify that the fibre laser exhibits high thermal resistance inherent to grating structures inscribed by a femtosecond laser, the laser was placed in a tube furnace and its output at 55mW pump power was monitored on an optical spectrum analyser over a temperature range from 20°C to 605°C. As shown in figure 6.12, the rate of the temperature dependent wavelength shift gradually increases from a rate of ~11pm/°C at temperatures up to 100°C to a rate of ~16pm/°C. In a separate experiment, the thermal response of a 8mm-long uniform fibre Bragg grating fabricated under the same conditions in the Er:Yb-codoped fibre was similarly evaluated showing very close agreement. Studies on the thermal dynamics of UV inscribed gratings at these temperatures are limited due to the low thermal stability of the UV inscribed structures. However the non-linear behaviour here demonstrated is reported as well in gratings inscribed in

Er-Sn fibre given that inscription in these fibres present improved thermal stability. The nonlinear thermal behaviour of fibre Bragg gratings was further investigated in chapter 5.

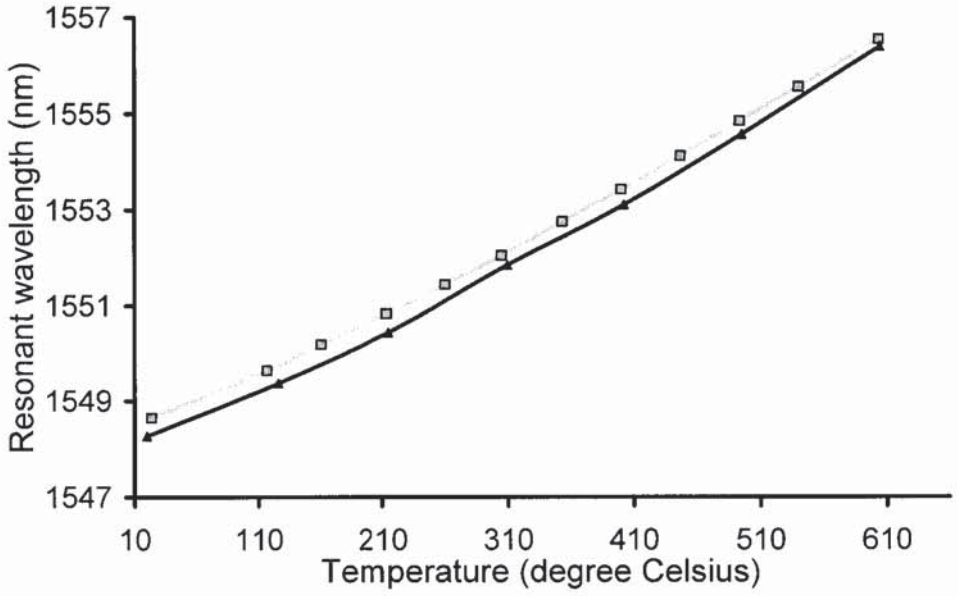

Figure 6.12: Thermal wavelength shifts of the fibre laser output (grey) and a uniform FBG (black) in Er:Yb-codoped fibre.

Due to the non-uniformity of the temperature along the open-ended tube furnace, the grating cavity was chirped and hence the output power characteristics over the temperature range cannot be quantified specifically in the experiment. However, the fibre laser can operate steadily at each temperature, and its high resistance to thermal decay is illustrated through a continuous operation at 500°C over 17 hours as shown in figure 6.13. No significant degradation in the performance of the laser was recorded throughout the whole period.

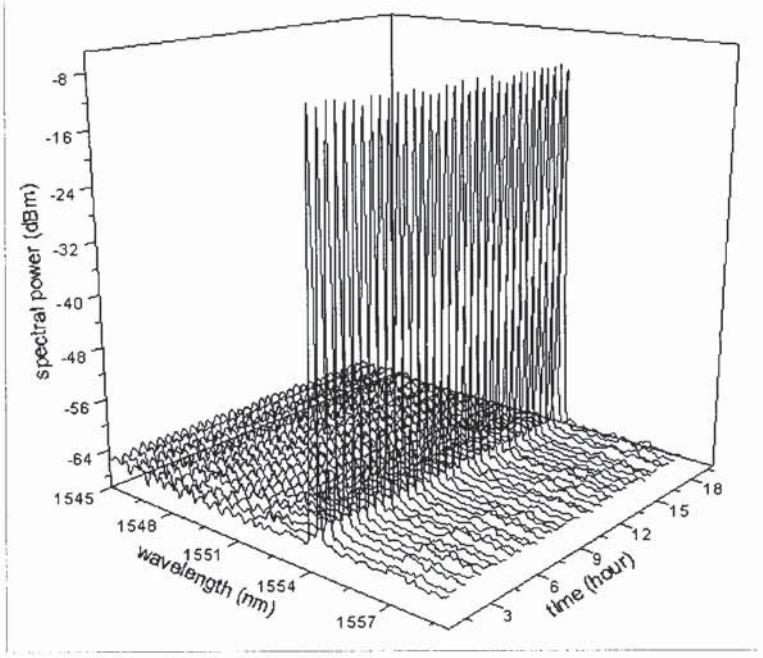

Figure 6.13: The fibre laser output sampled every half hour over 17 hours at ~500^{0}C.

It is worth noting that any degradation of the grating at high temperatures would prevent lasing operation, indicating that the gratings forming the resonator did not suffer any degradation. This is in contrast to various reports indicating high thermal stability of gratings inscribed by UV techniques [78], which degrade from an initial reflectivity of a 100% reflectivity to thermally stable reflectivity in the order of 80%, which may be suitable for sensing applications but does not permit lasing operation.

6.4.3. Distributed Feedback laser

DFB lasers offer better stability and stronger side-mode suppression than DBR lasers. It would therefore be advantageous to create such structure by means of femtosecond inscription. A DFB fibre laser consists of a long grating of at least 40cm to 50 cm in a high gain material such as Er-Yb fibre, with a gap in the periodicity at some point of the grating.

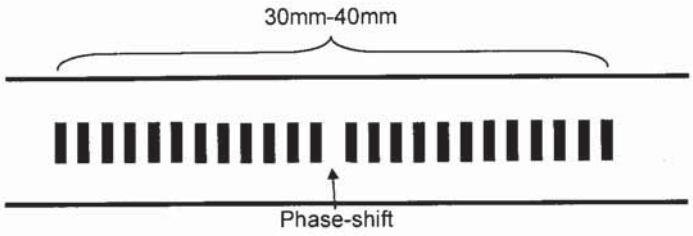

Figure 6.14: Illustration of a distributed feedback configuration.

The phase-shift can be achieved by post-processing the material after the inscription of the grating, or by omitting the inscription of one or various pitches during inscription. Either method has been employed successfully in UV inscription. Point-by-point inscription offers, in principle, the required flexibility to create such phase-shifted gratings, however, the high uniformity required for laser operation have prevented so far, the inscription of such structures by the method proposed in this work.

6.5. Conclusion

For the method developed in this work, fibre laser technology is simultaneously an area of great potential and great challenges. Fibre lasers require gratings of high spectral quality and low losses. Thus, the inscription method and set-up must be further developed to comply with those requirements. On the other hand, femtosecond inscription can provide a solution to major problems in fibre laser technology such as the low photosensitivity of the Er:Yb codoped fibre or the dual-polarisation beat frequency noise.

We proposed and demonstrated two fibre laser configurations. The first one was a ring cavity laser and the second a distributed Bragg reflector (DBR) fibre laser. The ring cavity laser represents the first demonstration of a fibre laser based on a grating inscribed by a femtosecond laser. The second laser produced was a short-length, linear cavity, DBR laser which was inscribed directly in a conventional Er:Yb codoped fibre overcoming the issue of the low photosensitivity of the gain fibre. Single-mode, single-polarisation operation was provided by the polarisation properties of the gratings that comprise the resonator cavity. In addition, stable lasing operation was observed at temperatures as high as 600°C, thus demonstrating the high thermal stability of the device.

CHAPTER 7: Conclusions

In this work, a novel method for direct, point-by-point writing of fibre Bragg gratings by means of femtosecond inscription was demonstrated. Unlike previously reported point-by-point methods, this scheme permits straightforward alignment and allows a rapid inscription process with the inscription time of several seconds. Point-by-point inscription is undoubtedly improved by using an infrared femtosecond laser compared to similar techniques based on other types of lasers. This superiority is evident from comparison of the inscription procedures and it is also confirmed by the detailed characterisation of the produced gratings. Some advantages of the technique arise generally from the physics of the femtosecond inscription process, whilst the other ones are specific to this particular writing technology.

We demonstrated, for the first time, the inscription of first order Bragg gratings by an infrared laser for a resonant wavelength of 1550nm. Incidentally, this represent also the first time that a first order grating is inscribed using a point by point method. Higher order gratings were also produced, the highest reflectivity was observed in the second order Bragg gratings. The strength of first order Bragg gratings was compromised by the reduced visibility of the refractive index modulation in the grating. Each pulse produced one grating pitch, but the region modified by the pulse was larger than the grating pitch for the first order gratings. This resulted on significant overlapping of individual modified regions.

All the gratings presented in this work were formed in commercial fibres without any photosensitisation and showed low insertion loss, narrow linewidth and strong, fundamental or higher order, resonance. The inscription process was fast and reliable, with a writing speed of approximately 1 mm/s.

We adopted a point by point method for the inscription of fibre Bragg gratings for its flexibility and simplicity. This method does not require a phase-mask and does not have stability requirements as stringent as interferometric set ups. In addition, by exploiting the characteristics of the infrared femtosecond laser, a fast and accurate method for alignment was developed. This was a major step in this project since alignment has been generally the key drawback of point by point techniques.

The relevance of this method in industry will depend fundamentally on the properties of these gratings compared to gratings inscribed by standard UV methods. The initial interest resided mainly in two points; the expected higher thermal stability and the possibility to inscribe gratings in non-photosensitive fibres. During the project, not only those two properties were demonstrated but we observed a number of unique characteristics such as; very high and

controllable birefringence, the possibility to inscribe gratings through the coating and small dimensions of the grating structure within the core.

It was demonstrated in this work, that inscription in untreated non-photosensitive fibre of highly reflective gratings is possible. This simplifies the inscription process since neither the use of hydrogenated or doped fibre is necessary. Moreover, it permits inscription in fibres where inscription was previously unattainable or inefficient, such as Er:Yb fibre.

Thermal stability is significantly higher for gratings inscribed by the method here proposed than gratings inscribed by UV-methods. Gratings inscribed using an infrared femtosecond laser exhibit stability at temperatures as high as 1000°C. Dynamics of reflectivity during the annealing-cooling cycles indicate, in particular, that the strain in the material volume adjacent to the modified region is a significant factor affecting the grating performance. Annealing at temperatures up to 700°C eliminates these strains leading to an increase in the overall reflectivity of the grating.

Gratings inscribed by other methods generally consist of periodical volumes which cover uniformly the cross-section of the core. On the other hand, the gratings presented in this work only cover a small region of the cross-section of the core with an estimated area of approximately $2\mu m^2$. The modified volume of material often consists of a central region with the negative refractive index change and a surrounding area with a positive index change. The refractive index change was estimated to be of the order of 10^{-3}. The small size of the grating structure has important effects on the spectral properties of the grating. Various ways in which to exploit this unique feature were investigated in this work.

A consequence of the small size of the grating structure is that the polarisation sensitivity of these gratings is significantly higher than it is observed in gratings inscribed by UV methods. Furthermore, we observed that by axially offsetting the gratings from the centre of the core the polarisation sensitivity could be enhanced. Controlling the polarisation properties of the grating may be useful for applications such as fabricating single-polarisation lasers, microwave signal generation, mode converters or rocking filters.

Inscription of highly reflective fibre Bragg gratings in standard, non-photosensitised SMF fibre through the coating, is possible with this technique. Standard coatings are transparent to infrared light however since the ablation threshold is lower for the polymer used in the coating than for the glass, tight focusing is critical to permit the inscription of the grating before ablation takes place at the surface of the coating. This indicates that inscription through the coating may not be achievable by phase-mask techniques based on femtosecond lasers. Inscription through the coating poses important technological advantages since it minimises the deterioration of the fibre by the inscription process as well as reducing the time and cost of the procedure.

One of the downsides of the method of inscription proposed in this work is the low quality of some of the gratings. This can be attributed to the lack of stability in the writing conditions but it is not an intrinsic characteristic of the gratings. This method requires higher mechanical stability and more precise motion control than diffractive methods, but the requirements are not as stringent as for interferometric methods. A further drawback arises from the strong changes in material structure as well as the non-circular shape of produced features leading to the increased scattering and coupling between the guided and the cladding modes, thus increasing the losses at wavelengths lower than the resonant wavelength. Furthermore, the insertion losses induced during the inscription of the grating are approximately 0.2dB/cm, higher than that observed in UV inscribed gratings.

A number of novel applications were demonstrated based on the exploitation of the characteristics of these gratings. A direction-sensitive bending sensor was implemented. The working principle of the device was based on breaking the symmetry of the fibre by inscribing a structure off the centre of the fibre. Other possible applications investigated and implemented included; superimposed but non-overlapping gratings and fibre lasers.

Whilst standard Bragg gratings are not sensitive to bending and long period gratings need to be inscribed in special asymmetric fibres in order to discern between bending directions. Axially offset gratings inscribed by the method study in this work offer directional sensitivity to the bending direction, allowing the fabrication of novel vectorial sensors based on fibre Bragg gratings. The inscription of arrays of superimposed, non-overlapping gratings in standard optical fibre is also possible with this technique, the inscription of various gratings leads to an increase in the out of band losses, and reduce the applicability in transmission applications. Nevertheless, since insertion losses are not critical for sensing applications, an omni-directional bending sensor is proposed in this work comprising four axially offset, non-overlapping gratings.

A ring cavity fibre laser and a distributed Bragg reflector (DBR) fibre laser were also produced in what represents, to the best of my knowledge, the first demonstrations of fibre lasers produce by an infrared femtosecond laser. In order to fabricate the DBR laser, highly reflective gratings with low insertion losses were inscribed in non-photosensitive, active Er:Yb codoped fibre. Due to the polarisation properties of the gratings that comprise the resonator cavity, single-mode and single-polarisation operation was achieved. Furthermore, stable lasing operation was observed at temperatures as high as 600°C, thus demonstrating the high thermal stability of the device.

Demonstrating the flexibility of the method, other in-fibre devices were implemented. Long period gratings were inscribed using the same set up arrangement as the one used for the inscription of fibre Bragg gratings. The only addition was a shutter synchronised with the laser which allowed extra flexibility on the exposure regime.

Finally, an alternative technique to create direction sensitive bending sensors was presented. This technique takes advantage of the possibility of inscribing structures in non-photosensitive regions. A method was presented in which long period gratings inscribed in standard fibre are made direction sensitive to bending, by embedding a track with a refractive index change in a given part of the cladding using the above technique and modifying the properties of the cladding propagating modes. Directional sensitivity of long period gratings after femtosecond induced asymmetrisation was demonstrated.

In this project, we focused mainly on developing the method of inscription, characterising the devices and finding suitable applications. Therefore, investigation of the physical mechanisms that take place during inscription was limited. However, the studies carried out to investigate the refractive index change and the thermal stability provides some information in the nature of the process.

We observed that the inscribed structures present a central part with a negative refractive index change surrounded by a ring-like structure with a positive index change. The structure inscribed is similar to a frozen pressure wave in a solid. This indicates that the central region is less dense while the area surrounding this point is denser. A possible explanation for such structure is that when the pulse is absorbed by the glass material, it creates an electron-plasma. The pulse energy is such that this plasma begins to expand into the surrounding areas creating an acoustic wave. This result indicates that we are operating at intensities in the level of micro-explosions, and not of exclusively positive refractive index modifications.

In the thermal stability studies, we observed that the reflectivity of the gratings increased after cycles of 24 hours at temperatures of 700°C. We believe this is a result of the annealing of parasitic strains introduced in the fibre during inscription that reduce the visibility of the grating structure while the central feature of the grating is unaffected by the high temperatures. At such high temperatures, the defects present in standard UV gratings are annealed. This result leads us to believe that defect formation is not a contributing factor in the reflectivity of gratings inscribed point-by-point by a femtosecond laser.

In summary, this work proposed a novel method for the inscription of in-fibre structures using a tightly focused femtosecond laser. Those include fibre Bragg gratings, long period gratings, fibre lasers, and asymmetric directional bending sensors. Their characteristics were examined and their merits compared to those of alternative techniques. Particular attention was drawn to novel applications that exploit the distinctive properties of the device.

CHAPTER 8: Future Work

Throughout this work, a set-up was built for the inscription of gratings, devices were characterised and applications proposed. It has been demonstrated that this technique offers a solution for a number of the shortcomings observed in structures inscribed by UV methods, however only a limited number of applications have been explored. This chapter offers an overview to the studies currently in progress and future projects, which aim to take full advantage of the method.

8.1 Optimisation of the fabrication set-up

The quality of the gratings inscribed has improved vastly throughout the development of the project. This has been due to improved understanding of the process, and minor improvements in the system. A complete optimisation of the system has not yet been done, since the demonstration of novel properties and applications were given priority, in order to demonstrate the validity an interest of the method. Therefore, the quality of the gratings, level of control and repeatability are still low compared to well-established UV technologies, which have been developed over two decades. Despite the evident flexibility of the system, in order to increase the complexity of the structures, optimisation of the system is required. One of the key parameters that must be monitored in order to produce long, high quality uniform gratings is the strain in the fibre.

Optimisation of the alignment and inscription will permit the inscription of high quality long uniform gratings. The inscription of chirped gratings is simple using this point by point technique since the only thing that needs to be change is the writing speed, although an important limiting factor, the strong coupling to cladding modes, ought to be addressed. The cladding modes are significantly reduced by inscribing through the coating and can be further reduced by obtaining a better control over the writing parameters and alignment. Apodisation is also possible, by varying the pulse energy throughout inscription, a detailed study on the effective refractive index in this gratings is necessary.

8.2 Inscription in other fibres and planar structures

It has been demonstrated that femtosecond inscription is suitable for a wide variety of materials. In this work, we demonstrated the inscription in standard non-photosensitive fibre and Er:Yb fibre, both of which cannot be modified by standard UV-based techniques. It would represent a significant achievement to expand the inscription to fibres such as polymer fibres or photonic crystal fibres, which are expected to become important components for photonic systems, in which the inscription of gratings poses an enormous challenge. Although we have recently inscribed a long period grating in a photonic crystal fibre using a femtosecond laser, the real challenge will be to overcome the diffraction of the pulse by the air holes that for the cladding and produce a confined structure within the core sufficient to produce Bragg gratings.

Inscription of waveguides using infrared femtosecond lasers is been the subject of intense research in recent years. The optimum conditions for the inscription of waveguides are based on high repetition rate lasers with a microscopic objective or using a low repetition rate and a beam shaped with a cylindrical telescope. In the second case, in order to integrate a grating in the femtosecond inscribed waveguide, it would be necessary to do it in a two-steps process, since the focusing conditions required for inscribing gratings and inscribing the waveguide are different. The aligning process in a planar structure is simplified by the fact that surfaces are planes, and the focusing conditions are improved.

8.3 Optimisation of focusing conditions

It has been demonstrated in this work that efficient, short-length fibre Bragg gratings can be produced by inscribing a second order structure using a tightly focused laser beam (100X microscopic objective with a numerical aperture of 0.55). This was done by inscribing with a pitch corresponding to a second order period. Achieving tighter focusing is therefore not necessary for general applications. It would be beneficial however for a number of special applications, such as inscribing several superimposed overlapping gratings, increasing the polarisation sensitivity, or inscribing gratings for shorter resonant wavelengths.

The lens effect of the surface of the fibre was mentioned in this work, as well as the relative advantage of using a long working distance objective. Tighter focusing is achievable by using an objective with a higher numerical aperture and by reducing the effect of the curvature of the fibre in the focusing conditions. This is possible by using immersion oil objectives with high numerical apertures. The alignment procedure in such case will be more complex due to the short working

distance of the objective and the need for homogeneous index-match fluid through the writing process.

8.4 Investigation on the birefringence

In this work, we demonstrated that gratings inscribed point-by-point exhibit a strong birefringence. We also observed the possibility to increase this birefringence by axially-offsetting the grating with respect to the geometrical centre of the fibre and indicated various parameters that may contribute to the polarisation sensitivity. Those were; the relative position of the grating structure with respect to the geometrical centre of the fibre, the asymmetric dimensions of the structure inscribed and the stresses induced in the surrounding area. Further investigation is necessary in order to understand the relative merits of each of these parameters. This investigation aims to have a better control on the polarisation of each inscribed grating, so higher birefringence can be achieved. In addition, and considering applications where birefringence is detrimental. We will work on finding ways in which to reduce the birefringence to the levels observed in gratings inscribed by standard UV methods. This is, in principle, possible by inscribing the gratings in a twisted fibre which would lead to the creation of a spiral-like structure.

8.5 Long Period Gratings

Several long period gratings of high quality have been inscribed and their characteristics are currently been investigated. The initial results indicate an appreciably different behaviour between long period gratings and fibre Bragg gratings, both in thermal and polarisation properties. The reason for the different conduct was commented on chapter 4. It is evident that unlike fibre Bragg gratings, the inscription of long period gratings requires a microscopic objective with lower numerical aperture. In the case of long period gratings, covering as much of the core as possible is advantageous in terms of improving the strength of the grating, and since the period is various order of magnitude larger than the spot size, overlapping of the grating pitches is not a concern. After a first demonstration, further work on the inscription of long period gratings in photonic crystal fibres is necessary.

Furthermore, a through study of the characteristics of long period gratings and particularly how they compare with fibre Bragg grating inscribed with the same approach inscribed using this technique could give further information regarding the nature of the process that leads to the inscription of structures in the fibre.

8.6 Fibre lasers

Lasing operation has been demonstrated with a ring cavity laser and a DBR laser, both based on a fibre Bragg grating inscribed point-by-point by an infrared femtosecond laser. A DFB configuration is however generally preferred, due to its compactness and tunability. A DFB laser consists on a phase-shift grating inscribed in a gain fibre with high gain efficiency. The challenge rises from the requirements of good uniformity of the grating over a length in the range between 40mm and 50mm in order to attain lasing operation. The necessary phase-shift can be produced by leaving a gap during inscription, by using a shutter synchronised with the femtosecond laser, or alternatively by post processing a given region using the femtosecond laser.

Particularly interesting is the integration of the fibre laser fabrication to implement omni-directional bending sensors. We have demonstrated the possibility of measuring the bending direction and strength. Polarisation and low sensitivity are nevertheless limiting factors to the feasibility in commercial applications of such device. By using a sensing device consisting on narrow band fibre lasers inscribed in the fibre, the polarisation problem is suppressed since single polarisation has been demonstrated, furthermore sensitivity would be increased due to the narrow linewidth of the laser source.

8.7 Alternative methods of inscription

In this work, we have demonstrated the benefits of using point-by-point inscription for numerous applications. It is however also clear that for some applications phase mask inscription is a more suitable method. One interesting development may be the inscription of tilted gratings through the core and cladding. Tilted gratings make use of coupling the light out of the core at wavelength-dependent angles. They are being used for a number of applications in sensing and for interrogation systems. In theory, efficiency of a tilted-grating may be increased by inscribing the structure not confined in the core but also spreading into the cladding, which is possible to achieve by femtosecond inscription with a phase-mask. The inscription with a phase-mask has also allowed the inscription of gratings with no coupling to the cladding modes. An interferometric set up may also be considered but of the three methods is the one that poses the most significant technological complexity.

References

1. BC Stuart, MD Feit, S Herman, AM Rubenchik, BW Shore and MD Perry, *'Nanosecond to femtosecond laser induced breakdown in dielectrics'*, Physical Review B, 53, 1749-1761 (1996)

2. X Liu, D Du and G Mourou, *'Laser Ablation and micromachining with ultrashort laser pulses'*, J. of Quantum Electronics, 33, 10, 1706-1716 (1997)

3. F Korte, S Adams, A Egbert C Fallnich, A Ostendorf, S. Nolte, M. Will, BN Chichkov and A. Tunnermann, *'Sub-diffraction limited structuring of solid targets with femtosecond laser pulses'*, Opt. Express. 7, 41-49 (2000)

4. KM Davies, K Miura, N Sugimoto and K Hirao, *'Writing waveguides in glass with a femtosecond laser'*, Optics Letters, 21, 21, 1729-1731 (1996)

5. J Zhai, Y Shen, J Si, J Qiu and K Hirao, *'The fabrication of permanent holographic gratings in bulk polymer medium by a femtosecond laser'*, J. Phys. D: Appl. Phys., 34, 3466-3469 (2001)

6. V Apostolopoulos, L Laversenne, T Colomb, C Depeursinge, RP Salathe, M Pollnau, R Ossellame, G Cerullo and P Laporta, *'Femtosecond irradiation induced refractive-index changes and channel waveguiding in bulk Ti^{3+}:sapphire'*, OSA Conf. Proc. CLEO/IQEC and PhAST Washington DC, 2004, CMY4

7. CB Schaffer, A Brodeur and E Mazur, *'Laser-induce breakdown and damage in bulk transparent materials induced by tightly focused femtosecond laser pulses'*, Meas. Sci. Technol. 12, 1784-1794 (2001)

8. D. Du, X. Liu, J. Squire, and G. Mourou, *'Laser induced breakdown by impact ionisation in SiO_2 with pulse widths from 7ns to 150fs'* Appl. Phys. Lett., Vol. 64, 3071-3073 (1994)

9. SH Cho, H Kumagai and K Midorikawa, *'In situ observation of dynamics of plasma formation and refractive index modification in silica glasses excited by a femtosecond laser'*, Opt. Commun., 207, 243-253 (2002)

10. CB Schaffer, A Brodeur, JF Garcia and E Mazur, *'Micromachining bulk glass using femtosecond laser pulses with nanojoule energy'*, Opt. Lett. 26, 93-95 (2001)

11. AM Streltsov and NF Borrelli, *'Study of femtosecond-laser-written waveguides in glasses'*, J. Opt. Soc. Am. B, 19, 2496-2504 (2002)

12. Y. Sikorski, AA Said, P Bado, R Maynard, C. Florea and KA Winick, *'Optical waveguide amplifier in Nd-doped glass written with near-IR femtosecond laser pulses'*, Elec. Lett., 36, 226-227 (2000)

13. H-B Sun, Y Xu, S Juodkazis, K Sun, M Watanabe, S Matsuo, H Misawa and J Nishii, *'Arbitrary-lattice photonic crystals created by multiphoton microfabrication'*, Opt. Lett., 26, 325-327, (2001)

14. E. N. Glezer, M. Milosavljevic, L. Huang, R. J. Finlay, T.-H. Her, J. P. Callan, E. Mazur, *'Three-dimensional optical storage inside transparent materials'*, Opt. Lett., 21, 2023-2025 (1996)

15. SJ Mihailov, CW Smelser, D Grobnic, RB Walker, P Lu, H Ding and J Unruh, *'Bragg gratings written in All-SiO2 and Ge-Doped core fibres with 800 nm femtosecond radiation and a phase mask'* J. Lightwave Tech., 22, 94-100 (2004)

16. Bennion I, Williams JAR, Zhang L, Sugden K, Doran NJ. *'UV-written in-fibre Bragg gratings'*, Optical and Quantum Electronics, 28, 93-135 (1996)

17. CR Giles, *'Lightwave applications of fibre Bragg gratings'*, J. Lightwave Tech.,15, 8, 1391-1404 (1997)

18. Kersey AD, Davies MA, Patrick HJ, LeBlanc M, Koo KP, Askins CG, Putnam, MA, Friebele EJ, *'Fibre Grating Sensors'*, J. Lightwave Tech. 15, 1442-1463 (1997)

19. A Othonos and K Kalli *'Fibre Bragg Gratings: Fundamentals and Applications in Telecommunications and Sensors'*, Artech House Books, (1999)

20. T Erdogan, V Mizrahi, PJ Lemaire, D Monroe, *'Decay of ultraviolet-induce fibre Bragg gratings'*, J. Appl. Phys. 76, 73-80 (1994)

21. Malo, B, Hill, KO, Bilodeau, F, Johnson, DC, and Albert, J, "Point-by-point fabrication of micro-Bragg gratings in photosensitive fibre using single excimer pulse refractive index modification techniques", Electron Lett. 29, 1668-1669 (1993)

22. E Wikszak, J Burghoff, M Will, S Nolte, A Tunnermann and T Gabler, *'Recording of fiber Bragg gratings with femtosecond pulses using a "point-by-point" technique'*, OSA Conf. Proc. CLEO/IQEC and PhAST Washington DC, 2004, CThM7

23. DS Starodubov, V Grubsky and J Feinberg, *'Efficient Bragg grating fabrication in a fibre through its polymer jacket using near-UV light'*, Electron. Lett., 33, 1331-1333 (1997)

24. K Imamura, T Nakai, K Moriura, Y Sudo, and Y Imada, *'Mechanical strength characteristics of tin-doped germanosilicate fibre Bragg grating by writing through UV-transparent coating'*, Electron. Lett., 34, 1016-1017 (1998)

25. RP Espindola, RM Atkins, NP Wang, DA Simoff, MA Paczkowski, RS Windeler, DL Brownlow, DS Shenk, PA Glodis, TA Strasser, JJ DeMarco and PJ Chandonnet, *'Highly*

reflective fibre Bragg Gratings written through a vinyl ether fibre coating', Photonics Tech. Lett., 11, 833-835 (1999)

26. L Chao, L Reekie and M Ibsen, *'Grating writing through fibre coating at 244 and 248nm'*, Electron. Lett., 35, 35-36 (1999)

27. JM Hopkins and W Sibbett, *'Ultrashort pulse lasers: Big payoffs in a flash'*, Scientific American, September, 55-61 (2000)

28. PF Moulton, *'Spectroscopic and laser characteristics of Ti:Al2O3'*, J. Opt. Soc. Am. B, 3, 1 125-133 (1986)

29. DE Spence, PN Kean and W Sibbett, *'60 fsec pulse generation from a self-modelocked Ti:Sapphire laser'*, Opt. Lett., 16, 1, 42-44 (1991)

30. R. Ossellame, S Taccheo, M. Marangoni, R. Ramponi, P. Laporta, D Polli, S. De Silvestri and G. Cerullo, *'Femtosecond writing of active optical waveguides with astigmatically shaped beams'*, J. Opt. Soc. Am. B, 20, 1559-1567 (2003)

31. EG Gamali, AV Rode, VT Tikhonchuck and B Luther-Davies, *"Ablation of solids by femtosecond lasers: ablation mechanism and ablation threshold for metals and dielectrics",* Phys. of Plasma, 9, 949-957 (2001)

32. D Strickland and G Mourou, *'Compression of amplified chirped optical pulses'* Opt. Commun., 56, 219-221 (1985)

33. L Shah, AY Arai, SM Eaton and PR Herman, *'Waveguide writing in fused silica with a femtosecond fibre laser at 522nm and 1MHz repetition rate'*, Opt. Express, 13, 1999-2006 (2005)

34. K Minoshima AM Kowalevicz, I Hartl, EP Ippen and JG Fugimoto, *'Photonic device fabrication in glass by use of nonlinear materials processing with a femtosecond laser oscillator'*, Opt. Lett., 26, 1516-1518 (2001)

35. S Taccheo, G Della Valle, R Osellame, G Cerullo, N Chiodo, P Laporta and O Svelto, *'Er:Yb-doped waveguide laser fabricated by femtosecond laser pulses'*, Opt. Lett., 29, 2626-2628 (2004)

36. Y Kondo, K Nouchi and T Mitsuyu, M Watanabe, PG Kazanski and K Hirao, Fabrication of long-period fibre gratings by focused irradiation of infrared femtosecond laser pulses, Opt. Lett., 24, 646-648 (1999)

37. A Dragomir, DN Nikogosyan, KA Zagorulko, PG Kryukov, EM Dianov, "Inscription of fibre Bragg gratings by ultraviolet femtosecond radiation", Opt. Lett., 28, 2171-2173 (2003)

38. A Martinez, M Dubov, IY Khrushchev, I Bennion, "Direct writing of fibre Bragg gratings by femtosecond laser", Electron. Lett., 40, 1170-1172 (2004)

39. MV Dubov, I Khrushchev, I Bennion, AG Okhrimchuk and AV Shestakov, *'Waveguide inscription in YAG:Cr^{4+} crystals by femtosecond laser irradiation'*, OSA Conf. Proc. CLEO/IQEC and PhAST Washington DC, 2004, CWA49

40. RR Thompson, S Campbell, G Brown, IJ Blewett, AK Kar, DT Reid, *'Femtosecond waveguide fabrication in bulk Lithium Niobate ($LiNbO_3$)'*, OSA Conf. Proc. CLEO/IQEC and PhAST Washington DC, 2005, CThV5

41. L Luo, C Li, S Wang, W Huang, C Wu, H Yang, H Jiang, Q Gong, Y Yang, S Feng, *'Optical microstructures fabricated by femtosecond laser two-photon polymerisation'*, J. Opt. A: Pure Appl. Opt. 3, 489-492 (2001)

42. Y Li, K Yamada, T Ishizuka, W Watanabe, K Itoh, Z Zhou, *'Single femtosecond pulse holography using polymethyl methacrylate'*, Opt. Express 10, 21, 1173-1178 (2002)

43. K Yamasaki, S Juodkakis, T Lippert, M Watanabe, S Matsuo, H Misawa, *'Dielectric breakdown of rubber materials by femtosecond irradiation'*, Appl. Phys. A, 76, 325-329 (2003)

44. E Bricchi, BG Klappauf and PG Kazansky, *"Form birefringence and negative index change created by femtosecond direct writing in transparent materials"*, Opt. Lett., 29, 119-121 (2004)

45. R Stoian, M Boyle, A Thoss, A Rosenfeld, G Korn, IV Hertel and EEB Cambell, *'Laser ablation of dielectrics with temporally shaped femtosecond pulses'*, Appl. Phys. Lett., 80, 353-355 (2002)

46. OM Efimov, K Gabel, SV Garnov, LB Glebov, S Grantham, M Richardson and MJ Soileau, *'Colour-centre generation in silicate glasses exposed to infrared femtosecond pulses'*, J. Opt. Soc. Am. B, 15, 193-199 (1998)

47. M Sakakura, M Terazima, *"Oscillation of the refractive index at the focal region of a femtosecond laser pulse inside a glass"*, Opt. Lett., 29, 1548-1550 (2004)

48. CB Schaffer, AO Jamison, JF Garcia and E Mazur, *"Structural changes induced in transparent materials with ultrashort laser pulses"*, Chapter from "Ultrafast lasers: Technology and applications", A Galvanauskas and GD Sucha. Ed. ME Ferman, Marcel dekker inc. New York (2002)

49. J Liu, Z Zhang, S Chang, C Flueraru, CP Grover, *'Directly writing of 1 to N optical waveguide power splitters in fused silica glass using a femtosecond laser'*, Opt. Comm. 253, 315-319 (2005)

50. S Juodkazis, S Matsuo, H Misawa, V Mizeikis, A Marcinkevicius, HB Sun, Y Tokuda, M Takahashi, T Yoko, J Nishii. *'Application of femtosecond laser pulses for microfabrication of transparent media'*, Appl. Surf. Sci. 8095, 1-5 (2002)

51. W Watanabe, T Asano, K Yamada, K Itoh, and J Nishii, *'Wavelength division with three dimensional couplers fabricated by filamentation of femtosecond laser pulses'*, Opt. Lett., 28, 2491-2493 (2003)

52. AM Streltsov and NF Borrelli, *'Fabrication and analysis of a directional coupler written in a glass by nanojoule femtosecond laser pulses'*, Opt. Lett., 26, 42-43 (2001)

53. M Ams, GD Marshall, DJ Spence and MJ Withford, *'Slit beam shaping method for femtosecond laser direct-write fabrication of symmetric waveguides in bulk glasses'*, Opt. Exp. 13, 5676-5681 (2005)

54. SH Cho, H Kumagai, K Midorikawa and M Obara, *'Fabrication of double cladding structure in optical multimode fibres using plasma channelling excited by a high-intensity femtosecond laser'*, Opt. Comms. 168, 287-295 (1999)

55. J Liu, Z Zhang, C Flueraru, X Liu, S Chang, CP Grover *'Waveguide shaping and writing in fused silica using a femtosecond laser'* J Sel. Top. Quantum Electron, 10, 169-173 (2004)

56. AG Okhrimchuck, AV Shestakov, I Khrushchev and J Mitchell, *'Depressed cladding buried waveguide laser formed in a YAG:Nd^{3+} crystal by femtosecond laser writing'*, Opt. Lett., 30, 2248-2250 (2005)

57. C Florea and KA Winick, *'Fabrication and characterisation of Photonic devices directly written in glass using femtosecond laser pulses'*, J. Lightwave Tech., 21, 246-253 (2003)

58. T Fukuda, S Ishikawa, T Fujii, K Sakuma and H Hosoya, *'Improvement on asymmetry of low-loss waveguides written in pure silica glass by femtosecond laser pulses' Optical Fibers and Passive components, Proc. SPIE 5279, 21-28 (2004)*

59. H Hosono, K Kawamura, S Matsuiishi, M Hirano, *'Holographic writing of micro-gratings and nanostructures on amorphous SiO2 by near infrared femtosecond pulses'*, Nuclear Instruments and Methods in Physics Research B 191 89-97 (2002)

60. Mills JD, Kazansky PG, Bricchi E, Baumberg JJ *'Embedded anisotropic microreflectors by femtosecond-laser nanomachining'* Appl. Phys. Lett., 81, 196-198 (2002)

61. E Wikszak, J Burghoff, M Will, S Nolte, A Tunnermann and T Gabler, *'Recording of fiber Bragg gratings with femtosecond pulses using a "point-by-point" technique'*, OSA Conf. Proc. CLEO/IQEC and PhAST Washington DC, 2004, CThM7

62. Grobnic D, Mihailov SJ, Smelser CW, Ding HM *'Sapphire fiber Bragg grating sensor made using femtosecond laser radiation for ultrahigh temperature applications'*, IEEE Photonic Technol. Lett., 16, 11, 2505-2507 (2004)

63. Grobnic D; Smelser CW; Mihailov SJ; Walker RB; Lu P., *'Fiber Bragg gratings with suppressed cladding modes made in SMF-28 with a femtosecond IR laser and a phase mask'* IEEE Photonics Technol. Lett., 16, 8, 1864-1866 (2004)

64. A Martinez, Y Lai, M Dubov, IY Khrushchev and I Bennion, *'Vector bending sensors based on fiber Bragg gratings inscribed by an infrared femtosecond laser'*, Electron. Lett., 41, 472-474 (2005)

65. A Martinez, I Khrushchev and I Bennion, *'Fabrication of Highly Reflective Bragg Gratings through Fiber Coating by Infrared Femtosecond* Laser', BGPP 2005, Sidney, Australia.

66. G Meltz, WW Morey, WH Glenn, *'Formation of Bragg gratings in optical fibers by a transverse holographic method'*, Opt. Lett. 14, 823-825 (1989)

67. Hill KO, Malo B, Bilodeau F, Johnson DC, Albert J, "Bragg Gratings fabricated in monomode photosensitive optical fiber by UV exposure through a phase mask", Appl. Phys. Lett. 62, 1035-1037 (1993)

68. R Kashyap, 'Fibre Bragg Gratings', Ed. Academic Press, (1999)

69. Othonos A, "Fiber Bragg gratings", Rev. Sci. Instrum. 68, (12), 4309-4341 (1997)

70. T Erdogan, 'Fibre Grating Spectra', J. Lightwave Tech., 15, 8, 1277-1294 (1997)

71. E Hetch, *'Optics'*, Addison Wesley Publishing Company; 3rd edition (1997)

72. J-L Archambault, L Reekie and P St J Russell, *'100% reflectivity Bragg reflectors produced in optical fibres by singer excimer laser pulses'*, Electron. Lett., 29, 453-455 (1993)

73. I Riant, F Haller, *'Study of the photosensitivity at 193 nm and comparison with photosensitivity at 240 nm influence of fiber tension: Type IIA aging'*, J. Lightwave Technol., 15, 1464-1469 (1997)

74. AG Simpson, K Kalli, K Zhou, L Zhang, I Bennion, *'Formation of type IA fibre Bragg gratings in germanosilicate optical fibre'* Electron. Lett., 40, 163-164 (2004)

75. H Patrick, SL Gilbert, A Lidgard, MD Gallagher, *'Annealing of Bragg gratings in Hydrogen-loaded optical fibre'*, J. Appl. Phys., 78, 2940-2945 (1995)

76. L Dong, WF Liu, 'Thermal decay of fibre Bragg gratings of positive and negative index changes formed at 193nm in a boron-co-doped germanosilicate fibre', Appl. Opt. 36, 224-226 (1997)

77. XW Shu, Y Liu, DH Zhao, B Gwandu, F Floreani, L Zhang, I Bennion, *'Dependence of temperature and strain coefficients on fiber grating type and its application to simultaneous temperature and strain measurement'* Opt. Lett., 27, 701-703 (2002)

78. Y Shen, J He, T Sun and KTV Grattan, *'High-temperature sustainability of strong fiber Bragg gratings written into Sb-Ge-codoped photosensitive fibre: decay mechanisms involved during annealing'*, Opt. Lett., 29, 554-556 (2004)

79. G Brambilla, V Pruneri, L Reekie, A Paleari, N Chiodini and H Booth, *'High photosensitivity in Sn_2:SiO_2 optical fibres'*, Fiber and Integrated Optics, 20, 553-564 (2001)

80. KO Hill, Y Fujii, DC Johnson, BS Kawasaki, *'Photosensitivity in optical fibre waveguides: Applications to reflection filter fabrication'*, Appl. Phys. Lett. 32, 647-649 (1978)

81. KO Hill, B Malo, KA Vineberg, F Bilodeau, DC Johnson and I Skinner, *'Efficient mode conversion in telecommunication fiber using externally written grating'*, Electron. Lett., 26, 1270-1272 (1990)

82. Q Zhang, DA Brown, L Reinhart, TF Morse, *'Simple prism-based scheme for fabricating Bragg gratings in optical fibers'*, Opt. Lett. 19 (23), 2030-2032 (1994)

83. H Patrick, SL Gilbert, *'Growth of Bragg gratings produced by continuous-wave ultraviolet light in optical fiber'*, Opt. Lett., 18, 1484-1486 (1993)

84. J Martin and F Ouellette, 'Novel writing technique of long and highly reflective in-fiber gratings' Electron. Lett., 30, 811-812 (1994)

85. HN Rourke, SR Baker, KC Byron, RS Baulcomb, SM Ojha and S Clements, *'Fabrication and characterisation of long, narrow-band fiber gratings by phase mask scanning'*, Electron. Lett., 30, 1341-1342 (1994)

86. Prohaska JD, Snitzer E, Rishton S, Boegli V, *'Magnification of mask fabricated fibre Bragg gratings'*, Electron. Lett., 29, 1614-1615 (1993)

87. Campbell RJ, Kashyap R, *'Spectral profile and multiplexing of Bragg gratings in photosensitive fibre'*, Opt. Lett., 16, 898-900 (1991)

88. JAR Williams, I Bennion, K Sugden and NJ Doran, *'Fiber dispersion compensation using a chirped in fibre Bragg grating'*, Electron. Lett., 30, 985-987 (1994)

89. PC Won, J Leng, Y Lai and JAR Williams *'Distributed Temperature Sensing Using a Chirped Fibre Bragg Grating'*, Meas. Sci. and Tech., 15, 1501-1505 (2004)

90. A Asseh, H Storoy, JT Kringlebotn, W Margulis, B Sahlgren, S Sandgren, R Stubbe, G Edwall, *'10cm Yb3+ DFB fiber laser with permanent phase-shifted grating'* electronics letters 31, 969-970 (1995)

91. GP Agrawal and S Radic, *'Phase-shifted fiber bragg gratings and their application for wavelength demultiplexing'*, Photon. Technol. Lett., 6, 995-997 (1994)

92. R Kashyap, R Wyatt and PF McKee, *'Wavelength flattened saturated erbium amplifier using multiple-side tap Bragg gratings'*, Electron. Lett., 29, 1025-1026 (1993)

93. Zhou K, Simpson AG, Zhang L, Bennion I *'Side detection of strong radiation-mode out-coupling from blazed FBGs in single-mode and multimode fibers'*, IEEE Photon. Technol. Lett., 15, 936-938 (2003)

94. F Bilodeau, *'An all-fibre dense-wavelength-division multiplexer/demultiplexer using photo-imprinted Bragg gratings'*, Photon. Tech. Lett., 7, 388-390 (1995)

95. JJ Pan and Y Shi, *'Steep skirt fibre Bragg grating fabrication using a new apodised phase mask'*, Electron. Lett., 33, 1895-1896 (1997)

96. R Kashyap, SV Chernikov, PF McKee, JR Taylor, *'30ps chromatic dispersion compensation of 400fs pulses at 100GBits/s in optical fibres using an all fiber photoinduced chirped reflection grating'*, Electron. Lett., 30, 1078-1080 (1994)

97. SW James, RP Tatam, *'Optical fibre long-period gratings sensors: characteristics and application'*, Meas. Sci. Technol., 14, R49-R61, (2003)

98. V Bhatia *'Applications of long-period gratings to single and multi-parameter sensing'*, Optics Express, 4, 457-466 (1999)

99. AG Simpson, KM Zhou, L Zhang, L Everall, I Bennion, *'Optical sensor interrogation with a blazed fiber Bragg grating and a charge-coupled device linear array'* Appl. Opt., 43, 33-40 (2004)

100. AM Vengsarkar, PJ Lemaire, JB Judkins, V Bhatia, T Erdogan and JE Sipe, *'Long-period gratings as band rejection filters'*, J. Lightwave Technol., 14, 58-64 (1996)

101. AM Vengsarkar, JR Pedrazzani, JB Judkins, PJ Lemaire, NS Bergano and CR Davidson, *'Long period fibre grating based gain equalizers'*, Opt. Lett., 21, 336-338 (1996)

102. DD Davis, TK Gaylord, EN Glytsis, SG Kosinski, SC Mettler, Am Vengsarkar, *'Long period fibre grating fabrication with focused CO_2 laser beams'*, Electron. Lett., 34, 302-303 (1998)

103. EM Dianov, VI Karpov, MV Grekov, KM Golant, SA Vasiliev, OI Medvekov and RR Khrapko, *'Thermo-induced long period fibre grating' IOOC-ECOC, Vol.2, 53-56 (1997)*

104. CS Kim, Y Han, BH Lee, W-T Han, U-C Paek and Y Chung, *'Induction of the refractive index change in B-doped optical fibres through relaxation of mechanical stress'*, Opt. Commun., 185, 337-342 (2000)

105. G Rego, O Okhotnikov, E Dianov and V Sulimov, *'High-temperature stability of long, period fibre gratings using an electric arc'*, J. Lightwave Technol., 19, 1574-1579 (2001)

106. SA Slattery, DN Nikogosyan and G Brambilla, *'Fibre Bragg grating inscription by high-intensity femtosecond UV laser light: comparison with other existing methods of fabrication'*, J. Opt. Soc. Am. B, 22, 354-361 (2005)

107. J Nishii, N Kitamura, H Yamanaka, H Hosono and H Kawazoe, *'Ultraviolet-radiation-induced chemical reactions through one and two photon absorption processes in GeO_2-SiO_2 glasses'*, Opt. Lett. 20 1184-1186 (1995)

108. Y. Lai, A. Martinez, I. Khrushchev, I. Bennion, *'Er:Yb Fiber Grating Laser Based On Femtosecond Laser Inscription Technique'* Accepted for oral presentation at BGPP 2005, Sidney, Australia.

109. T. Allsop, M. Dubov, A. Martinez, F. Floreani, I. Khrushchev, D.J. Webb and I. Bennion, *"A long period grating directional bend sensor based upon an asymmetric index modification of the cladding"*, Electron. Lett. 41, 59-60 (2005)

110. CW Smelser, SJ Mihailov and D Grobnic, *'Hydrogen loading for fiber grating writing with a femtosecond laser and a phase mask'*, Opt. Lett., 29, 2127-2129 (2004)

111. LMD Delbridge, AA Kabbara, C Bellair, BE Allman, L Nassis, A Roberts and KA Nugent, *'Quantitative Phase Imaging- a new way to 'see' cells'*, Today's Life Science, March/April 1-6 (2002)

112. ED Barone-Nugent, A Barty and KA Nugent, *'Quantitative phase-amplitude microscopy I: optical microscopy'*, J. of Microscopy, 206, 194-203 (2002)

113. A Barty, KA Nugent, D Paganin and A Roberts, *'Quantitative optical phase microscopy'*, Opt. Lett., 23, 817-819 (1998)

114. PP Pronko, SK Dutta, J Squier, JV Rudd, D Du, G Mourou, *'Machining of submicron holes using a femtosecond laser at 800-nm'*, Opt. Commun., 114, 106-110 (1995)

115. M Janos, J Canning and MG Sceats, *'Incoherent scattering losses in optical fibre Bragg gratings'*, Opt. Lett., 21, 1827-1829 (1996)

116. V Mizrahi and JE Sipe, *'Optical properties of photosensitive fiber phase gratings'* J. of Lightwave Technol., 11, 1513-1517 (1993)

117. Komukai T., Nakazawa M., *'Efficient fiber gratings formed on high NA dispersion-shifted fiber and dispersion flattened fiber'* Jpn. J. of Appl. Phys. 2, 34, L1286-L1287 (1995)

118. Dong L, Reekie L, Cruz JL, Caplen JE, de Sandro JP, Payne DN *'Optical fibers with depressed claddings for suppression of coupling into cladding modes in fiber Bragg gratings'* IEEE Photonic Technol. Lett. 9, 64-66, (1997)

119. E Delavaque, S Bog, JF Bajyon, H Poignat, J Le Mellt, and M Monerie, Opt. Fiber Commun. Conf. Paper PD5 (1995)

120. Hill, KO, Malo, B, Vineberg, KA, Bilodeau, F, Johnson, DC and I Skinner, *'Efficient mode conversion in telecommunication fiber using externally written gratings'* Electron. Lett. 26, 1270-1272 (1990)

121. Hill, KO, Bilodeau, F, Malo, B,and Johnson, DC, *'Birefringent photosensitivity in monomode optical fiber - application to external writing of rocking filters'*, Electron. Lett. 27, 1548-1550 (1991)

122. Meltz, G, Morey, WW, Glenn, WH, *'Formation of Bragg gratings in optical fibers by a transverse holographic method'*, Opt. Lett. 14, 823-835 (1989)

123. WH Loh and RI Laming, *'1.55μm phase-shifted distributed feedback fiber laser'*, Electron. Lett., 31, 1440-1442 (1995)

124. T Erdongan and V Mizrahi, *'Characterisation of UV-induced birefringence in photosensitive ge-doped silica optical fibers'* J. Opt. Soc. Am. B, 11, 2100-2105, (1994)

125. AM Vengsarkar, S Zhong, D Inniss, WA Reed, PJ Lemaire, SG Kosinski, *'birefringence reduction in side-written photoinduced fiber devices by a dual-exposure method'*, Opt. Lett. 19, 1260-1262 (1994)

126. VR Bhardwaj, PB Corkum, DM Rayner, C Hnatovsky, E Simova and RS Taylor, *'Stress in femtosecond-laser-written waveguides in fused silica'*, Opt. Lett., 29, 1312-1314 (2004)

127. SR Baker, NH Rourke, V Baker, D Goodchild, *'Thermal decay of fiber Bragg gratings written in Boron and Germanium co-doped silica fiber'*, J. Lightwave Technol. 15, 1470-1477 (1997)

128. J Mandal, T sun, KTV Grattan, AT Augousti, SA Wade, SF Collins, GW Baxter, B Dussardier and Monnom, *'A wide temperature tunable fibre laser using a chirped grating and a type IIA fibre Bragg grating'*, Meas. Sci. Technol. 15, 1113-1119 (2004)

129. F Farahi, DJ Webb, JD Jones, DA Jackson, *'Simultaneous measurement of temperature and strain: Cross-sensitivity considerations'*, J. Lightwave Technol., 8, 138-142 (1990)

130. S Pal, T Sun, KTV Grattan, SA Wade, SF Collins, GW Baxter, B Dussardier, G Monnom, *'Non-linear temperature dependence of Bragg gratings written in different fibres, optimised for sensor applications over a wide range of temperatures'* SENSORS AND ACTUATORS A-PHYSICAL 112 (2-3): 211-219 (2004)

131. Longman and JH de Bussy, *'Materials and technology Vol.2: Non-metallic minerals and rocks'*, Longman Group Ltd. (1971)

132. A. Martinez, I. Khrushchev, I. Bennion, *'Thermal properties of fibre Bragg gratings inscribed point-by-point by an infrared femtosecond laser'*, Electron. Lett., 41, 176-178 (2005)

133. L Dong, JL Archambauldt, L Reekie, P St J Russell, and DN Payne, *'Single pulse Bragg gratings written during fibre drawing'*, Electron. Lett., 29, 1577-1578 (1993)

134. R Feced, MP Roe-Edwards, SE Kanellopoulos, NH Taylor, VA Handerek, *'Mechanical strength degradation of UV exposed optical fibres'*, Electron. Lett., 33 157-159 (1997)

135. YW Song, SA Havstad, D Starodubov, Y Xie, AE Willner and J Feinberg, *'40nm wide tunable fibre ring laser with single-mode operation using a highly stretchable FBG'*, Photon. Technol. Lett., 13, 1167-1169 (2001)

136. GA Ball and WW Morey, *'Compression-tuned single-frequency Bragg grating fibre laser'*, Opt. Lett., 19, 1979-1981 (1994)

137. D Zhao, L Zhang and I Bennion, *'Implementation of vector bending sensors using long-period gratings UV-inscribed in Flat-Clad and 4-core fibres'* in Proceedings of 16th International Conference on Optical Fiber Sensors, 794 (2003)

138. FM Araujo, LA Ferreira, JL Santos and F Farahi, *'Temperature and Strain insensitive bending measurements with D-type fibre Bragg gratings'*, Meas. Sci. Technol. 12, 829-833 (2001)

139. H Kumazaki, K Nakashima, S Inaba and K Hane, *'Tunable wavelength filter through bending control of asymmetric single-mode grating fibre'*, Opt. Express, 10, 469-474 (2002)

140. HJ Patrick, *'Self-aligning, bipolar bend transducer based on long period grating written in eccentric core fibre'*, Electron. Lett., 36, 1763-1764 (2000)

141. W Du, H Tam, M Liu, X Tao, *'Long period grating bending sensors in laminated composite structures'*, SPIE Conf. Proc. Smart structures and materials, 3330, 284 (1998)

142. JX Cai, KM Feng, AE Willner, V Grubscky, DS Starodubov and J Feinberg, *'Simultaneous tunable dispersion compensation of many WDM channels using a sampled nonlinearly chirped fiber Bragg grating '*, Photon. Technol. Lett. 11, 1455-1457 (1999)

143. D. Wei, T. Li, Y. Zhao, and S. Jian, '*Multiwavelength erbium-doped fiber ring lasers with overlap-written fiber Bragg gratings'*, Opt. Lett. 25, 1150-1152 (2000)

144. A. Arigiris, M Kostantantanaki, A. Ikiades,Chronis, P Florias, K Kallimani and G. Pagiatakis, *'Fabrication of high-reflectivity superimposed multiple-fiber Bragg gratings with unequal wavelength spacings'* , Opt. Lett. 27, 1306-1308 (2002)

145. DCJ Reid, CM Ragdale, I Bennion, DJ Robbins, J Buus and WJ Stewart *'Phase-shifted Moire grating fibre resonators'*, Elec. Lett. 26, 10-12 (1990)

146. L Dong, WH Loh, JE Caplen, JD Minelly, K Hsu, L Reekie, *'Efficient single-frequency fibre lasers with novel photosensitive Er:Yb optical fibres'*, Opt. Lett. 22, 694-696 (1997)

147. RJ Mears, L Reekie, IM Jauncy, DN Payne, *'High gain rare-earth doped fibre amplifier at 1.54μm'*, Proc. Optical Fibre Communications Conference (OFC), WI1 (1987)

148. RJ Mears, L Reekie, SB Poole, DN Payne, *'Low Threshold tunable CW and Q-switched fibre laser operating at 1.55μm'*, Electron. Lett., 22, 159-160 (1986)

149. RI Laming, SB Poole and EJ Tarbox, *'Pump excited state absorption in erbium doped fibres'*, 13, 1084-1086 (1988)

150. RI Laming, MC Farries, PR Morkel, L Reekie, and DN Payne, *'Efficient pump wavelengths of erbium doped fibre optical amplifiers'*, Electron. Lett., 25, 12-14 (1989)

151. M Yamada, M Shimizu, T Takeshita, M Okayasu, M Horiguchi, S Uehara, E Sugita, *'Er^{3+} doped fibre amplifier pumped by 0.98μm laser diodes'* Photon. Technol. Lett., 1, 422-424 (1989)

152. M Yamada, M Shimizu, M Okayasu, T Takeshita, M Horiguchi, Y Tachikawa, E Sugita, *'Noise characteristics of Er^{3+} doped fibre amplifiers pumped by 0.98 and 1.48μm laser diodes'*, Photon. Technol. Lett., 2, 205-207 (1990)

153. WL Barnes, PR Morkel, L Reekie, and DN Payne, *'High quantum efficiency Er^{3+} fibre lasers pumped at 980nm'*, Opt. Lett., 14, 1002-1004 (1989)

154. JE Townsend, WL Barnes, KP Jedrzejewski, *'Yb^{3+} sensitised Er^{3+} doped silica optical fibre with ultrahigh transfer efficiency and gain'*, Electron. Lett., 27, 1958-1959 (1991)

155. WL Barnes, PR Morkel, L Reekie, DN Payne, *'High quantum efficiency Er^{3+} fibre lasers pumped at 980nm'*, J. Lightwave Technol., 7, 1461-1465 (1989)

156. DC Hanna RM Percival, IR Perry, RG Smart and AC Tropper, *'Efficient operation of an Yb^{3+} sensitised Er fibre laser pumped in the 0.8μm region'*, Electron. Lett., 24, 1068-1069 (1988)

157. M Ding, PK Cheo, *'Effects of Yb:Er-codoping on suppressing self-pulsing in Er-doped fibre lasers'*, Photon. Technol. Lett., 7, 1461-1465 (1997)

158. HL An, XZ Lin, HD Liu, *'Intensity noise suppression by Ytterbium codoping in heavily erbium doped fibre lasers partly clustered erbium ions'*, Opt. Lett., 25, 1747-1749 (2000)

159. Z Ahmed, HF Liu, D Novak, M Pelusi, Y Ogawa, DY Kim, *'Low phase noise millimetre wave signal generation using a passively modelocked monolithic DBR laser injection locked by an optical DSBSC signal'*, Electron. Lett., 31, 1254-1255 (1995)

160. WH Loh, L Dong and JE Caplen, *'Single-sided output Sn/Er:Yb distributed feedback laser'*, Appl. Phys. Lett., 69, 2151-2153 (1996)

161. GA Ball, CE Holton, G Hull-Hallen and WW Morey, *'60mW 1.5μm single-frequency low noise fibre laser MOPA'*, IEEE Photon. Technol. Lett., 6, 192-194 (1994)

162. D Zhao, Y Lai, X Shu, L Zhang and I Bennion, *'Supermode-noise suppression using a nonlinear Fabry-Perot filter in a harmonically mode-locked fibre ring laser'*, Appl. Phys. Lett., 81, 4520-4522 (2002)

163. JT Kringlebotn, JL Archambault, L Reekie, JE Townsend, GG Vienne, DN Payne, *'Highly-efficient, low-noise grating-feedback Er3+:Yb3+ codoped fiber laser'*, Electron. Lett., 30, 972-973 (1994)

164. SL Woodward, V Mizrahi, TL Koch, U Koren, PJ Lemaire, *'Wavelength stabilisation of a dbr laser using an in-fiber bragg filter'*, Photon. Technol. Lett., 5, 628-630 (1993)

165. JT Kringlebotn, PR Morkel, L Reekie, JL Archambault, Dn Payne, *'Efficient diode-pumped single frequency erbium-ytterbium fibre laser'*, Photon. Technol. Lett., 5, 1162-1164 (1993)

166. ZE Harutjunian, WH Loh, RI Laming, DN Payne, *'Single polarisation twisted distributed feedback fibre laser'*, Electron. Lett., 32, 346-348 (1996)

167. M Douay, T Feng, P Bernage, P Niay, E Delevaque, T Georges, *'Birefringence effect of optical fibre laser with intracore fibre Bragg grating'*, Photon. Technol. Lett., 4, 844-846 (1992)

Publications arising from this work

Patents:

'Laser inscribed structures', UK Patent Application, GB 0410821.3, 14th May 2004.

'Er:Yb fibre grating laser based on femtosecond laser inscription technique' GB 0509920.5, 14th May 2005.

Publications:

1. A. Martinez, M. Dubov, I.Y. Khrushchev and I. Bennion, *"Point-by-point FBG inscription by a focused NIR femtosecond laser"*, OSA Conf. Proc. CLEO/IQEC and PhAST Washington DC, 2004, CMY6
2. A. Martinez, M. Dubov, I. Khrushchev and I. Bennion, *"Direct writing of fibre Bragg gratings by femtosecond laser"*, Electron. Lett. 40, 1170-1172 (2004)
3. A. Martinez, M. Dubov, I. Khrushchev, I. Bennion, *"Femtosecond Inscription of Superimposed, Non-Overlapping Fibre Bragg Gratings"*, 30th European Conference on Optical Communications (ECOC2004), Stockholm, Sweden, September 2004, Paper Tu.1.3.2.
4. A. Martinez, M. Dubov, I. Khrushchev, I. Bennion, *"Direct femtosecond inscription of fibre Bragg gratings"* MRS 2004
5. T. Allsop, M. Dubov, A. Martinez, F. Floreani, I. Khrushchev, D.J. Webb and I. Bennion, *"A long period grating directional bend sensor based upon an asymmetric index modification of the cladding"*, Electron. Lett. **41**, 59-60 (2005)
6. A. Martinez, I. Khrushchev and I. Bennion, *"Thermal properties of fiber Bragg gratings inscribed point-by-point by an infrared femtosecond laser"* Electron. Lett. **41** 176-177 (2005)
7. A. Martinez, Y. Lai, M. Dubov, I.Y. Khrushchev and I. Bennion, *"Vector bending sensors based on fiber Bragg gratings inscribed by an infrared femtosecond laser"* Electron. Lett. **41**, 472-474 (2005)
8. A. Martinez, I. Khrushchev, I. Bennion *"Dynamics of thermal annealing of fiber gratings directly written by an infrared femtosecond laser"* OptoIreland 2005 accepted for presentation 2005.
9. T. Allsop, M. Dubov, A. Martinez, F. Floreani, I. Khrushchev, D.J. Webb, I. Bennion, *"A long period grating directional bend sensor incorporating index modification of the cladding"* Accepted for presentation OFS 2005.

10. A. Martinez, Y. Lai, M. Dubov, I. Khrushchev and I. Bennion *"Vector bending sensors based on fiber Bragg gratings inscribed by an infrared femtosecond laser"*, Accepted for oral presentation at CLEO 2005.

11. A. Martinez, I. Khrushchev and I. Bennion, *"Thermal Annealing of Fiber Bragg Gratings Directly Inscribed by an Ultrafast Infrared Laser"*, Accepted for oral presentation at CLEO 2005.

12. T. Allsop, M. Dubov, A. Martinez, F. Floreani, I. Khrushchev, D.J. Webb, I. Bennion, *"Directional bend sensor based on an asymmetric modification of the fibre cladding by a femtosecond laser"* Accepted for oral presentation CLEO 2005.

13. A. Martinez, I. Khrushchev and I. Bennion, *'Fabrication of Highly Reflective Bragg Gratings through Fiber Coating by Infrared Femtosecond Laser'* Accepted for oral presentation at BGPP 2005, Sidney, Australia.

14. Y. Lai, A. Martinez, I. Khrushchev, I. Bennion, *'Er:Yb Fiber Grating Laser Based On Femtosecond Laser Inscription Technique'* Accepted for oral presentation at BGPP 2005, Sidney, Australia.

15. V. Mezentsev, M. Dubov, A. Martinez, T.P. Allsop, I.Y. Khrushchev, I. Bennion, Y. Lai, D.J. Webb, F. Floreani, *'Micro-fabrication of advanced photonic devices by means of direct point by point femtosecond inscription in silica'*, *SPIE* Photonics West 2006.

16. KT O'Mahoney, AS Main, A Martinez and D Webb, *'Implications of losses at high optical powers in Bragg gratings written by femtosecond laser pulses in coated fibre', SPIE* Photonics Europe 2006.

17. TD Allsop, H Dobb, AS Main, A Martinez, M Dubov, K Kalli, DJ Webb and I Bennion, *'A comparison of the spectral properties of high-temperature annealed long-period gratings inscribed by a femtosecond laser, UV and fusion arc' SPIE* Photonics Europe 2006.

18. T. Allsop, M. Dubov, A. Martinez, F. Floreani, I. Khrushchev, D.J. Webb, I. Bennion *'Bend Characteristics of Fibre Long Period Gratings with Cladding Index Modified by Femtosecond Laser',* J. Lightwave Technol. to be published.

19. A. Martinez, M. Dubov, I. Khrushchev and I. Bennion "Structure of fiber gratings directly written by infrared femtosecond laser", Submitted to CLEO 2006

20. A. Martinez, I. Khrushchev and I. Bennion, "Direct inscription of Bragg gratings in coated fibers by infrared femtosecond laser" submitted to Opt. Lett.